CHAPTER IV

RESULTS AND DISCUSSION

Based on the research work of N. Ogata and S. Chujo (28, 29), the phenomenon of the free volume in solution where the morphology of the matrix polymer was changed in the solvent, as shown in Figure 4.1, is used as a guidance of this research work. Considering the nature of styrene and methyl methacrylate monomers, the former is rather hydrophobic while the latter is somewhat hydrophilic. It can be explained that, when using the good solvent for the matrix polymer such as ethanol, the copolymer particles have a narrow size distribution because of equal free volume within the matrix polymer chains when using the poor solvent for the matrix polymer such as water, the copolymer particles have a broad size distribution.

In this research work, poly(styrene-*co*-methyl methacrylate) microbeads were prepared in a dispersion media of a solvent mixture of ethanol and water by dispersion polymerization. The solubility of styrene and methyl methacrylate monomers in the above dispersion media strongly depends on the water content and their solubility in ethanol. Different dispersion media having various polarities by changing the water content in the solvent mixture of ethanol and water were used.

Dispersion copolymerization of styrene and methyl methacrylate in the solvent mixture of ethanol and water in the presence of PVP K-30 as a matrix polymer was homogeneous and clear at the beginning. The single phase solution was thus formed, because the monomer, initiator, matrix polymer are soluble in the medium. After an

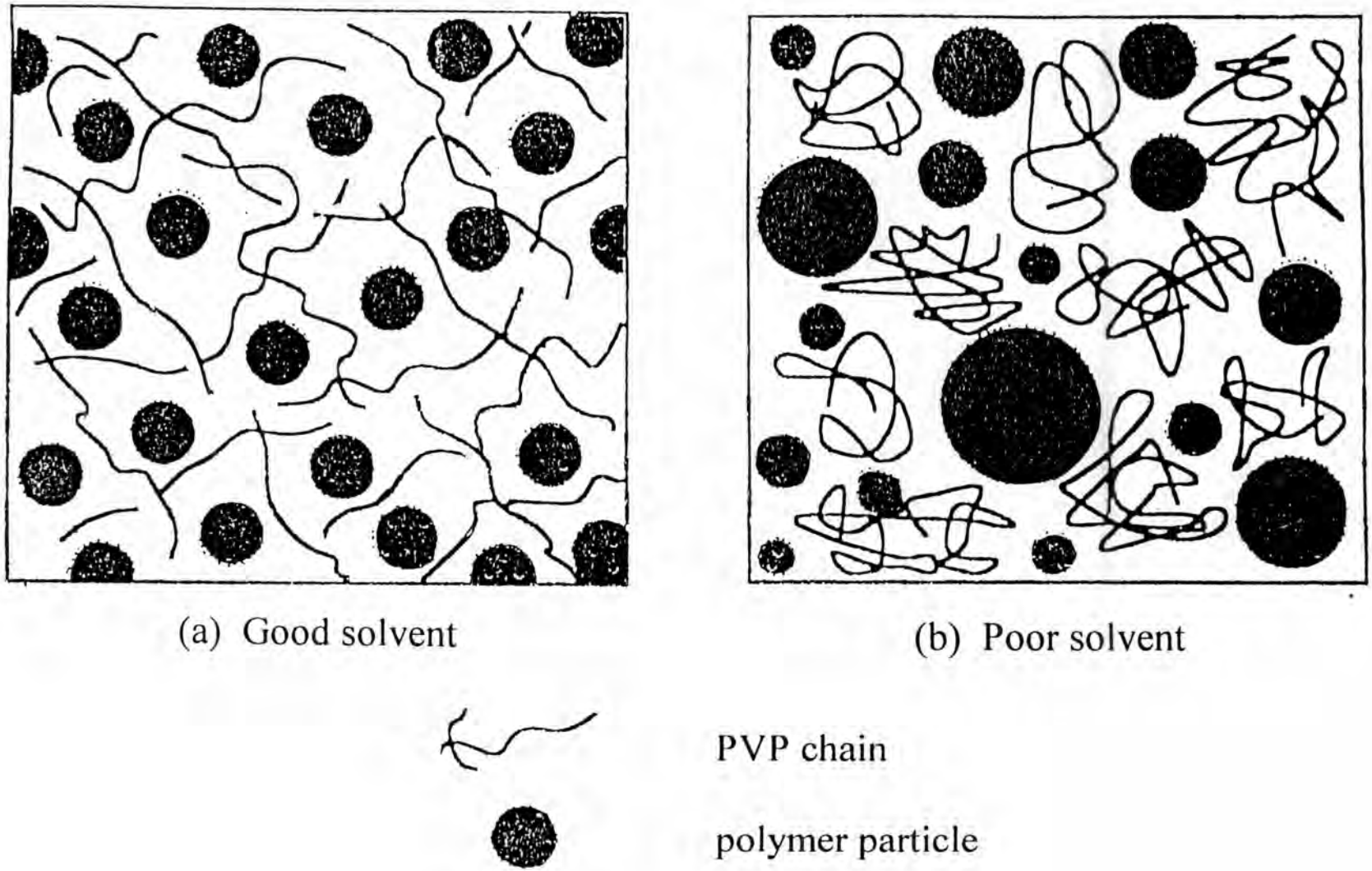

Figure 4.1 Schematic views of PVP matrix polymer in a good and poor solvent

induction period of about 15 mins a faint opalescence was observed. It becomes more opalescence after a longer while (25 mins) and turns into a milky white stable dispersion afterwards. After the polymerization had been completed, the copolymer particles were removed from the reaction mixture by centrifugation, and were washed with methanol, and dried under vacuum. After drying, the polymer particles were a fine powdery form.

Further investigations using the ethanol/water mixture were then carried out to establish the effect of reaction variables such as the solvency of the reaction medium, PVP concentration, the agitation rate, the reaction time and temperature on the dispersion polymerization. These effects of variables are presented below.

4.1 The Effect of Matrix Polymer Concentration on

4.1.1 The Particle Size and Particle Size Distribution of Poly(Styrene-*co*-Methyl Methacrylate)

The selection of an effective matrix polymer is very important in the preparation of monosized polymeric particles by dispersion polymerization. The matrix polymer is used for stabilization of dispersion polymerization. The soluble polymer which processes active ∝-hydrogens as possible chain transfer sites, is used as a matrix polymer. The matrix polymer is must not only be soluble in the system but also be able to cover the particle surface sufficiently to prevent coagulation (30). Typically, the structure of matrix polymer contain active hydrogen atoms, because it is believed that during particle nucleation, in situ grafting of the matrix polymer occurs via generation of free radical sites, that is the grafting of the matrix polymer involves

abstraction of hydrogen radicals from the PVP molecule creating free radical sites which can add more monomer (31).

The following reactions can occur :

$$\text{AIBN} \rightarrow 2R\bullet + N_2 \quad (4.1)$$

$$R\bullet + M \rightarrow \text{R-M}\bullet \rightarrow \text{Pdisp (precipitated)} \quad (4.2)$$

$$R\bullet + \text{PVP-H} \rightarrow \text{PVP}\bullet + \text{RH} \quad (4.3)$$

$$\text{PVP-H} + \text{R-M}\bullet \rightarrow \text{PVP}\bullet + \text{Pdisp} \quad (4.4)$$

$$\text{PVP}\bullet + n\text{M} \rightarrow \text{PVP-}g\text{-Pdisp} \quad (4.5)$$

$$\text{PVP}\bullet + \text{R-M}\bullet \rightarrow \text{PVP-}g\text{-Pdisp} \quad (4.6)$$

$$\text{PVP-}g\text{-Pdisp} + \text{Pdisp} \rightarrow \text{stabilized dispersed polymer} \quad (4.7)$$

where Pdisp = dispersed phase polymer

PVP = soluble matrix polymer

The above process is represented in Figure 4.2.

In dispersion polymerization, during or immediately following the precipitation of the insoluble disperse phase polymer, the dispersant becomes adsorbed on the polymer surface. The equilibrium between the adsorbed dispersant, single dispersant molecules and dispersant micelles may be represented as shown in Figure 4.3 (32).

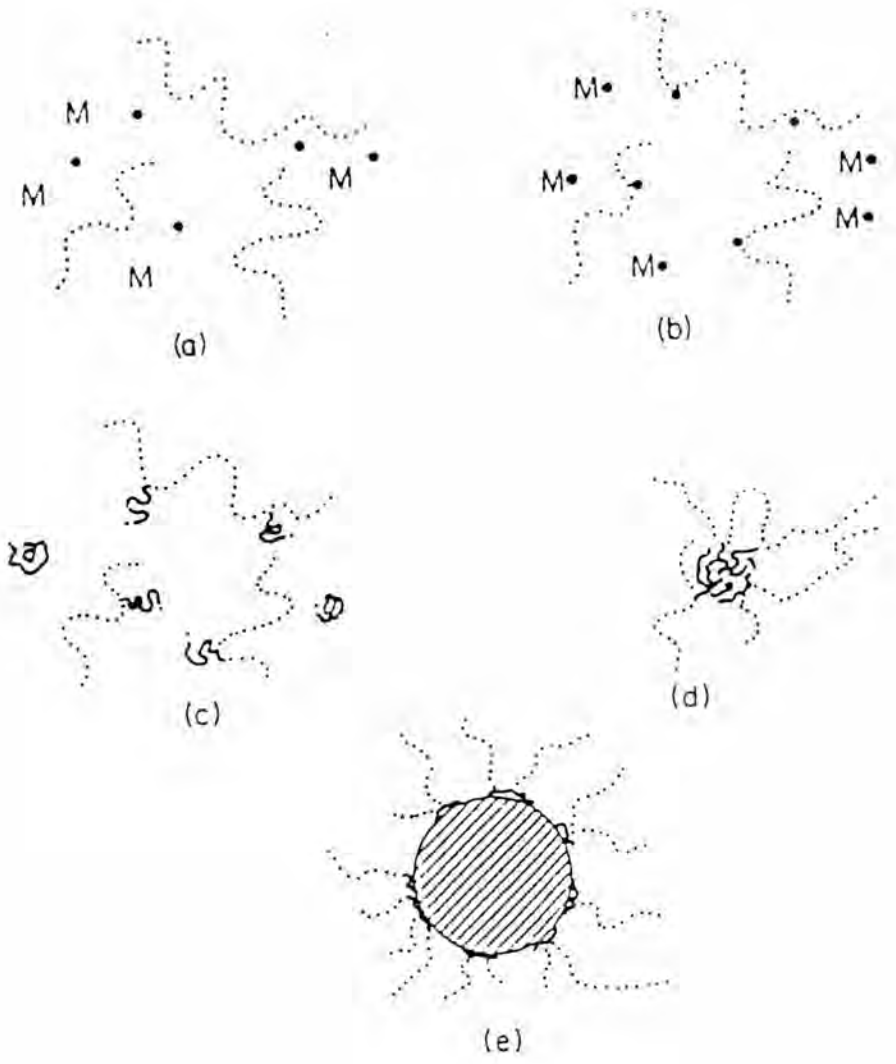

Figure 4.2 Stages in the formation of random graft stabilizers in dispersion polymerization: (a) Radical formation (initiation); (b) radical transfer; (c) random grafting; (d) aggregation; (e) particle growth; (.....) soluble chain; (—) insoluble chain (•) free radicals; (M) monomer

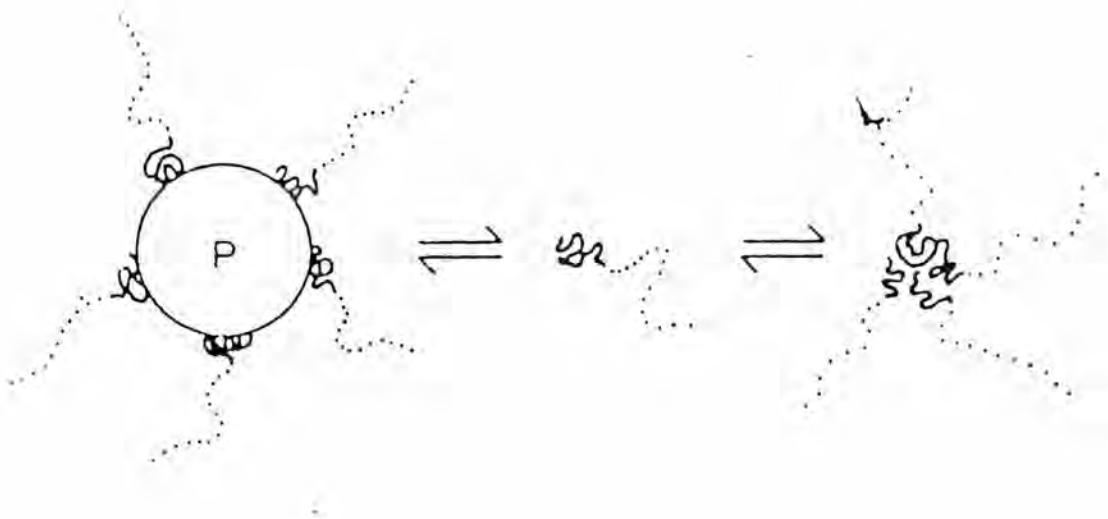

Figure 4.3 Dispersant equilibria during dispersion polymerization; (.....) soluble group; (___) insoluble or anchor group; P, growing polymer particle

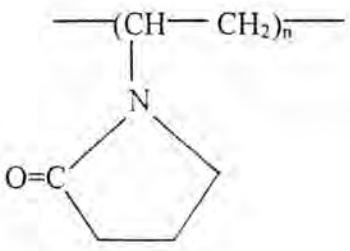

Figure 4.4 The structure of poly(N-vinyl pyrrolidone) matrix polymer

In this research, poly(N-vinyl pyrrolidone), with a molecular weight of 40,000 was used as a matrix polymer in the dispersion copolymerization of styrene and methyl methacrylate. The structure of the matrix polymer, poly(N-vinyl pyrrolidone), is shown in Figure 4.4.

Dispersion copolymerization systems were performed with six different PVP K-30 concentrations (0, 2, 6, 8, 10, and 12 wt%) in ethanol/water ratio of 70/30.

In this research, the reaction involving the dispersion copolymerization in ethanol/water media is a single stage or "one-shot" process, utilizing an initially homogeneous solution of reactants in a media which is then polymerized to completion in a single stage.

In the "one-shot" process, a solution of monomer, initiator and graft copolymer dispersant (PVP-g-Pdisp) in a diluent, is heated together with stirring generally under reflux conditions. After a short period under reflux during which solution polymerization takes place, the reaction mixture becomes opalescent due to the formation of very small, "molecular" particles of polymer precipitated from solution. These primary particles can aggregate with each other to form larger species but are prevented from complete aggregation by their association with the graft copolymer dispersant which provides a barrier of soluble polymer around the particles formed as shown in Figure 4.2-d. After the formation of dispersed polymer, styrene or methyl methacrylate monomer are absorbed into the polymer particles and polymerization then proceeds at an increasing rate within the particle. Dispersion polymerization continues at a fast rate until the monomer concentration in the

continuous phase has fallen to a low level. At this point, the polymerization rate is decreased (33).

Barrett proposed three possible nucleation mechanisms for dispersion polymerization, that is micelle, self and aggregative nucleations. The micelle nucleation mechanism was eliminated because no micelles were present in the reaction system before polymerization took place. The important difference between the aggregative nucleation and self nucleation process is that the nuclei are formed almost at sometime resulting in a narrower particle size distribution (34). Therefore, the aggregative nucleation mechanism fits the picture of dispersion polymerization in organic media most closly. A distinct characteristic of the aggregative nucleation mechanism is that each nucleus contains several oligomer chains. Therefore, the size of each nucleus depends on the chain length and number of chains.

The characteristic and the surface of the copolymer particles prepared with different PVP K-30 concentrations are shown in Figures 4.5-4.10. It can be seen that these copolymer particles which are controlled by the matrix polymer have a microspherical shape with a smooth surface. Different matrix polymer concentrations gave also various copolymer particle sizes. The copolymer particle sizes obtained were in the range of 0.3-1.5 μm. The copolymer particles have a spherical shape and stabilized in dispersion polymerization because of the forces of repulsion generated by barriers of the soluble matrix polymer. That is, as two surfaces, each covered by a layer of adsorbed soluble polymer chains, approach each other within a distance less than the combined thickness of the adsorbed layers, an interaction between the polymer

layers will occur. This interaction, which is the source of steric stabilization will in most cases, generate a repulsive force between the opposing surfaces (35).

When the system was polymerized without the matrix polymer, PVP K-30, agglomerated particles or even sheets were formed. It is explained that the polymerizing system without a matrix polymer brings about the instability of the growing particles and leads to their rapid coalescence because of the forces of attraction among the particles. This attractive force which operates between two adjacent particles, usually called the Van der waals force, originates in the interactions between the atoms and molecules of which the particles are composed (36).

The SEM photographs of the copolymer which indicate the particle size distribution of the copolymer controlled by different PVP K-30 concentrations are given in Figures 4.11-4.15. For the particle size, as the PVP K-30 concentration was increased from 2 to 8 wt%, the average particle size decreased from 1.5 to 0.6 μm. The copolymer particle sizes became smallest from 0.6 to 0.3 μm when increasing the PVP K-30 concentration to about 12 wt%. At low PVP K-30 concentration (2 wt%), the rate of adsorbtion of the matrix polymer is very low, resulting in very larger particles (1.5 μm). This is the largest particle size with a narrow size distribution (CV = 4.75%) of the dispersion copolymerization, in the research. The effect of the matrix polymer concentration on particle size of poly(styrene-*co*-methyl methacrylate) is tabulated in Table 4.1 and shown in Figure 4.16.

From the work of Tseng et al. (37), it can be seen that above PVP K-30 concentration of 2.76 wt% in combination with Aerosol OT co-stabilizer in ethanol, the average particle size of polystyrene decreased slightly with the increasing of the

matrix polymer concentration from which a narrow particle size distribution were obtained. The later, the results of the research of Tuncel et al. (38) indicated that the average particle size of polystyrene decreased with increasing PAA concentration in isopropanol/water media. Moreover, Shen et al. (39) studied the control of particle size in dispersion polymerization of methyl methacrylate by varying the PVP concentrations from 1 to 10 wt% in methanol media. It was found that the resulting polymer particle size increased with decreasing PVP concentration.

The chart of the polymer particle size distribution with different PVP concentrations and relationship between average particle size and CV of poly(styrene-*co*-methyl methacrylate) microspheres are shown in Appendice D-a1 to D-a5 and Figure 4.17, respectively. It is found that the smaller particle size gave a broad size distribution. For particle size, increasing the PVP K-30 concentration means an increase in both the physical adsorption rate of PVP and the viscosity of the continuous phase (39), which in turn, reduced the mobility of oligomer chains, decreased the diffusion velocity of the precipitated oligomer radicals to result in a decrease of the aggregation of precipitated oligomer radicals, and decrease the number of precipitated oligomer chains and the chain length in each nucleus. The above phenomena increase the number of particle nuclei and smaller particles have a larger total surface area and a broader size distribution. When 12 wt% PVP was used, the smallest particle size was found because increasing PVP concentration in a good solvent resulted in an increase of PVP expanded soluble chains. The free volume in the polymeric solution that controlls the particle sizes of the copolymer became smaller.

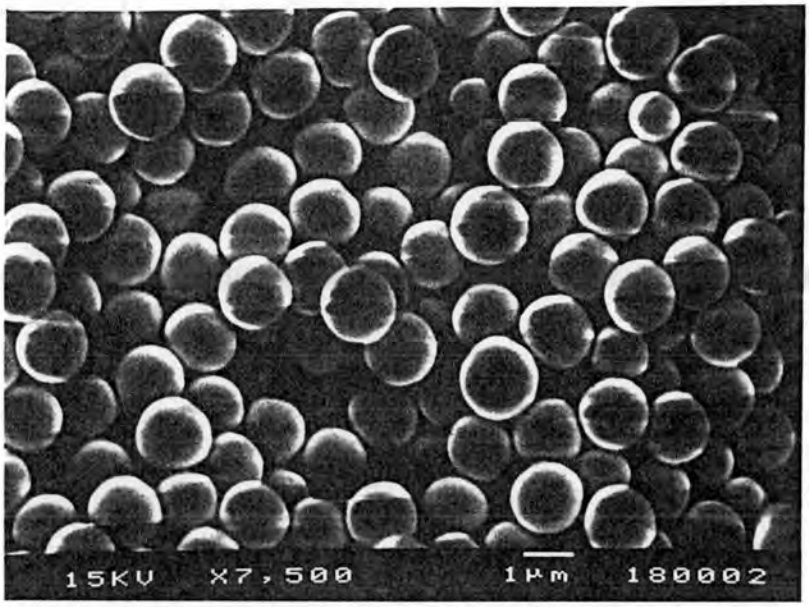

Figure 4.5 SEM micrograph of poly(styrene-*co*-methyl methacrylate) controlled by 2 wt% PVP K-30

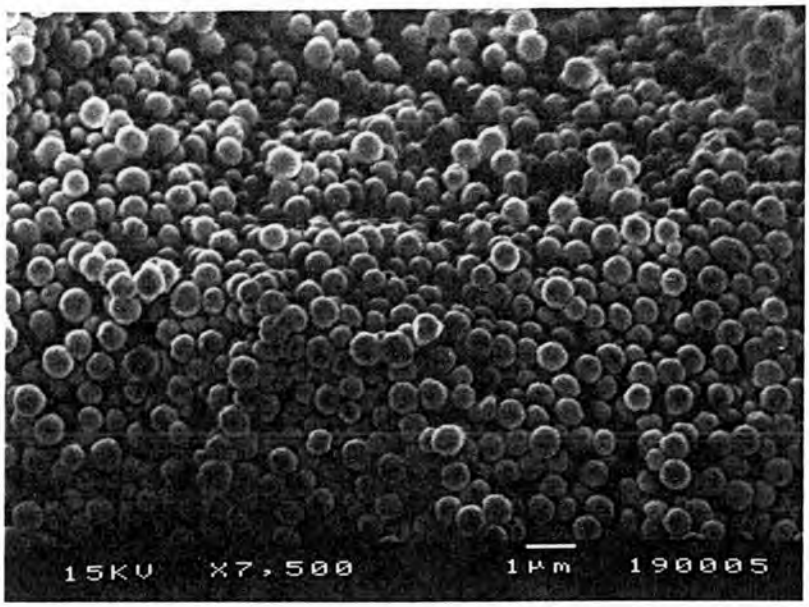

Figure 4.6 SEM micrograph of poly(styrene-*co*-methyl methacrylate) controlled by 6 wt% PVP K-30

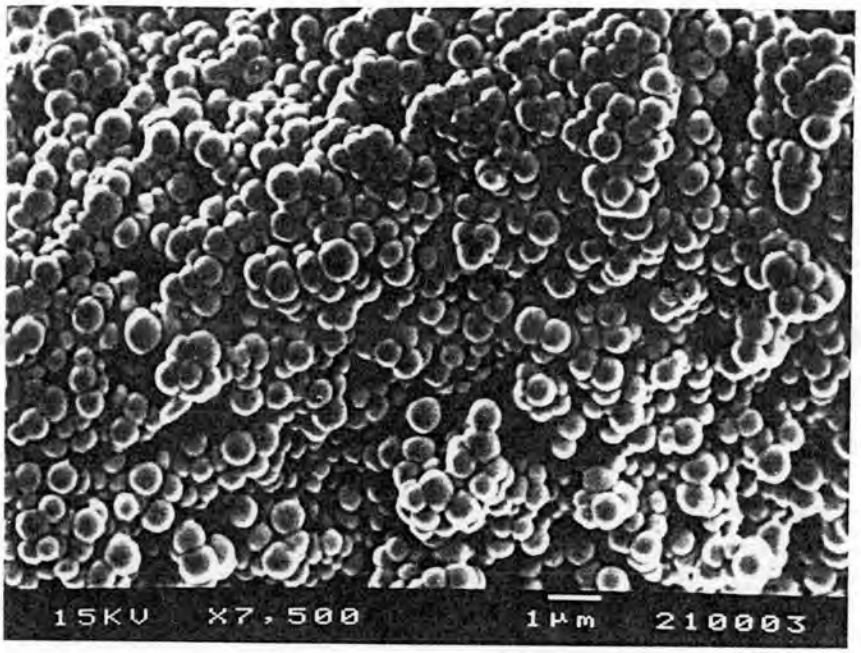

Figure 4.7 SEM micrograph of poly(styrene-*co*-methyl methacrylate) controlled by 8 wt% PVP K-30

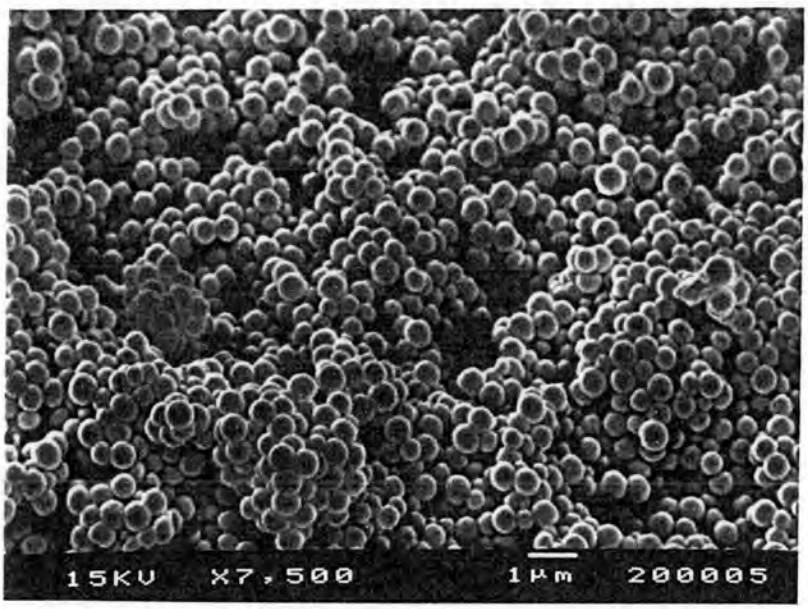

Figure 4.8 SEM micrograph of poly(styrene-*co*-methyl methacrylate) controlled by 10 wt% PVP K-30

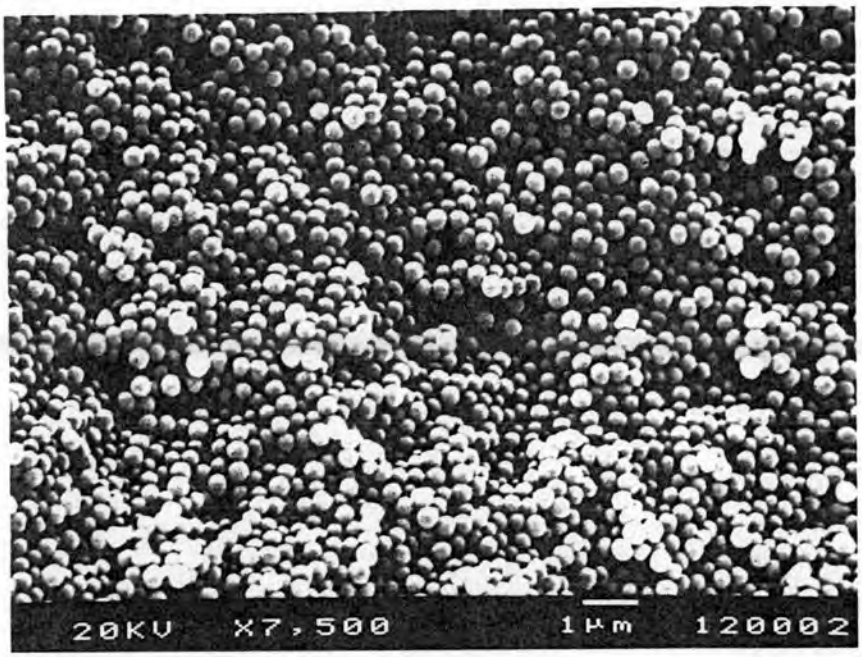

Figure 4.9 SEM micrograph of poly(styrene-*co*-methyl methacrylate) controlled by 12 wt% PVP K-30

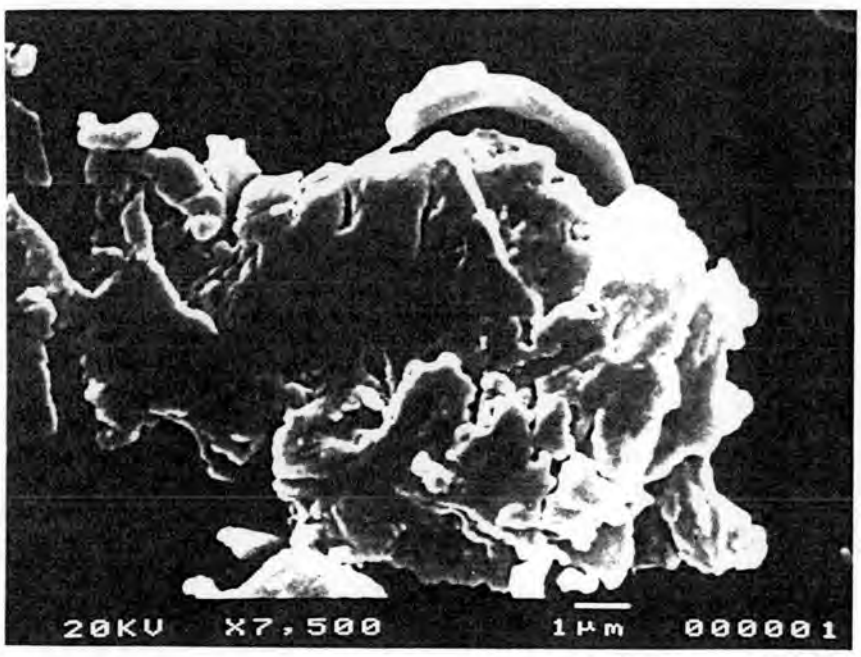

Figure 4.10 SEM micrograph of poly(styrene-*co*-methyl methacrylate) with out the matrix polymer

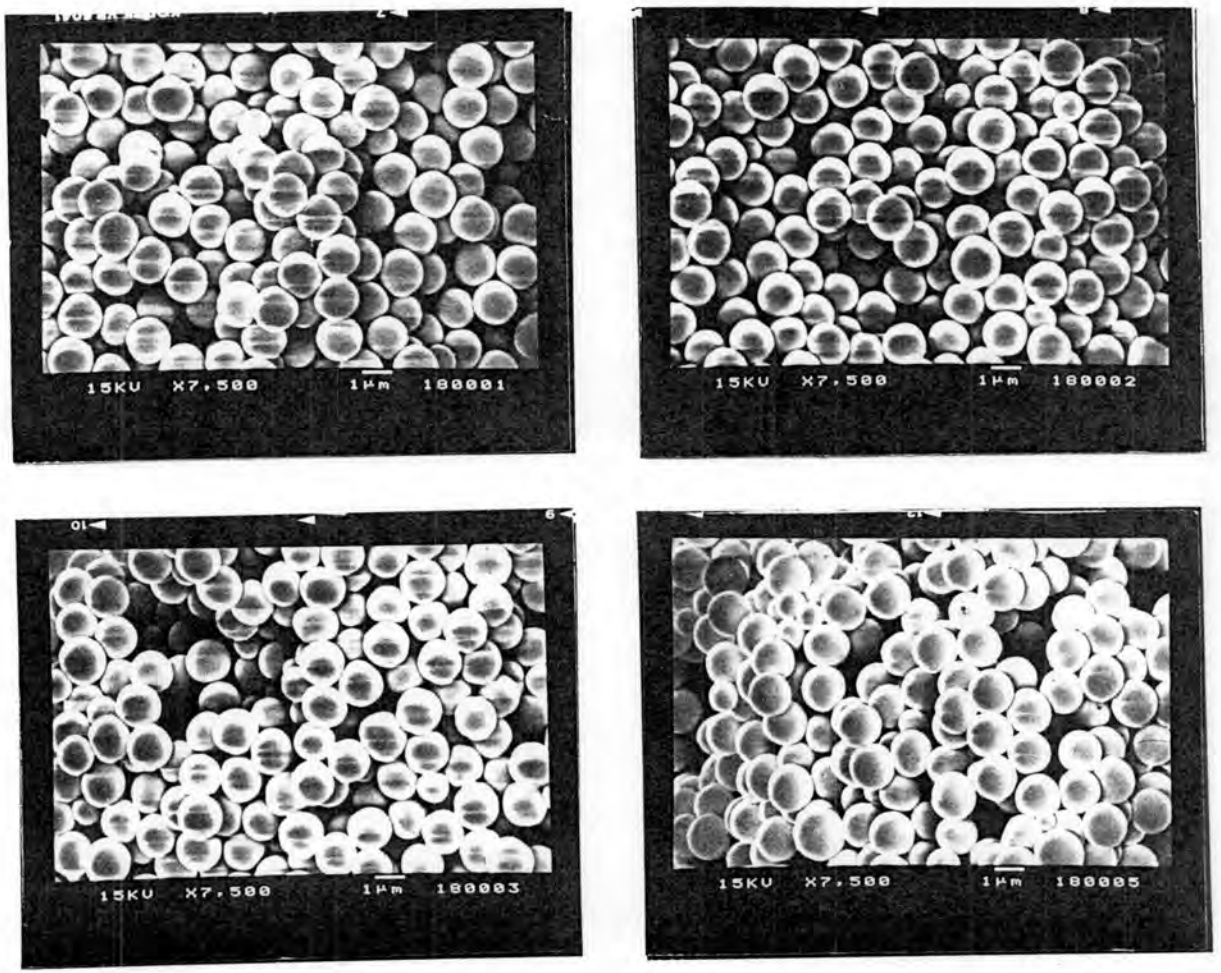

Figure 4.11 SEM micrographs for PSD measurement of poly(styrene-*co*-methyl methacrylate) controlled by 2 wt% PVP K-30

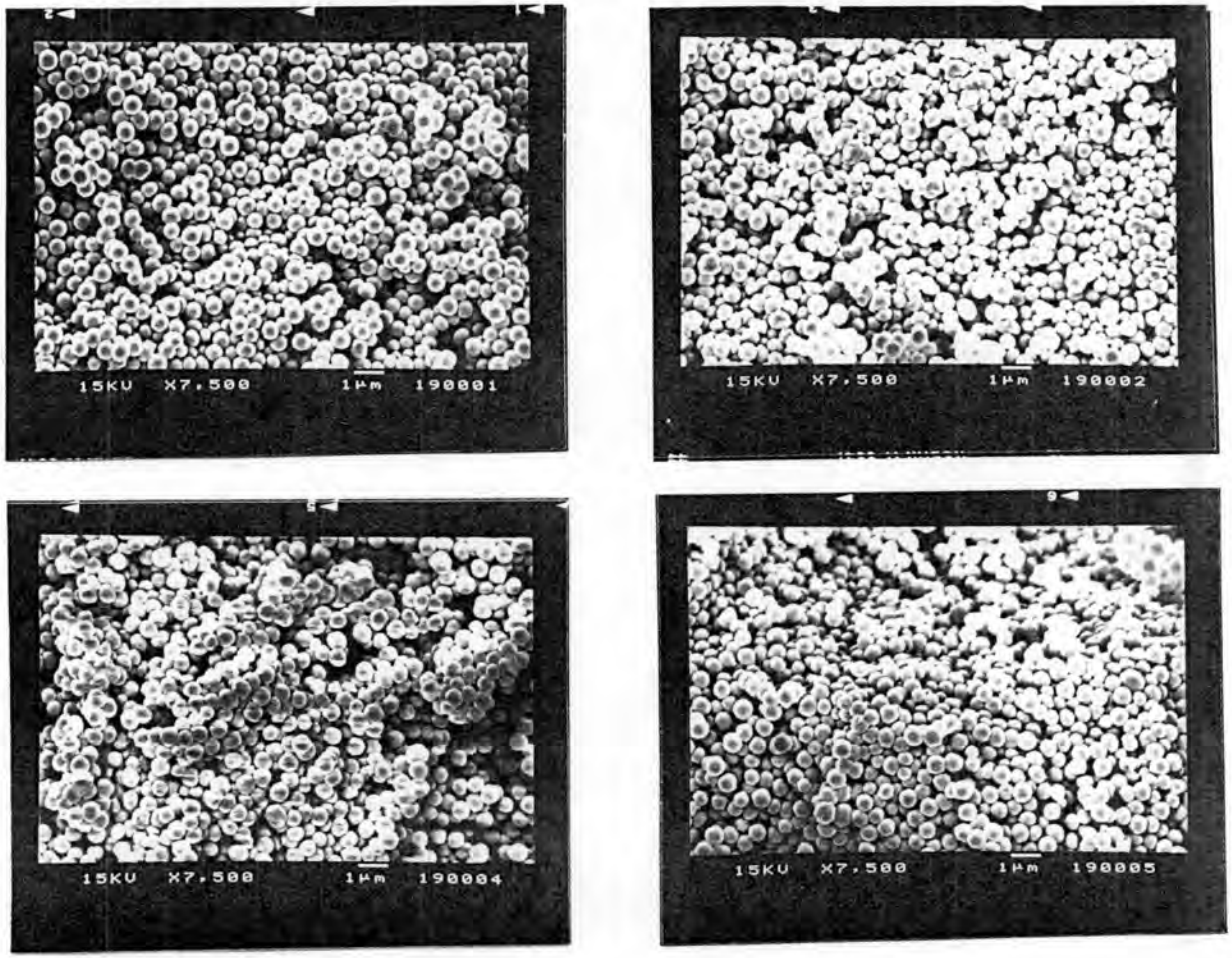

Figure 4.12 SEM micrographs for PSD measurement of poly(styrene-*co*-methyl methacrylate) controlled by 6 wt% PVP K-30

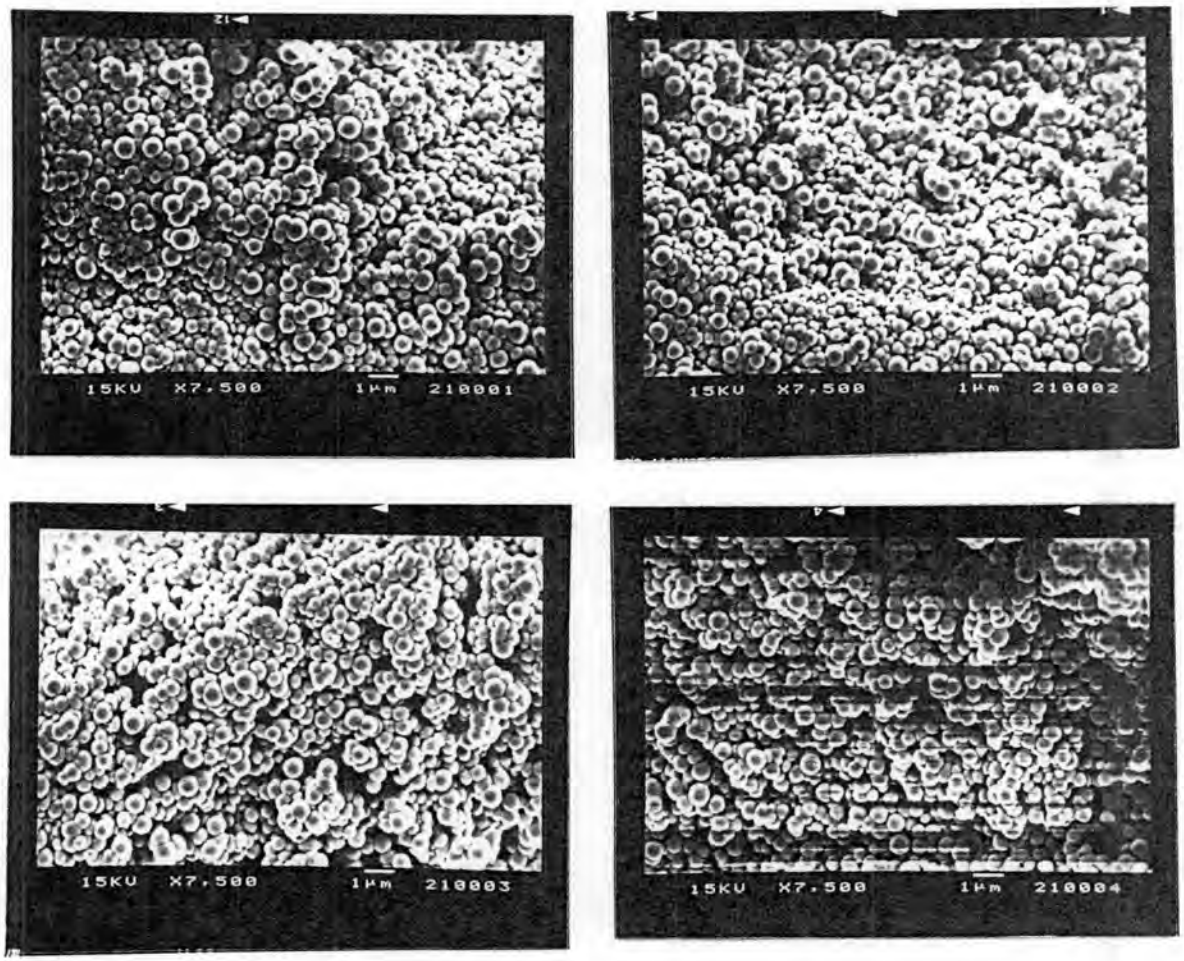

Figure 4.13 SEM micrographs for PSD measurement of poly(styrene-*co*-methyl methacrylate) controlled by 8 wt% PVP K-30

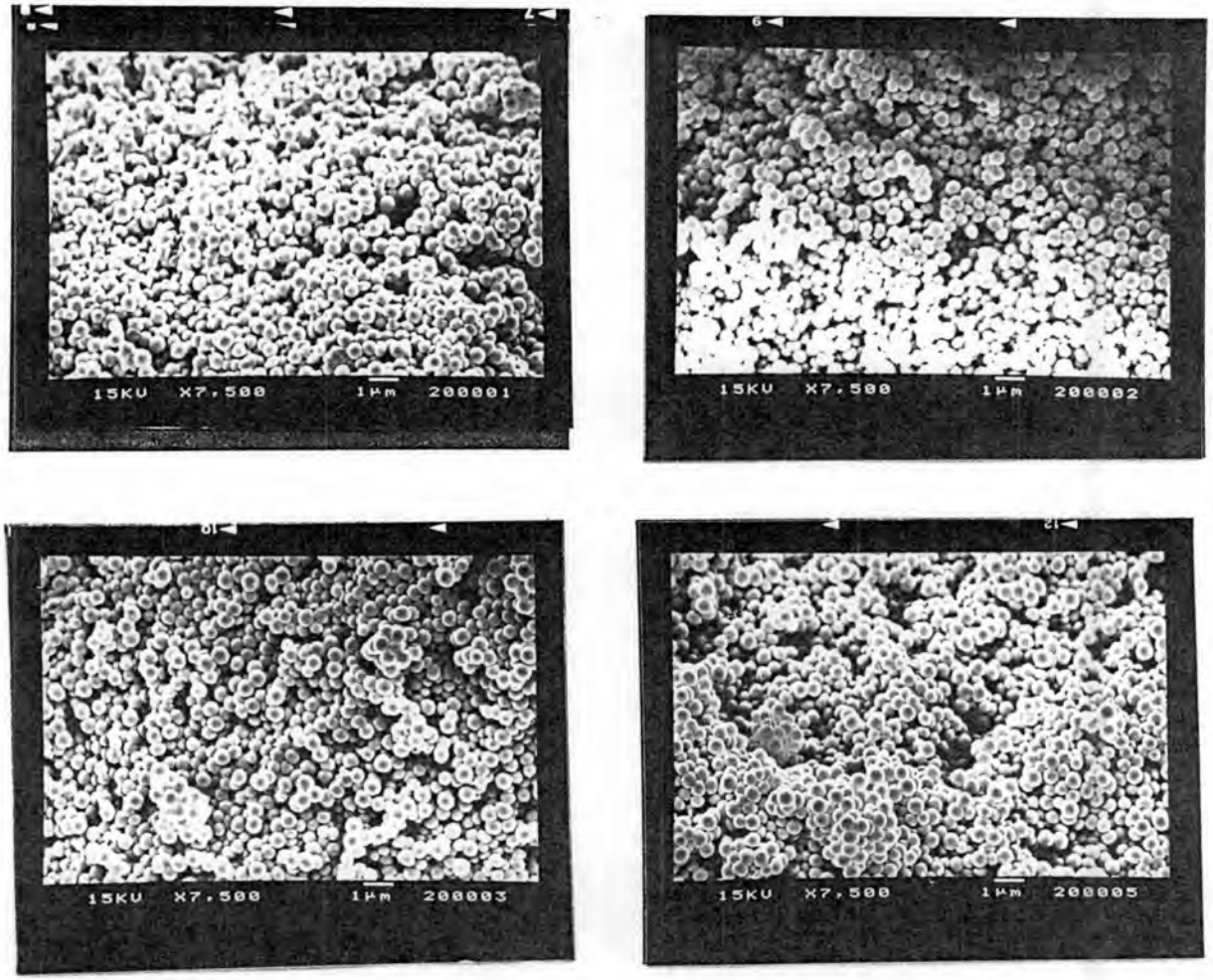

Figure 4.14 SEM micrographs for PSD measurement of poly(styrene-*co*-methyl methacrylate) controlled by 10 wt% PVP K-30

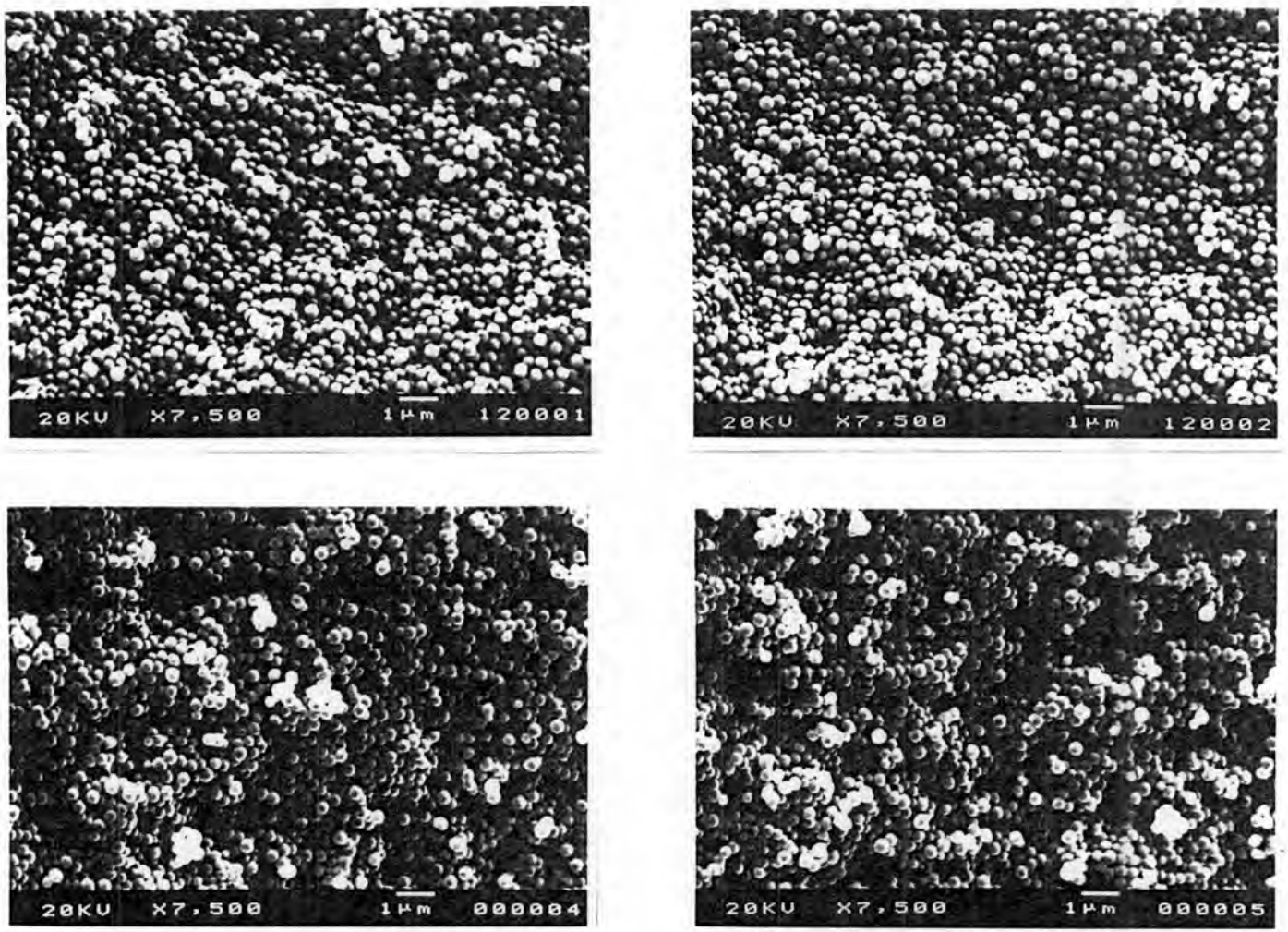

Figure 4.15 SEM micrographs for PSD measurement of poly(styrene-*co*-methyl methacrylate) controlled by 12 wt% PVP K-30

Table 4.1 Effects of Matrix Polymer Concentration on Dispersion Copolymerization of Styrene and Methyl Methacrylate[a]

No.	PVP (wt%)	$\overline{D}_n$[b,c] (μm)	CV[d,c] (%)	SD[e,c] (μm)	PSD[f]	$\overline{M}_n$	$\overline{M}_w$	$\overline{M}_w/\overline{M}_n$
P1[g]	0	-	-	-	-	-	-	-
P2	2	1.5	4.75	0.07	1.01	29884	79214	2.65
P3	6	0.6	8.72	0.05	1.02	119717	216576	1.81
P4	8	0.6	7.53	0.04	1.02	11619	37123	3.20
P5	10	0.5	8.59	0.05	1.02	39629	157979	3.99
P6	12	0.3	9.07	0.03	1.02	15087	34016	2.25

[a]Reaction time = 10 h, reaction temperature = 60°C

[b]Calculated diameter

[c]Determined by Scanning Electron Microscope from which each particle diameter is obtained from measurements on SEM and the $\overline{D}_n$

[d]Coefficient of variation of number-average size

[e]Standard Deviation [f]Particle size distribution [g]Agglomerated particles

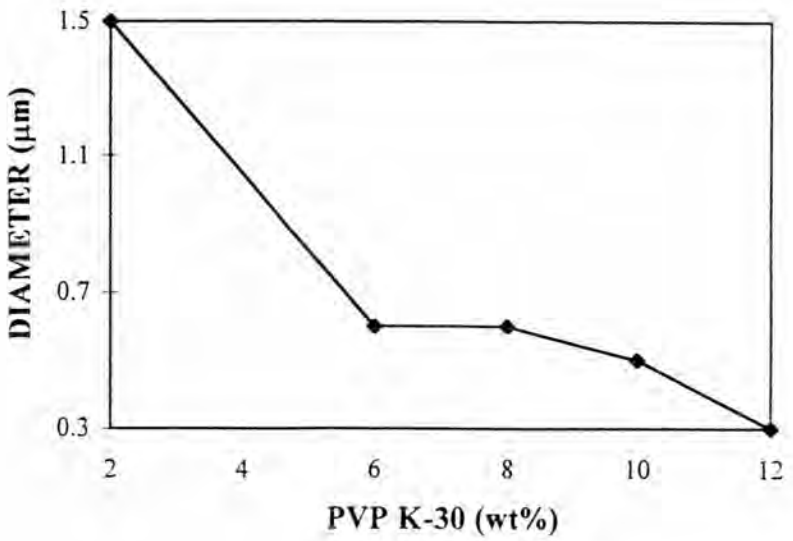

Figure 4.16 Effect of PVP K-30 concentration on the particle size of poly(styrene-*co*-methyl methacrylate)

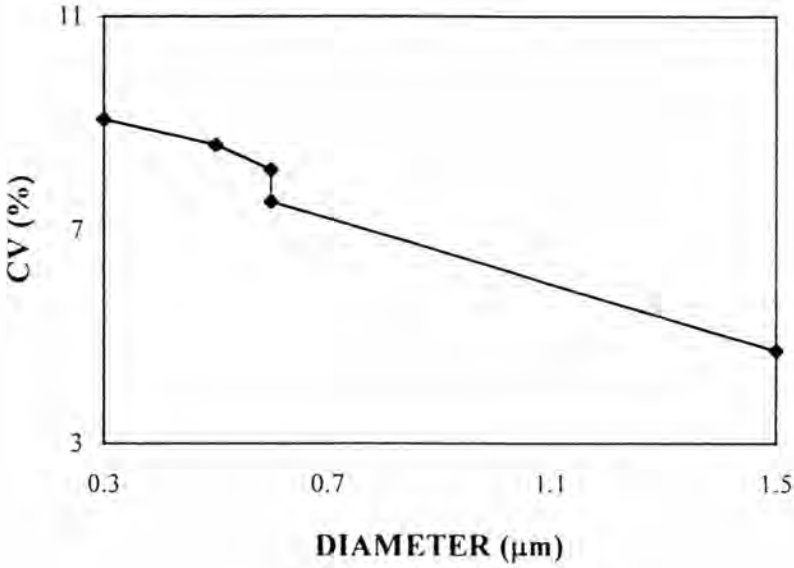

Figure 4.17 Relationship between the average particle size and CV of poly (styrene-*co*-methyl methacrylate) prepared by various PVP K-30 concentrations

4.1.2 Characterization of the Adsorption of the Matrix Polymer

4.1.2.1 The Physical Adsorption

The adsorption of the matrix polymer onto poly(styrene-*co*-methyl methacrylate) particles can be divided into two cases (40). The first case is physical adsorption of PVP, which is relatively weak and reversible by washing with methanol. The other case is anchoring adsorption of graft copolymer (PVP-g-Pdisp), which is an irreversible adsorption, it could not be desorbed by washing with methanol because the matrix polymer radicals continue to react (propagate, transfer, terminate) as part of the polymer particle. In this term, propagation is far more probable and would create polymers which would be chemically bound ('anchored') to the particles and thus be incapable of being desorbed. The anchoring adsorption gives a dead polymer which is terminated by a free radical in the continuous phase prior to adsorption. Both anchoring adsorptions are irreversible and remained on the particle surface after washing with methanol.

In this research, the polystyrene, poly(methyl methacrylate) and copolymer prepared by dispersion polymerization with PVP matrix polymer were isolated from the colloidal system by the washing with methanol. Initially, removal of physically adsorbed PVP by polymer particles were allowed to sediment for 2-3 days at the room temperature. After the PVP matrix polymer in the serum was decanted and then the polymer particles were allowed to sediment again. The occurrence of the physical adsorption of PVP on the surface of the polymer particles during the course of a dispersion polymerization was clearly confirmed by the above procedure.

It is important to distinguish between the stability of dispersions in practice and the ideal or thermodynamic concept of stability (41). An ideal stable dispersion is the one in which the particles undergo no mutual attraction but only short-range, elastic repulsions. They behave, in fact, rather like the molecules of an ideal gas. Simple calculations using the Stokes' law sedimentation rate and the Brownian diffusion rate make it quite clear that only under the most exceptional circumstances (usually a near identity in density between the particles and the liquid medium) will such ideal systems be free from settlement under gravity.

Since the particles of an ideal dispersion can definitely slip past one another very easily, settlement continues until a close-packed array of particles is achieved in the sediment. This close-packed array is mechanically quite strong. As a result, while such clay-like sediments are readily re-dispersed by gentle agitation over very long periods of time, they are extremely difficult to re-disperse rapidly by vigorous mechanical agitation. The formation of such an intractable sediment after prolonged storage constitutes an 'unstable' system in the eyes of the practical paint formulator or other technological users. For these applications it is preferable that the dispersions either do not settle at all, or at least settle to a soft and easily re-incorporated, open-textured sediment. This type of behaviour requires a critical degree of instability or non-ideality in the behaviour of the dispersion. When particles come together, they undergo an attraction of the order of a few kT, so that they flocculate rather than move freely past one another to pack into a close sediment; at the same time the strength of the attraction must be sufficiently small to enable the floc structure to be readily redispersed by mild agitation.

The structure of flocs formed from dispersions in which the particles form contacts of finite attractive energy, has been discussed by Vold (42). Interestingly, it is found that the stronger the attraction between the particles (i.e. the more energy that would be available if the system formed a compact floc), the more open-textured is the floc which is actually formed. Negligible rearrangement of the primary floc structure is possible in these cases because of the larger activation energies associated with such processes. Thus, the phase volume of the most open-textured flocs may be as low as a few percent, compared with a value of about 60% for the phase volume of the closely-compacted sediment from an ideal stable dispersion.

4.1.2.2 The Anchoring Adsorption

When the cleaned copolymer particles were dried. The PVP segments of graft copolymer could be analyzed by infrared spectrophotometry. It is confirmed by comparing the spectrum to the reference peak of the standard PVP and standard polystyrene.

The FTIR spectra of PVP K-30 standard is shown in Figure 4.18. The vibration at 1666 cm^{-1} indicates C=O group. In spectrum of poly(methyl methacrylate) prepared by dispersion polymerization, the characteristic adsorption peaks of C=O group of poly(methyl methacrylate) and PVP K-30 overlap at 1700-1800 cm^{-1}, as shown in Figure 4.19. The FTIR spectra of polystyrene standard (43) are shown in Figures 4.21, and 4.22. In Figure 4.21, the vibration bands at 1940, 1870, 1800, and 1740 cm^{-1} indicate monosubstituted aromatic rings. The band at 1600 cm^{-1} indicate the

aromatic ring 'breathing' vibration. Besides the band at 1600 cm^{-1} and the bands of monosubstituted aromatic rings, there are no additional bands indicative of other functional groups especially the C=O group. The FTIR spectrum of polystyrene prepared by dispersion polymerization in the presence of PVP is shown in Figure 4.23. It is seen that the additional peak of C=O group at 1684 cm^{-1} in the spectrum of polystyrene prepared by dispersion polymerization indicates the residual PVP in the polymer. The above results clearly prove the importance of the anchoring adsorption of the PVP. Therefore, it can be concluded that the adsorption of the matrix polymer on poly(styrene-*co*-methyl methacrylate) particles can be explained by both a physical adsorption and anchoring adsorption from which the latter case is an irreversible adsorption and the matrix polymer could not be desorbed by a simple washing with methanol.

4.1.3 The Average Molecular Weights and Molecular Weight Distribution of Poly(Styrene-*co*-Methyl Methacrylate)

The effects of PVP K-30 concentration on the average molecular weights and molecular weight distribution of poly(styrene-*co*-methyl methacrylate) are also investigated. The values of Q-Factor (weight of the polymer per angstrom of backbone length) (QF = 1) and Mark-Houwink constants (α = 0.76, k = 0.00716) (44) were used to interpret all the copolymer chromatograms. Before the analysis of the copolymer, the polystyrene standards with the average molecular weights of 3,160,000, 156,000, 28,500, and 2,950 were dissolved in $CHCl_3$ eluent to determine the retention times. All chromatograms of polystyrene standard are shown in

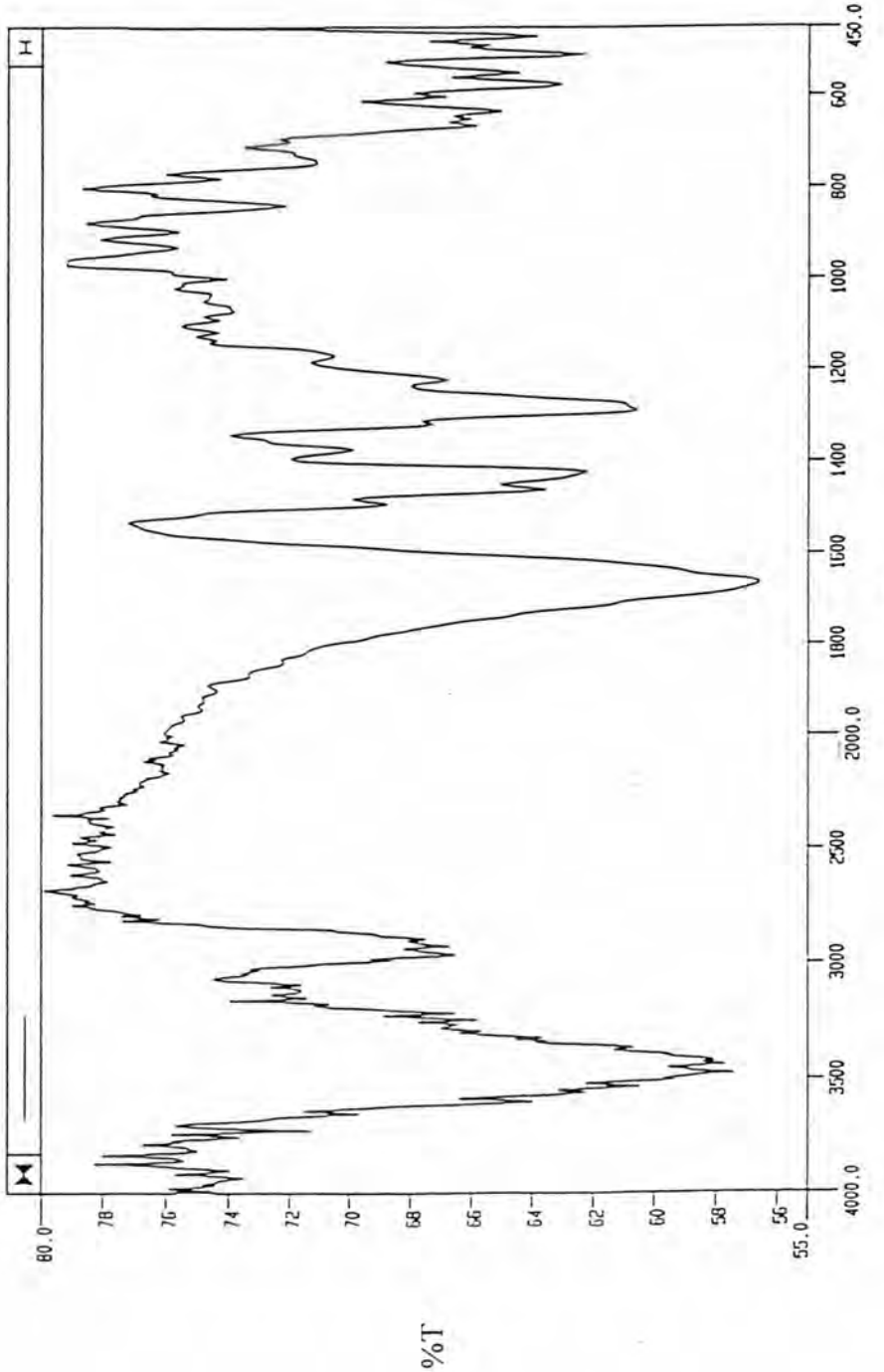

Figure 4.18 FTIR spectra of poly(N-vinyl pyrrolidone)

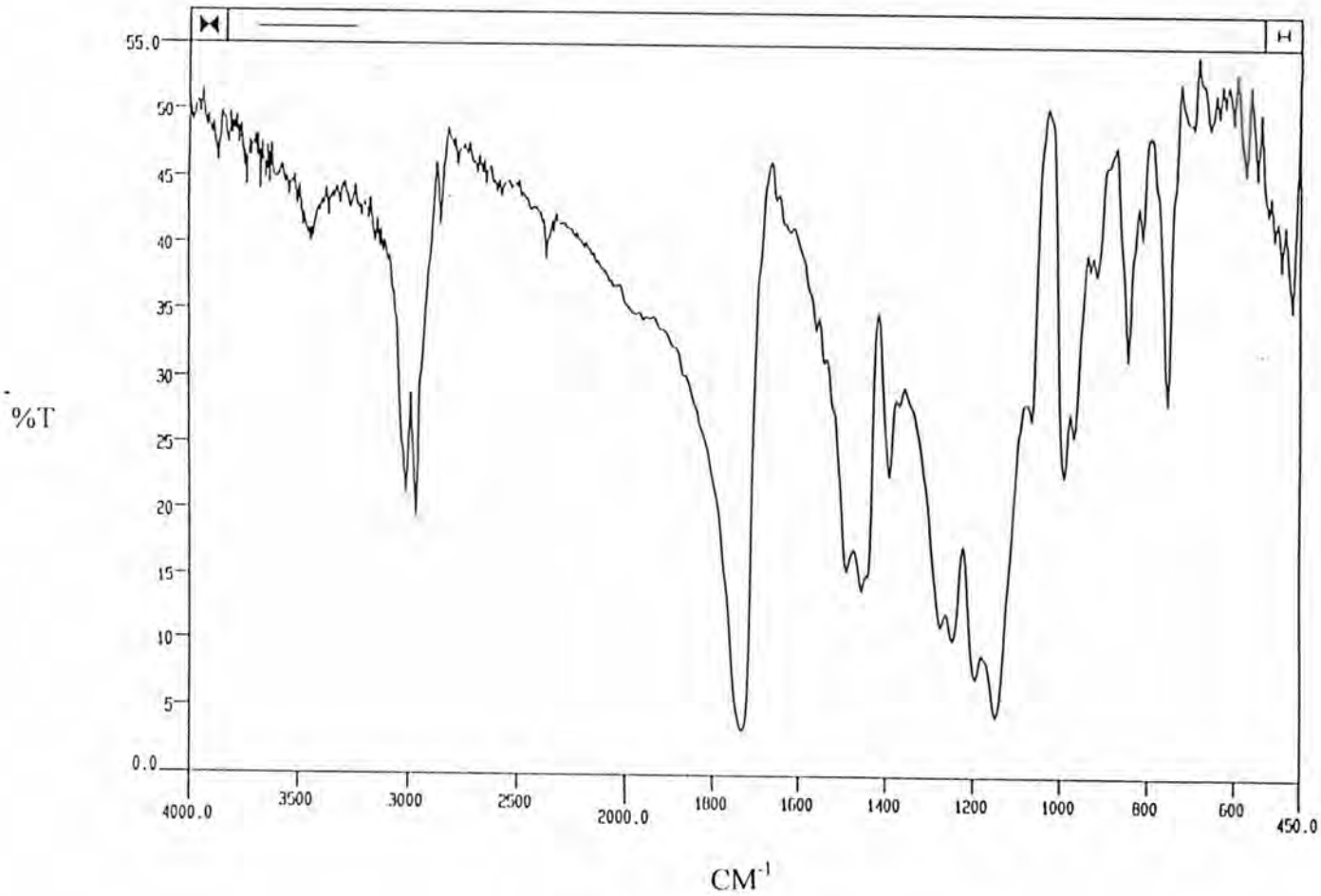

Figure 4.19 FTIR spectra of poly(methyl methacrylate) prepared by dispersion polymerization

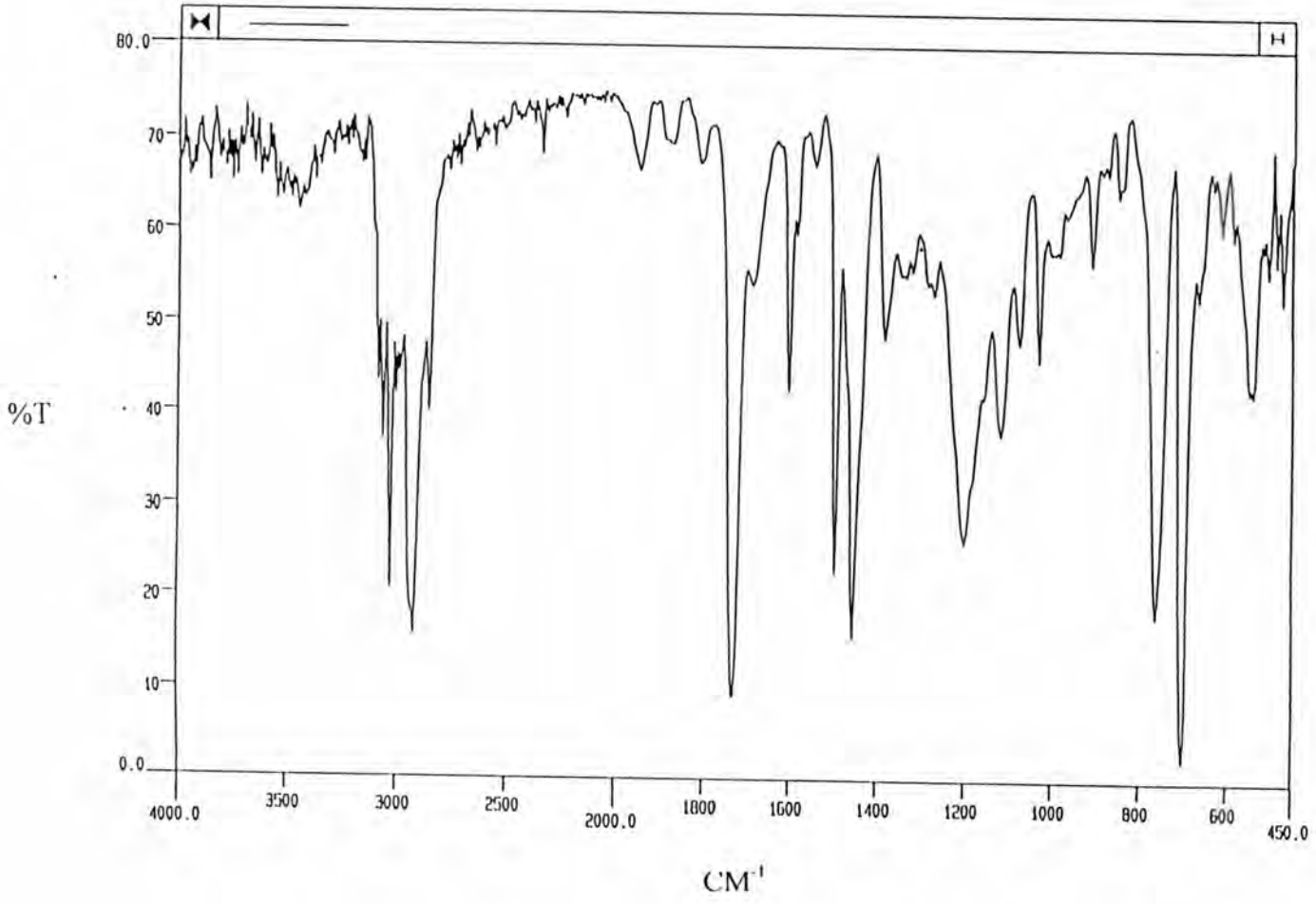

Figure 4.20 FTIR spectra of poly(styrene-*co*-methyl methacrylate) prepared by dispersion polymerization

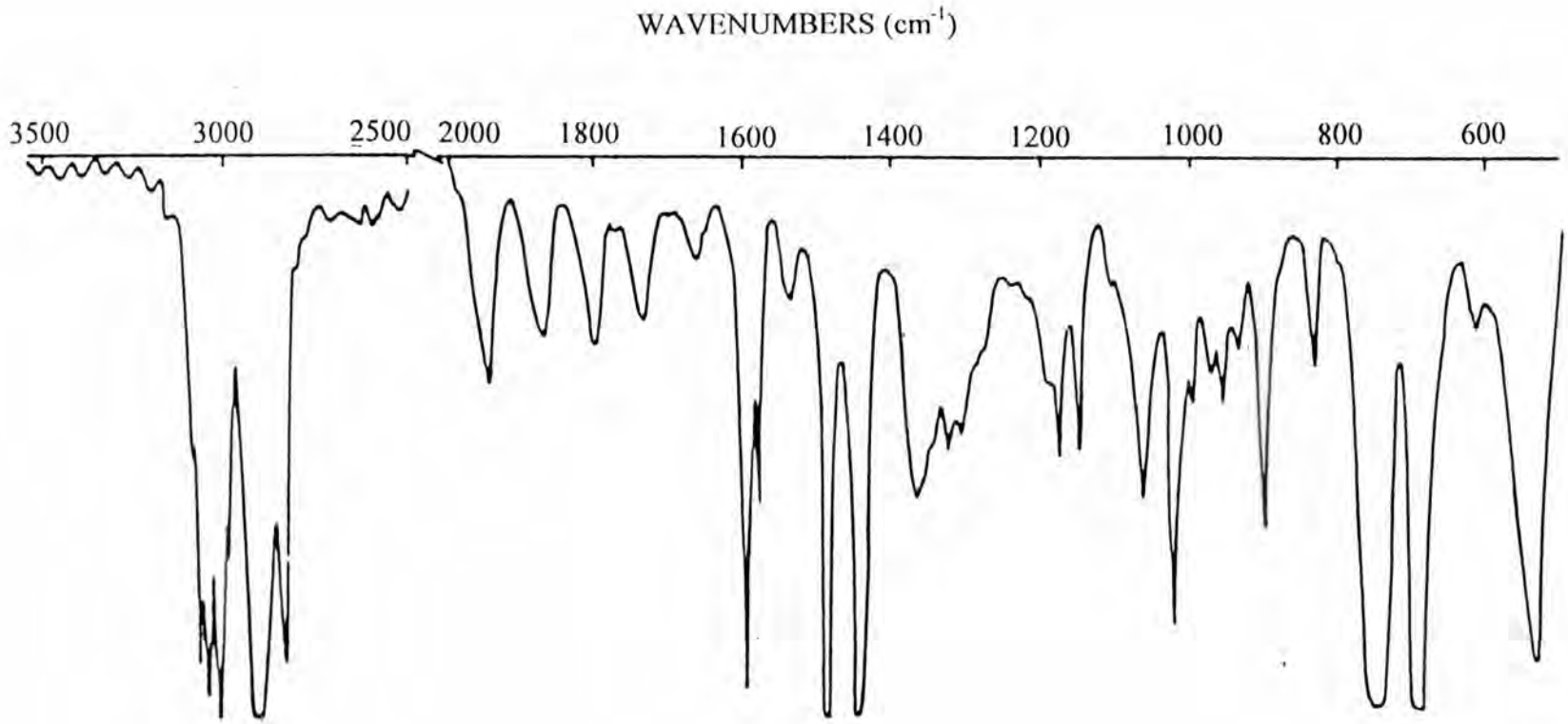

Figure 4.21 FTIR spectra of polystyrene standard (I)

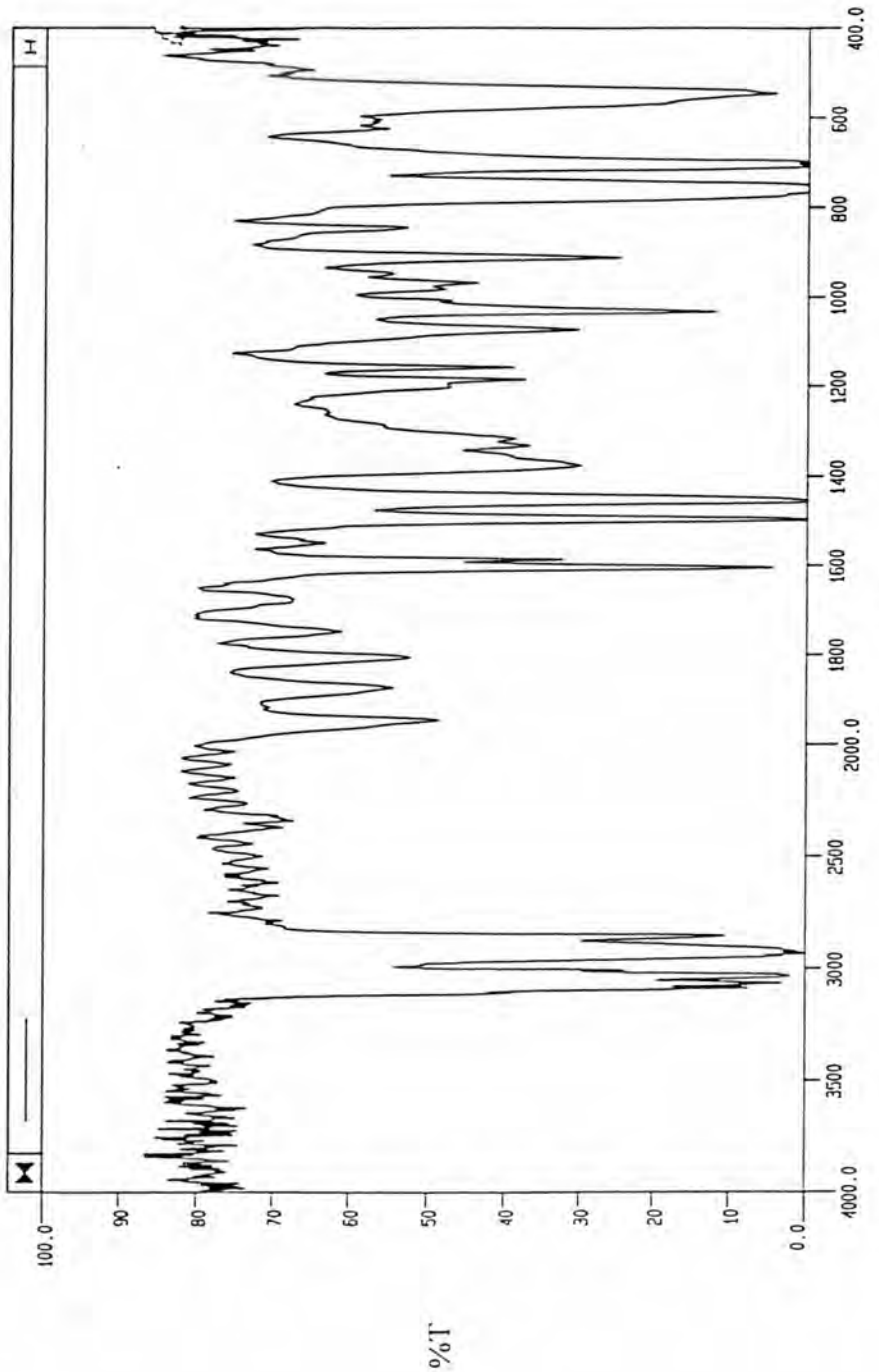

Figure 4.22 FTIR spectra of polystyrene standard (II)

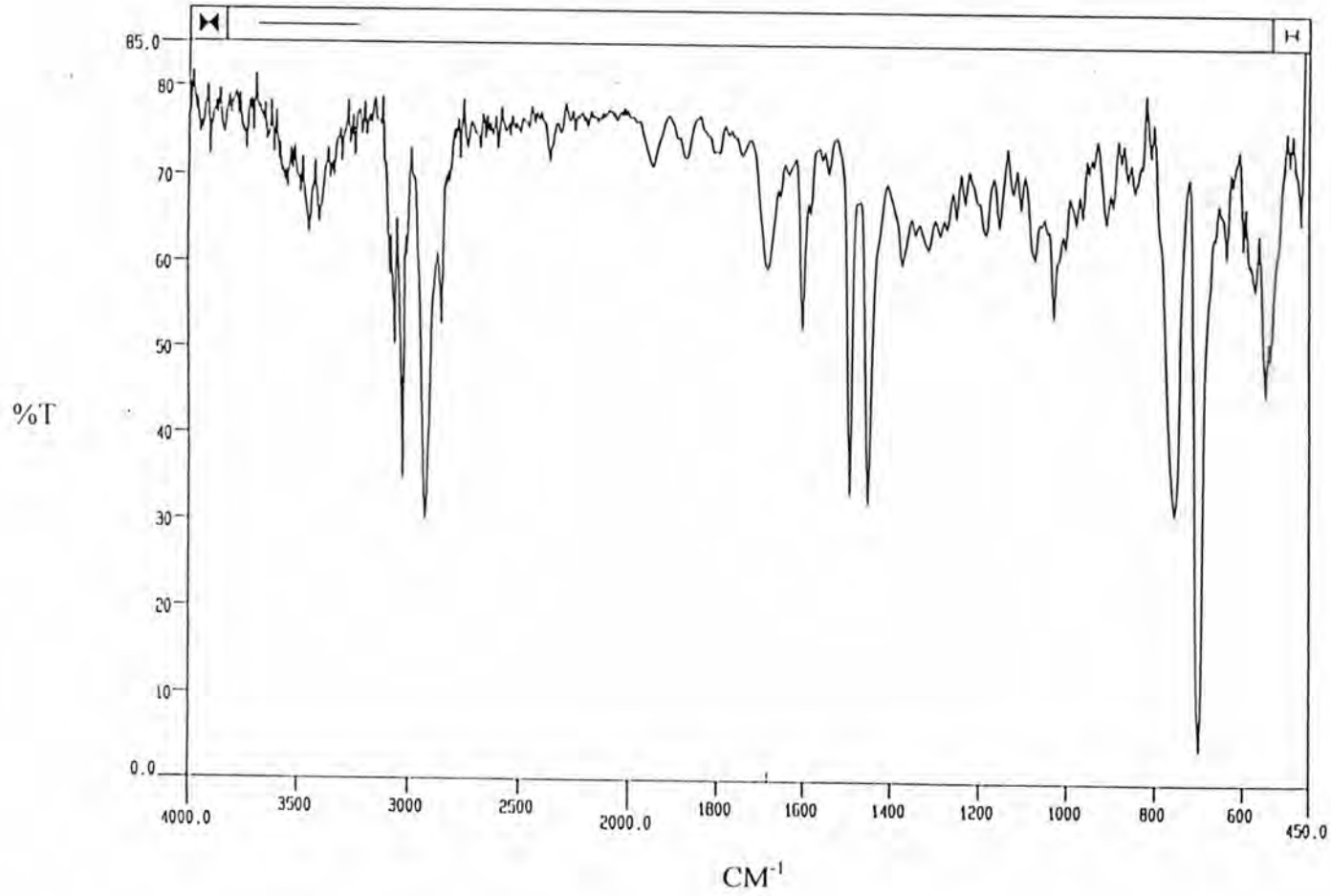

Figure 4.23 FTIR spectra of polystyrene prepared by dispersion polymerization

Appendice E-1 to E-4. The calibration curve of Shodex polystyrene standard S-66.0 is shown in Figure 4.24. The calibration curve is linear in molecular weight range from about 2,950 to 3,160,000. The average molecular weights and molecular weight distribution of poly(styrene-*co*-methyl methacrylate) were measured after the setting of a basic calculation of parameters and the retention times of polystyrene standard were completed. The data of average molecular weights and molecular weight distribution of poly(styrene-*co*-methyl methacrylate) with different PVP concentrations are shown in Table 4.1 and Appendice E-5 to E-9, respectively. When the concentration of PVP K-30 was further increased to 6 wt%, the copolymer particles have a higher molecular weight and narrower molecular weight distribution as shown in Figures 4.25 and 4.26. The GPC chromatograph of poly(styrene-*co*-methyl methacrylate) with 6 wt% PVP K-30 is shown in Figure 4.27. Further increase in PVP K-30 concentration to 8 wt% resulted in minimum average molecular weights and a broader molecular weight distribution. With the use of PVP K-30 concentration of 10 wt%, the average molecular weights increased rapidly, their molecular weight distribution was broad. However, the copolymer particles have a lower molecular weight again when the system was polymerized with PVP K-30 concentration of 12 wt% and narrower molecular weight distribution but broader than the use of PVP K-30 concentration of 6 wt%.

In this group of experiments, values of $\overline{M}_w/\overline{M}_n$ are in the range 1.81-3.99 among which the narrowest molecular weight distribution ($\overline{M}_w/\overline{M}_n = 1.81$) was found in the polymerizing system with PVP K-30 concentration of 6 wt% and the broadest molecular weight distribution ($\overline{M}_w/\overline{M}_n = 3.99$) was found in the polymerizing system

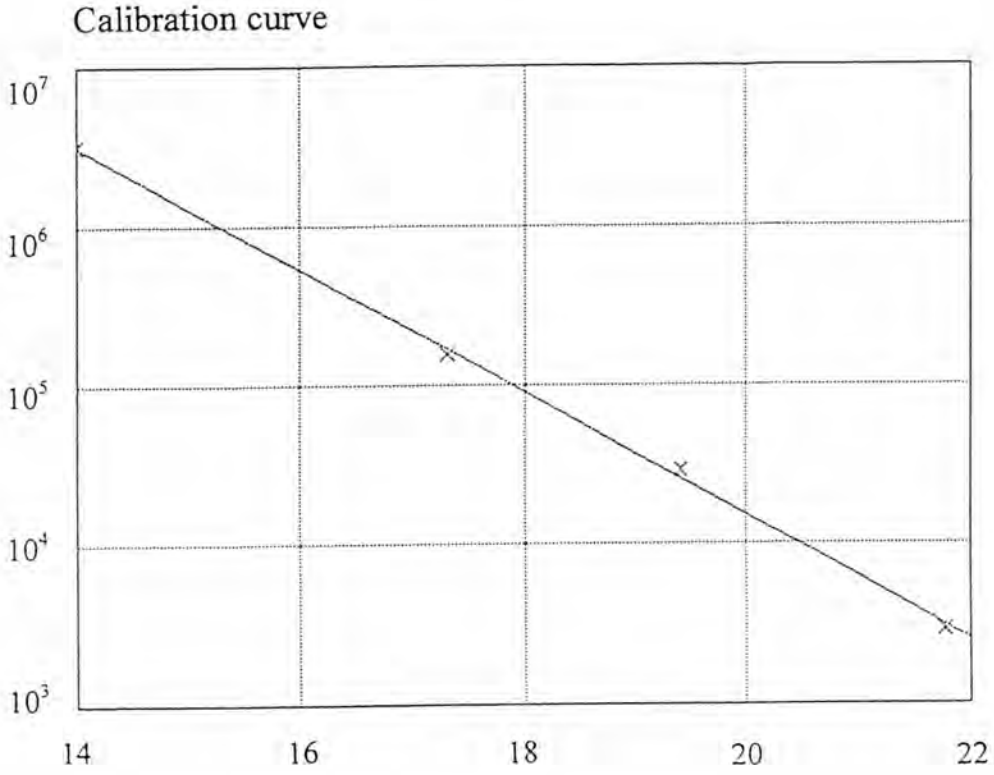

Figure 4.24 Calibration curve of Shodex polystyrene standard S-66.0

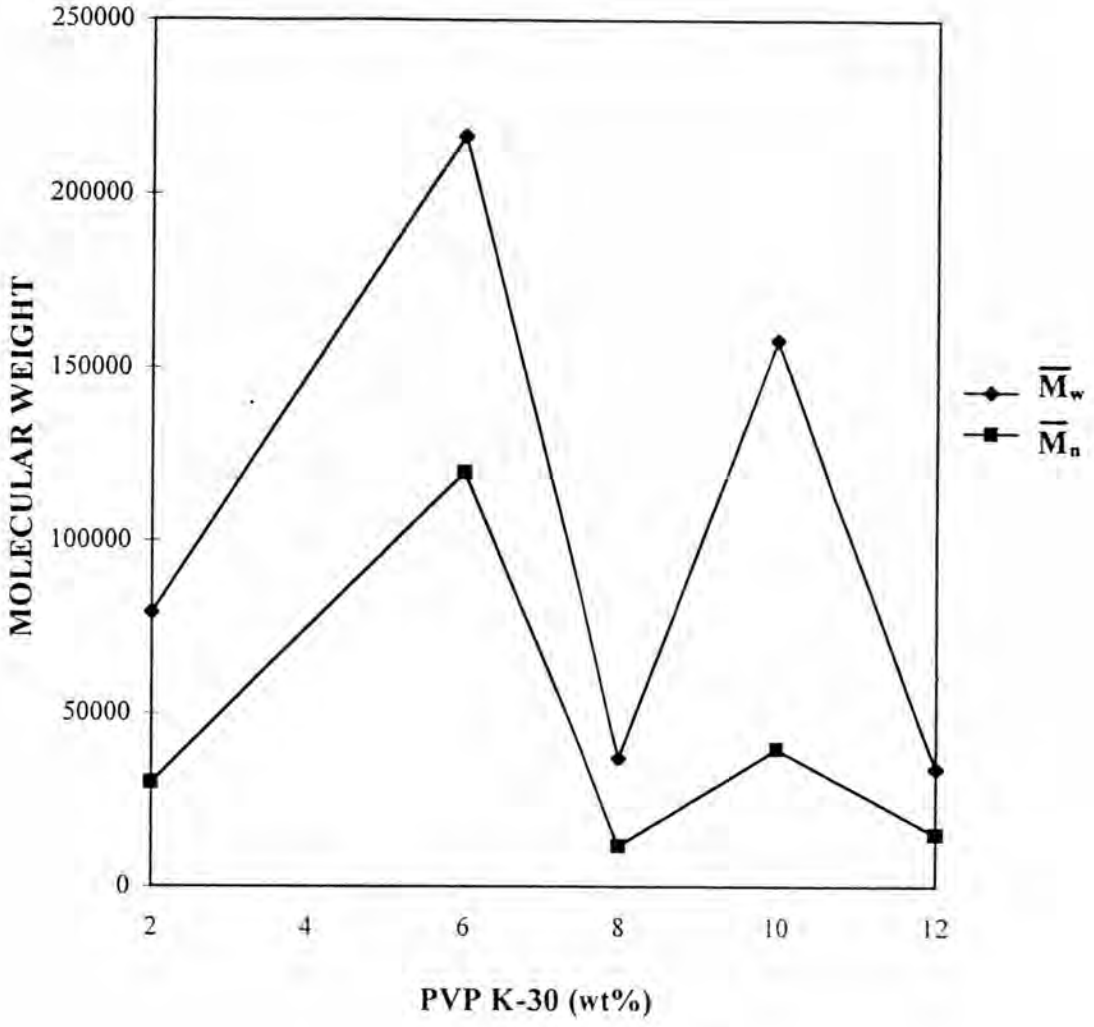

Figure 4.25 Effect of PVP K-30 concentration on the average molecular weights of poly(styrene-*co*-methyl methacrylate)

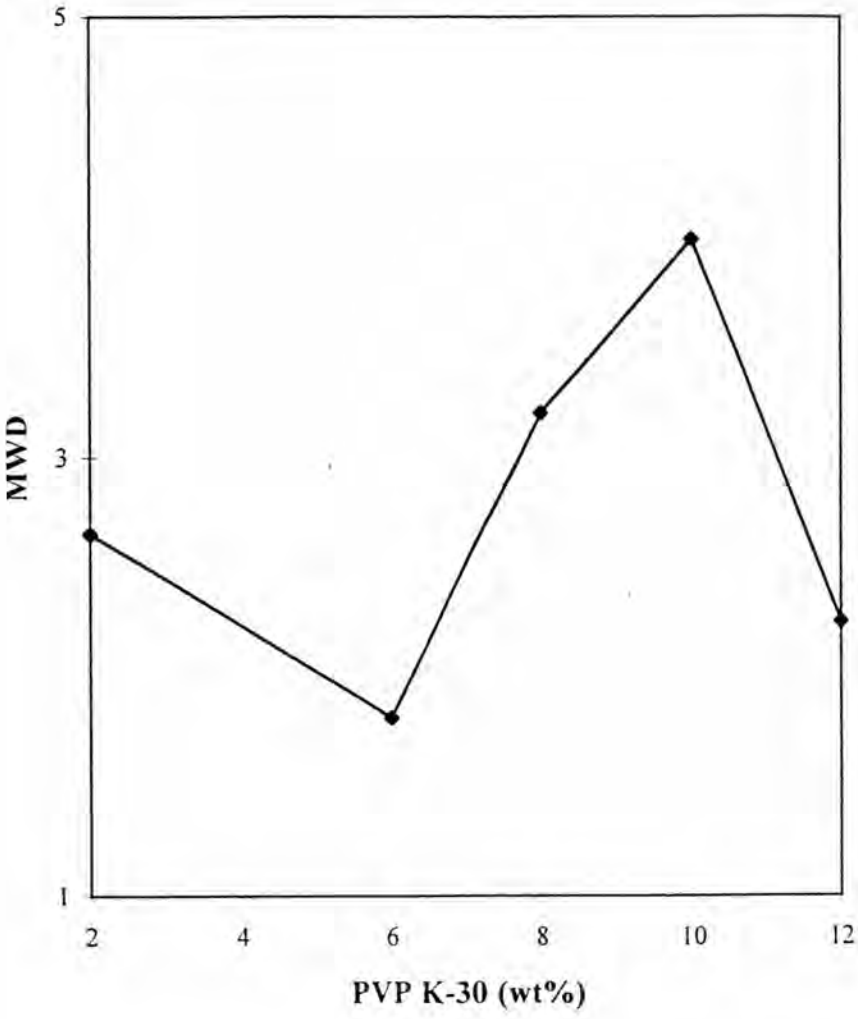

Figure 4.26 The curve of MWD of poly(styrene-*co*-methyl methacrylate) for various PVP concentrations

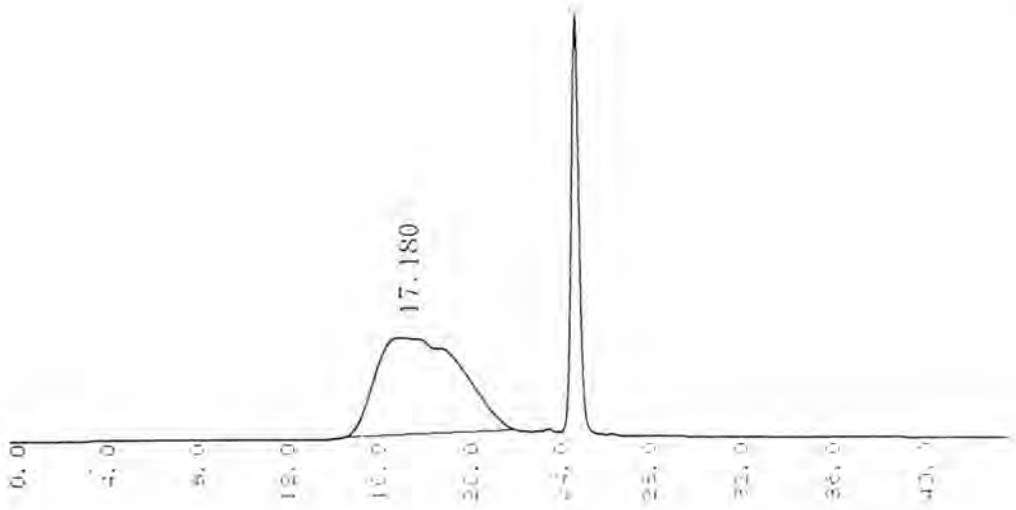

Peak information	Time (min)	Mol. size	Height
start	14.85	1478767	26
top	17.18	185661	5753
end	18.85	41979	5015

Number-A.M.W.	$\overline{M}_n$ =	119717	Weight-A.M.W.	$\overline{M}_w$ =	216576
z-A.M.W.	$\overline{M}_Z$ =	376382	Visc-A.M.W.	$\overline{M}_v$ =	201178
Dispersity	$\overline{M}_w/\overline{M}_n$ =	1.80907	Dispersity	$\overline{M}_z/\overline{M}_w$ =	1.73788
Dispersity	$\overline{M}_v/\overline{M}_n$ =	1.68045	I. Viscosity	I. VISC =	6.84814

Figure 4.27 The GPC chromatograph of the copolymer controlled by 6 wt% PVP

with PVP K-30 concentration of 10 wt%. Table 4.1 summarizes the data obtained in this section of experiments.

At 12 wt% PVP K-30, the copolymer has a lowest average molecular weight because the viscosity in the polymerizing system is high. High viscosity affects the termination process much more than the propagation process, because termination involves the ending reaction of two large polymer radicals, while propagation involves the adding reaction of small monomer molecules and the larger radicals. Therefore, the quantity $k_p/k_t^{1/2}$ in eq 4.8 increases leading to an increase in the rate of polymerization. The overall rate of dispersion polymerization is given by

$$R_p = \alpha C_m k_p (\nu R_i/k_t)^{1/2} \qquad (4.8)$$

where C_m = the overall monomer concentration

ν = volume fraction

The kinetic chain length (ν) of a radical polymerization is given by

$$\nu = R_p/R_i = R_p/R_t \qquad (4.9)$$

Since the rate constants for all the propagation steps are the same, one can express the polymerization rate by

$$R_p = k_p[M\bullet][M] \qquad (4.10)$$

where [M] = the monomer concentration

$[M\bullet]$ = the total concentration of all chain radicals, that is, all radicals of size M1• and larger

The rate of initiation is defined as

$$R_i = 2k_t[M\bullet]^2 \tag{4.11}$$

Combination of Eqs. 4.9, 4.10, and 4.11 yields

$$\nu = \frac{k_p[M]}{2k_t[M\bullet]} \tag{4.12}$$

$$\nu = \frac{k_p^2[M]^2}{2k_tR_p} \tag{4.13}$$

From equation 4.13, shows the kinetic chain length is inversely dependent on the rate of polymerization.

Equation 4.8 can be substituted into Eq. 4.13 to yield

$$\nu = \frac{k_pC_m}{\overline{2\alpha\nu R_ik_t}^{1/2}} \tag{4.14}$$

Therefore, increasing of the rate of polymerization means a decrease in the average molecular weights.

4.2 The Effect of Ethanol-to-Water Ratios on

4.2.1 The Particle Size and Particle Size Distribution of Poly(Styrene-*co*-Methyl Methacrylate)

Another variable that has a considerable influence on the particle sizes and size distribution of poly(styrene-*co*-methyl methacrylate) prepared by dispersion polymerization is the solvency of the reaction medium. The solvency of the reaction medium controls the critical chain length of precipitated oligomers which effects on critical molecular weight and the size of the copolymer particles (45). The experiments were carried out in polar solvents of ethanol/water mixture for controlling the formation of polymeric microspheres. The solvency of the polymerization mixture can be fine tuned by adjustments in the concentration of water.

Table 4.2 presents the data of the effects of ethanol/water ratio on dispersion copolymerization of styrene and methyl methacrylate monomers. The SEM photographs of microspheres prepared with different ethanol/water ratios in the presence of 8 wt% PVP K-30 are given in Figures 4.28-4.31. Figures 4.32-4.35 show SEM photographs, for particle size distribution measurement of poly(styrene-*co*-methyl methacrylate) controlled by 8 wt% PVP K-30 in different ethanol/water ratios. Figures 4.36-4.41 show SEM photographs of microspheres prepared with different ethanol/water ratios in the presence of 6 wt% PVP K-30. Figures 4.42-4.47 show SEM photographs, which indicate the particle size distribution controlled by 6 wt% PVP K-30 in different ethanol/water ratios.

For pure ethanol, the copolymers have a largest size and broad size distribution because the pure ethanol is a very good solvent for the oligomer radicals;

(styrene-methyl methacrylate) the formation of the critical chain length of the oligomer radicals is very long resulting the formation of particle nuclei from these growing oligomer chains is self-nucleation mechanism. However, some oligomer radical chains have a shorter chain resulting from the aggregative mechanism, the smaller particle size was thus produced. These various particle sizes led to a broad particle size distribution. At 100% water (δ_p = 16 $(MPa)^{1/2}$) (46), the copolymer containing more styrene (δ_p = 1.0 $(MPa)^{1/2}$) monomers than methyl methacrylate (δ = 18 $(MPa)^{1/2}$) monomer ($\Delta\delta_{pSTY\text{-}H2O}$ is large than $\Delta\delta_{MMA\text{-}H2O}$). The critical chain length of oligomer radical chains in water is shorter than in ethanol. So, in 100% water, the copolymer particle size becames smaller. Besides, the copolymers have a broad size distribution because pure water (δ_T = 47.9 $(MPa)^{1/2}$) acts as a poor solvent for the PVP matrix polymer (δ_T = 25.6 $(MPa)^{1/2}$). The PVP matrix polymer chains entangle or aggregate to become a coiled form in the poor solvent. The particle size distribution is thereby controlled by the excluded free volume in solution of the matrix polymer, the broad particle size distribution of the copolymer was consequently obtained.

The copolymer particles prepared in the solvent mixture of ethanol and water have a narrower size distribution. This results can be explained by the phenomenon of the free volume in solution in good solvent as shown in Figure 4.1-a. The copolymer prepared in 90/10 ethanol/water have a narrower size distribution than that in 80/20 ethanol/water, and 70/30 ethanol/water gave a broader size distribution than that in 80/20 ethanol/water.

The copolymer prepared in 60/40 ethanol/water have a broadest size distribution because the poor solvent for matrix polymer was increased, the PVP

chains entangle and precipitate in the poor solvent resulting in the morphology of the PVP matrix polymer as a coil form and give bigger solution free volume within the matrix polymer chains. The particle size distribution is additionally controlled by the excluded free volume in solution of the matrix polymer. Therefore, the broad particle size distribution was found as shown in Figure 4.1-b. When using a good solvent for matrix polymer in the reaction medium the resulting particle size distribution is narrow because the morphology of the matrix polymer is in an expanded chain as shown in Figure 4.1-a. More importantly, when the water content was increased, the high generation rate of nuclei and the high adsorption rate of stabilizer would make it more difficult for existing particles to capture all the nuclei and aggregates from the continuous phase before they become stable particles. Therefore, the particle formation stage would be extended, resulting in broader size distributions (47).

The particle sizes was shown to be dependent on the polarity of the reaction medium. Obviously, below 80% ethanol (increasing the water content), the particle sizes became smaller. An increase of the water content resulted in polymers with broader size distributions, as discussed previously. Figure 4.48 shows the variation in particle size data for poly(styrene-*co*-methyl methacrylate) carried out in mixed solvents from 10% to 30% water in presence of 8 wt% PVP K-30 at 60°C and 6 wt% PVP K-30 at 70°C.

The higher the polarity of the reaction medium, the smaller the average size at a constant matrix polymer concentration because water is a poorer solvent for poly (styrene-*co*-methyl methacrylate) than ethanol, the critical chain length of precipitated oligomers decreased while the rate of adsorption of the matrix polymer onto the nuclei

and the rate of nuclei formation increases with increasing water content. Accordingly, the above behavior might affect the decrease of free volume in the polymeric solution that controls particle sizes of the copolymer when increasing water content.

The variation of average particle size with the average solubility parameter of the dispersion medium is shown in Figure 4.49. The average solubility parameters of the dispersion medium were calculated as shown in eq 4.15 (48).

$$\delta_m = (\chi_a\delta_a^2 + \chi_w\delta_w^2)^{1/2} \qquad (4.15)$$

where χ_a, χ_w = the volume fraction of alcohol and water

δ_m, δ_a, and δ_w = the solubility parameters of the dispersion medium, alcohol, and water, respectively.

The volume fractions of alcohol and water were calculated as shown in eq. 4.16 and 4.17.

$$\chi_a = \frac{\text{the volume of alcohol}}{\text{the volume of the solvent mixture}} \qquad (4.16)$$

$$\chi_w = \frac{\text{the volume of water}}{\text{the volume of the solvent mixture}} \qquad (4.17)$$

From Figure 4.49, it can be explained that the average particle size decreased with increasing solubility parameter of the reaction medium. Therefore, it can be concluded that there is a certain relation between the polarity of the dispersion medium and the average particle size. Increasing the polarity of dispersion medium increases the solubility parameter of dispersion medium that affects the average particle size as discussed previously.

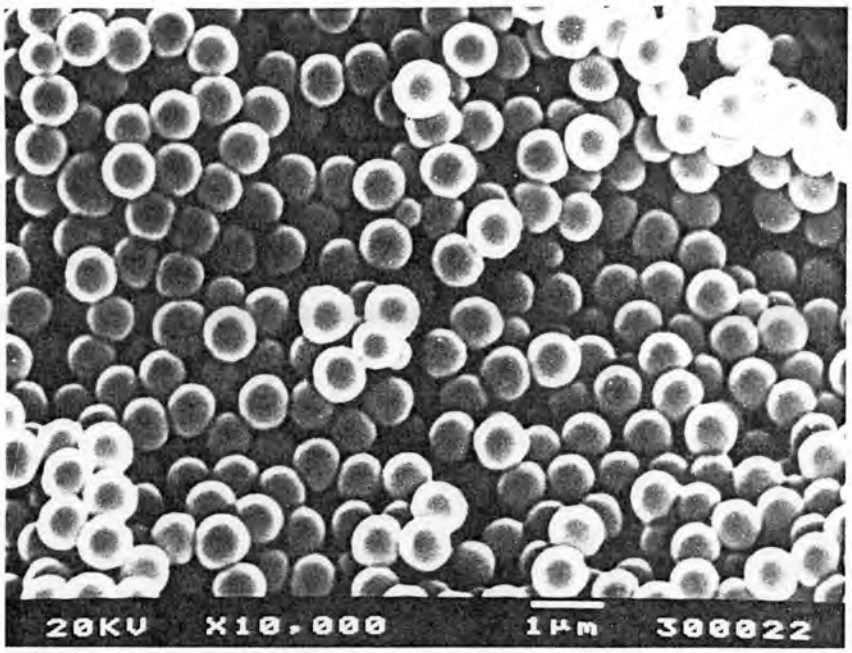

Figure 4.28 SEM micrograph of poly(styrene-*co*-methyl methacrylate) synthesized in 90/10 EtOH/H_2O controlled by 8 wt% PVP K-30

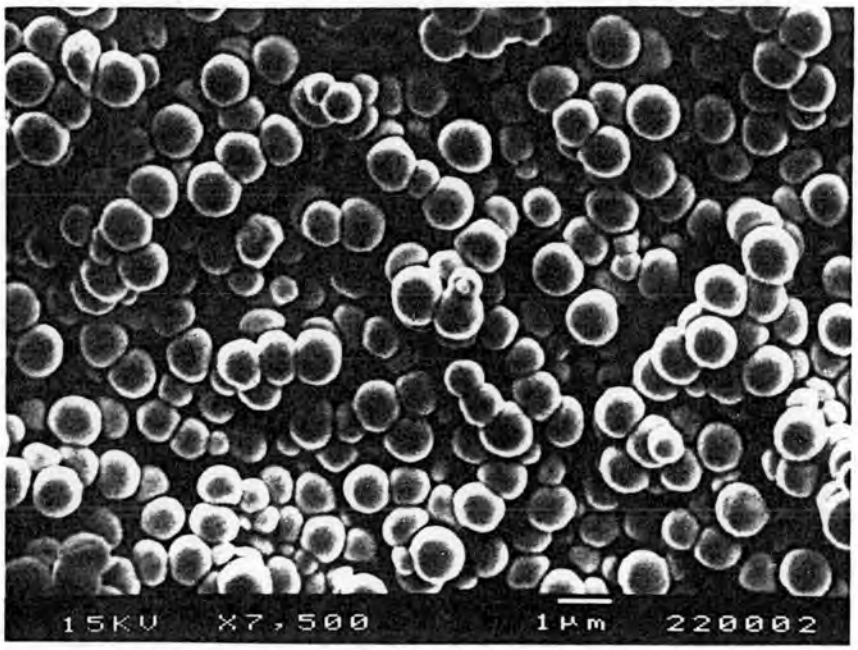

Figure 4.29 SEM micrograph of poly(styrene-*co*-methyl methacrylate) synthesized in 80/20 EtOH/H_2O controlled by 8 wt% PVP K-30

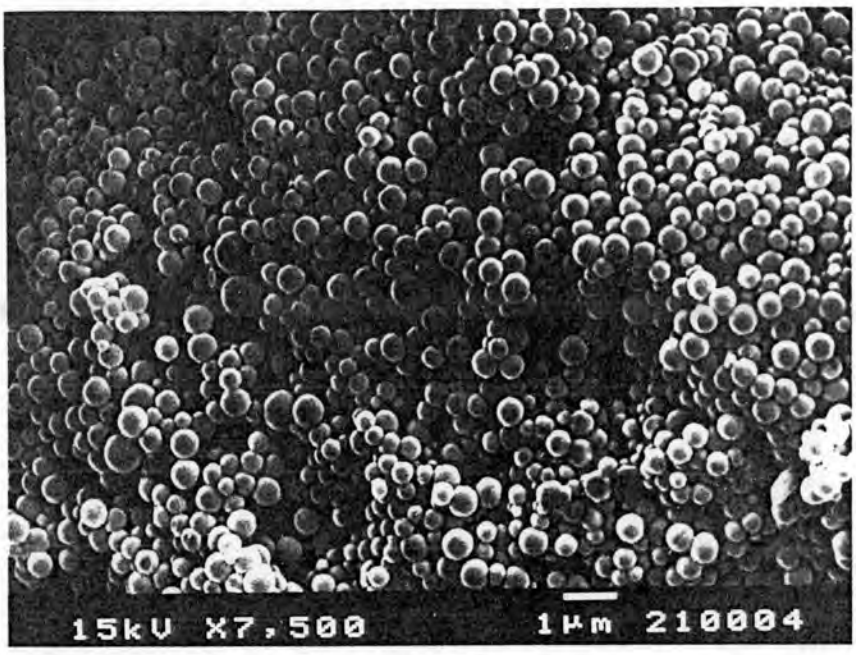

Figure 4.30 SEM micrograph of poly(styrene-*co*-methyl methacrylate) synthesized in 70/30 EtOH/H_2O controlled by 8 wt% PVP K-30

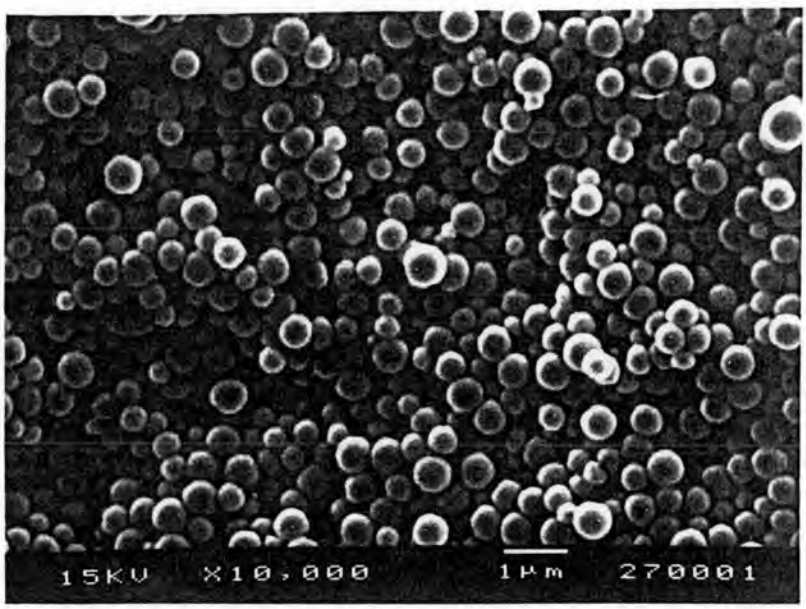

Figure 4.31 SEM micrograph of poly(styrene-*co*-methyl methacrylate) synthesized in 60/40 EtOH/H_2O controlled by 8 wt% PVP K-30

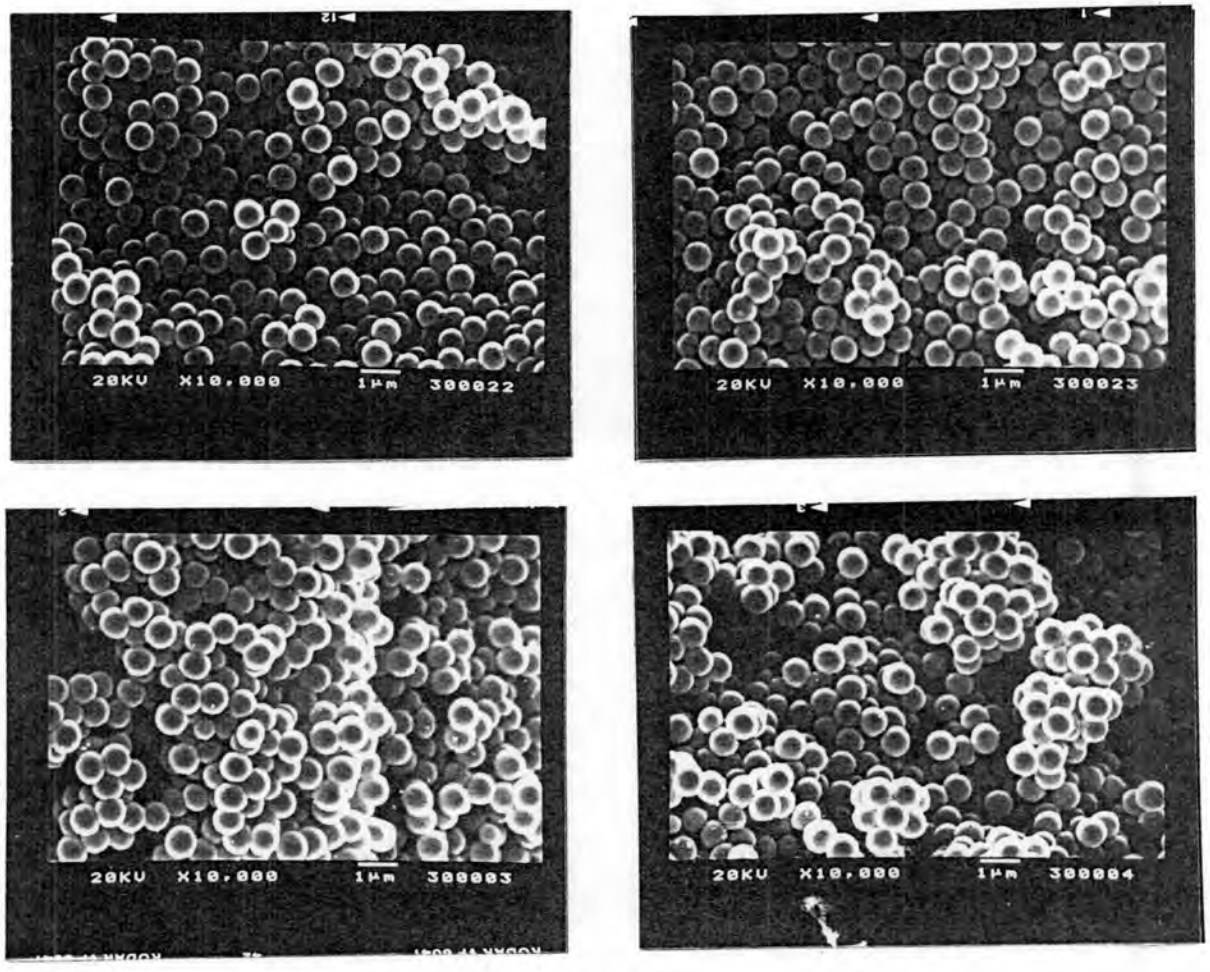

Figure 4.32 SEM micrographs for PSD measurement of poly(styrene-*co*-methyl methacrylate) synthesized in 90/10 EtOH/H_2O controlled by 8 wt% PVP K-30

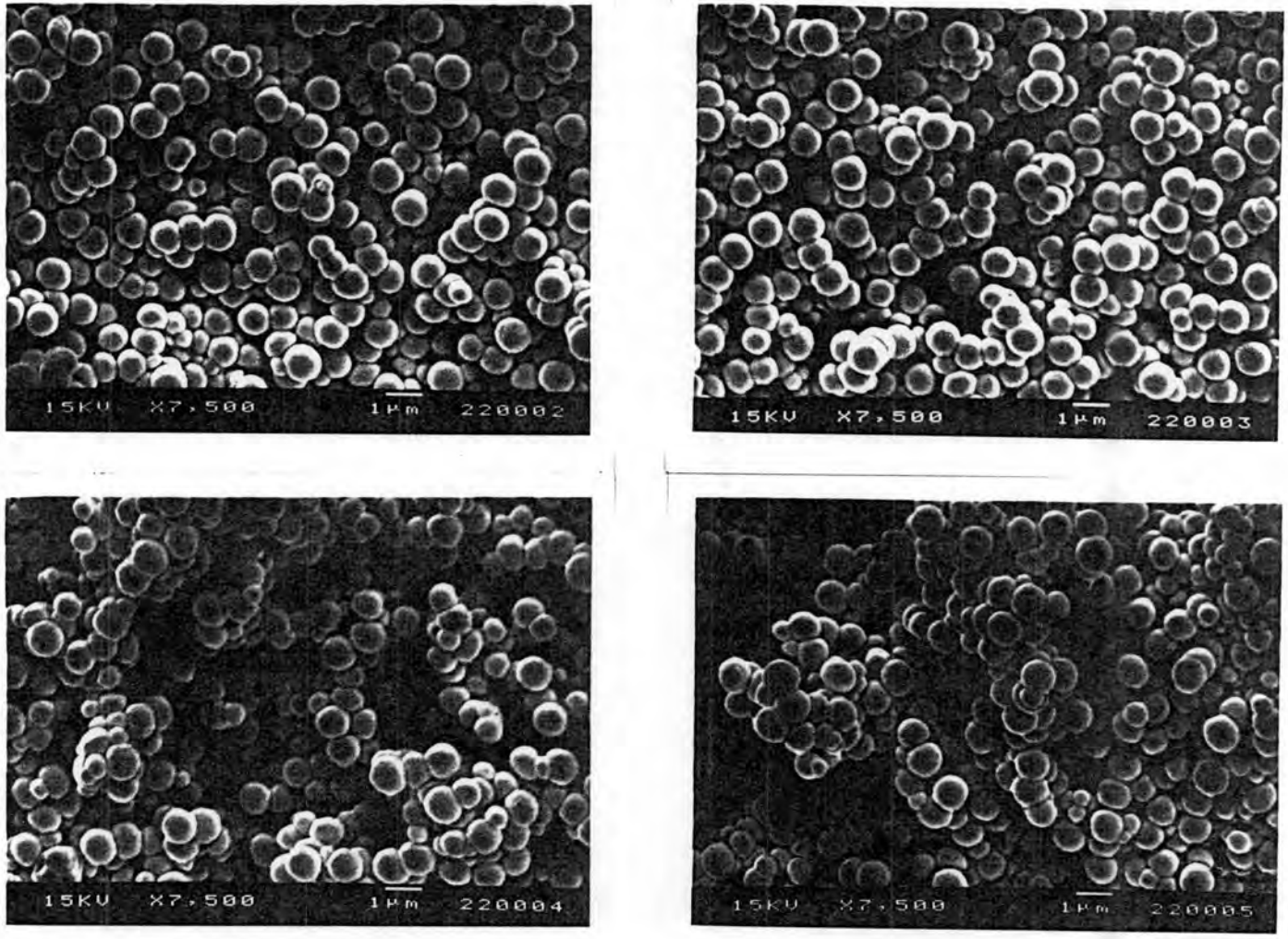

Figure 4.33 SEM micrographs for PSD measurement of poly(styrene-*co*-methyl methacrylate) synthesized in 80/20 EtOH/H_2O controlled by 8 wt% PVP K-30

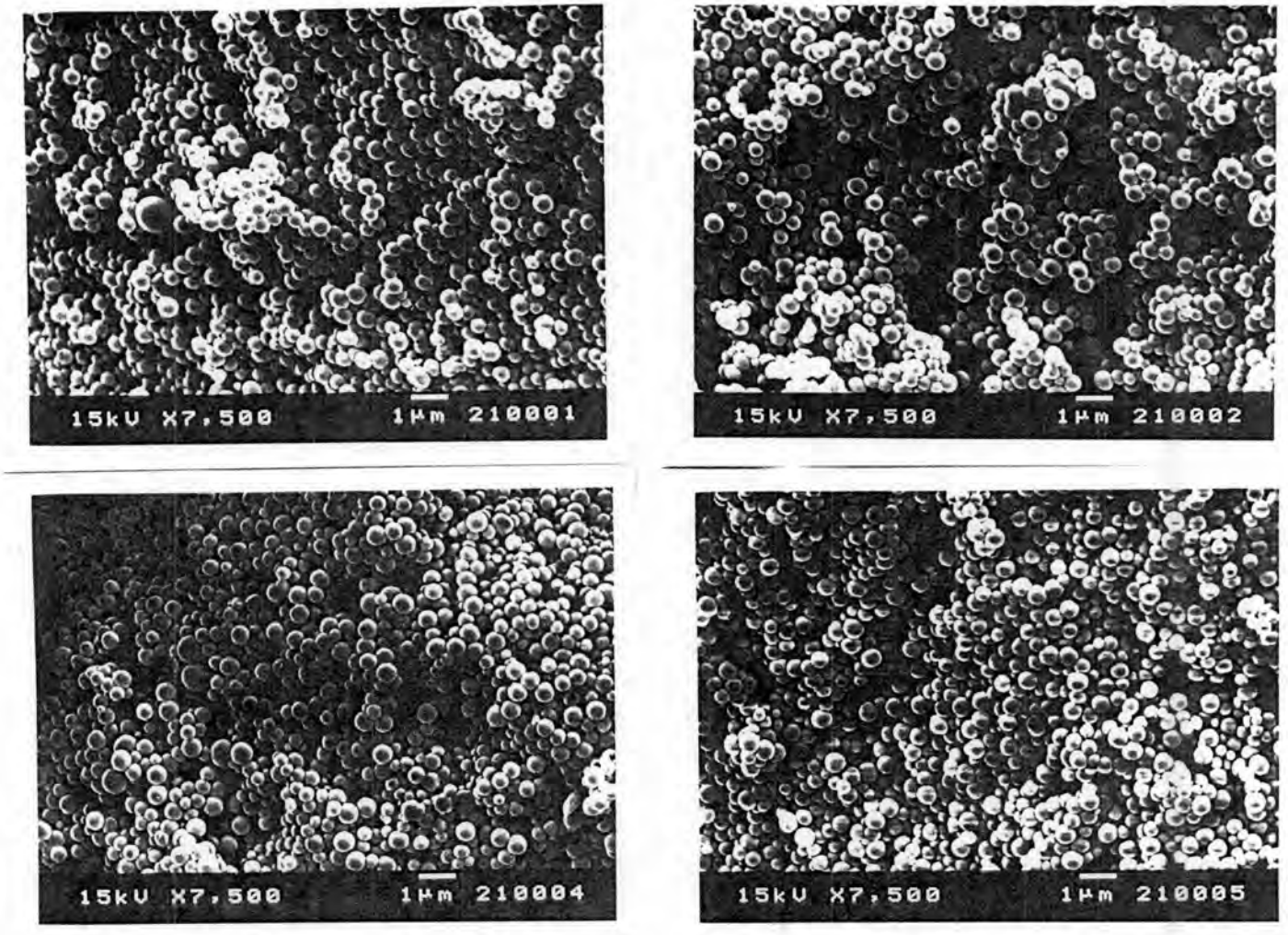

Figure 4.34 SEM micrographs for PSD measurement of poly(styrene-*co*-methyl methacrylate) synthesized in 70/30 EtOH/H_2O controlled by 8 wt% PVP K-30

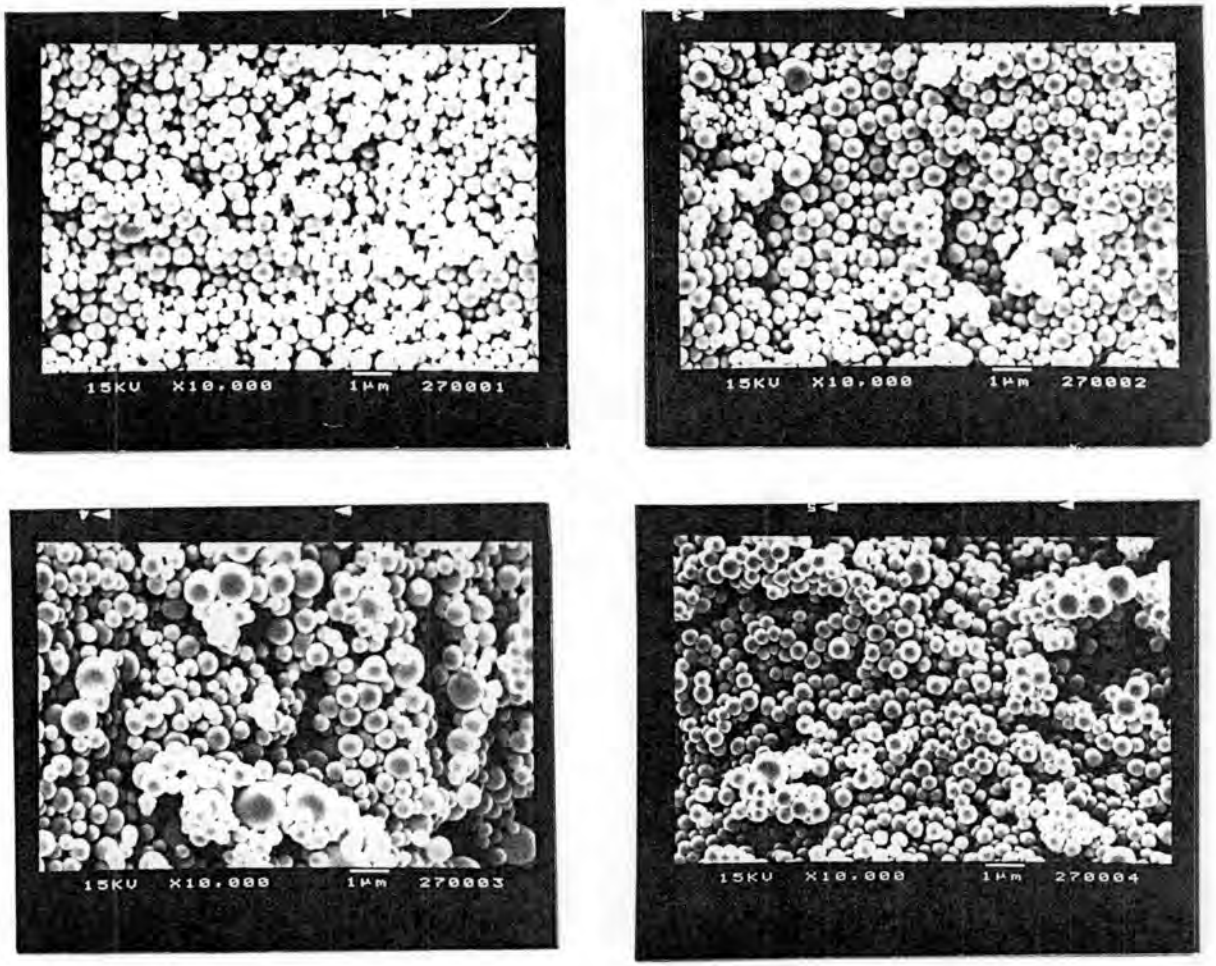

Figure 4.35 SEM micrographs for PSD measurement of poly(styrene-*co*-methyl methacrylate) synthesized in 60/40 EtOH/H_2O controlled by 8 wt% PVP K-30

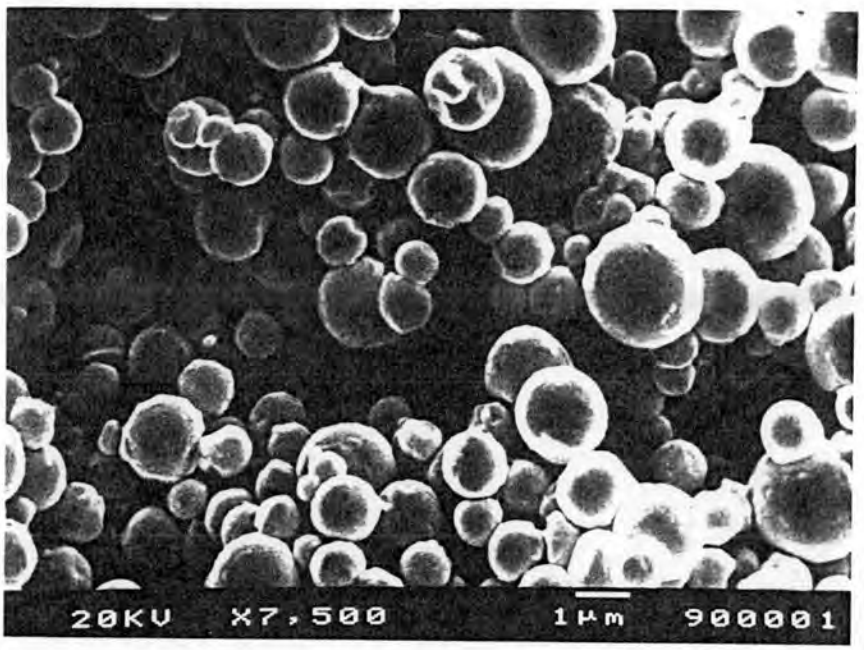

Figure 4.36 SEM micrograph of poly(styrene-*co*-methyl methacrylate) synthesized in ethanol

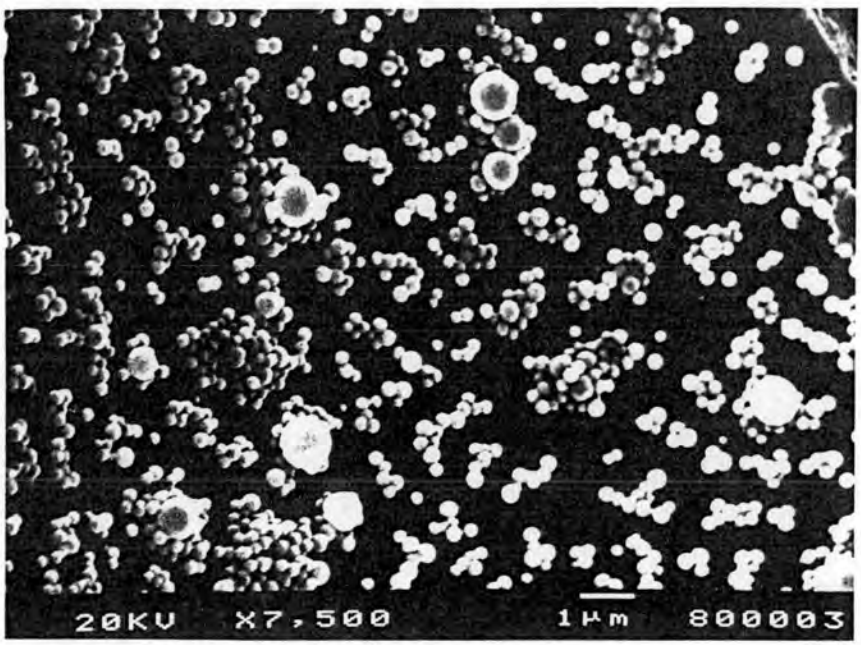

Figure 4.37 SEM micrograph of poly(styrene-*co*-methyl methacrylate) synthesized in water

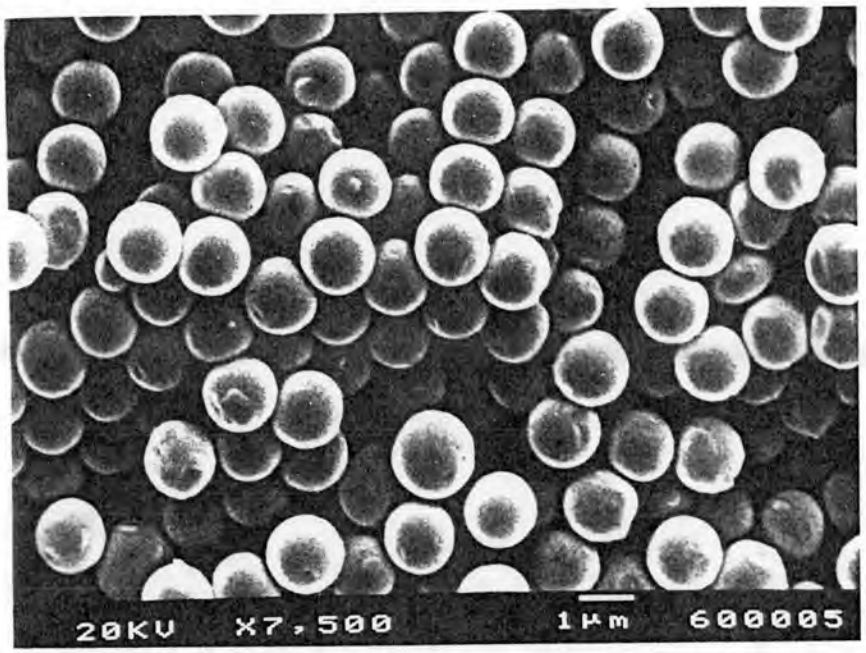

Figure 4.38 SEM micrograph of poly(styrene-*co*-methyl methacrylate) synthesized in 90/10 EtOH/H_2O controlled by 6 wt% PVP K-30

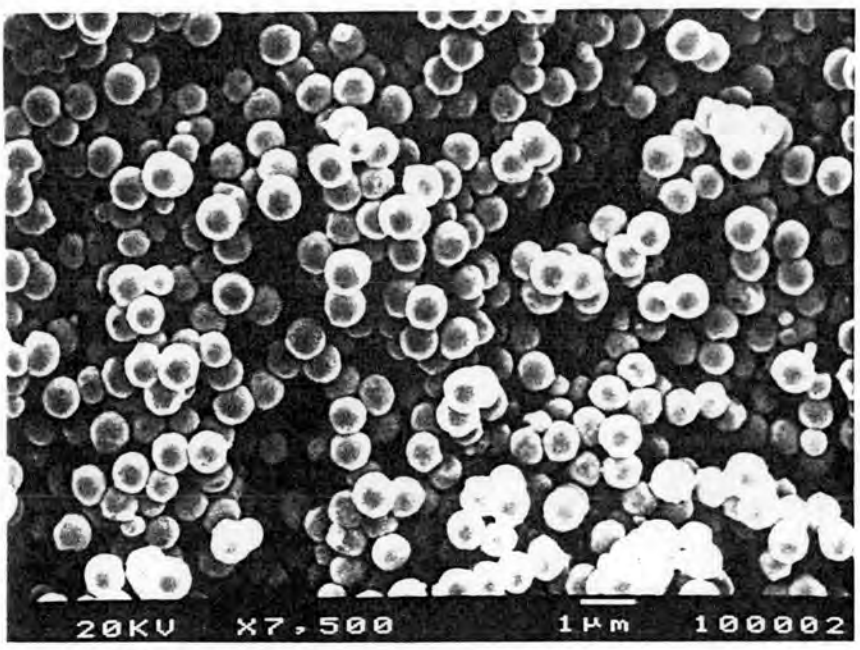

Figure 4.39 SEM micrograph of poly(styrene-*co*-methyl methacrylate) synthesized in 80/20 EtOH/H_2O controlled by 6 wt% PVP K-30

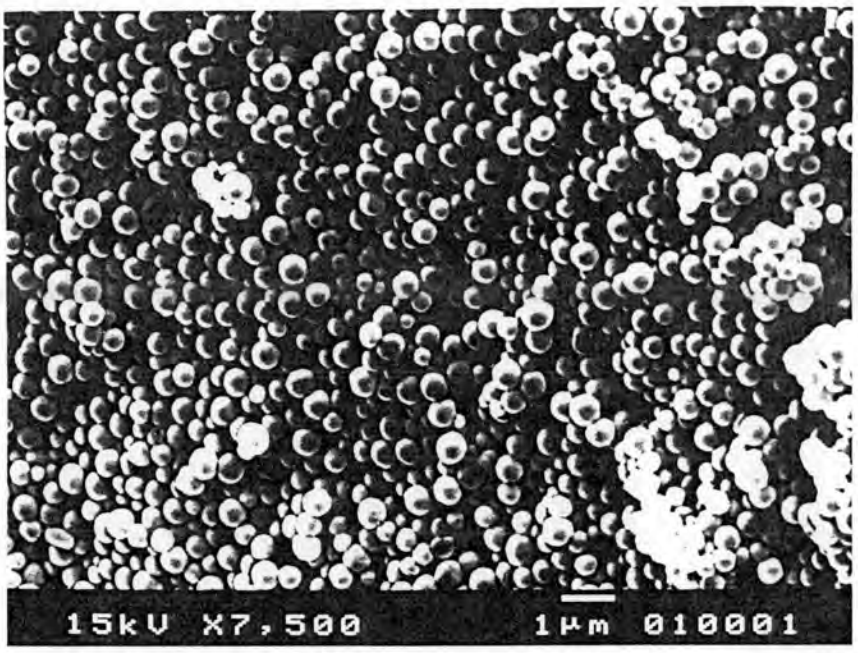

Figure 4.40 SEM micrograph of poly(styrene-*co*-methyl methacrylate) synthesized in 70/30 EtOH/H_2O controlled by 6 wt% PVP K-30

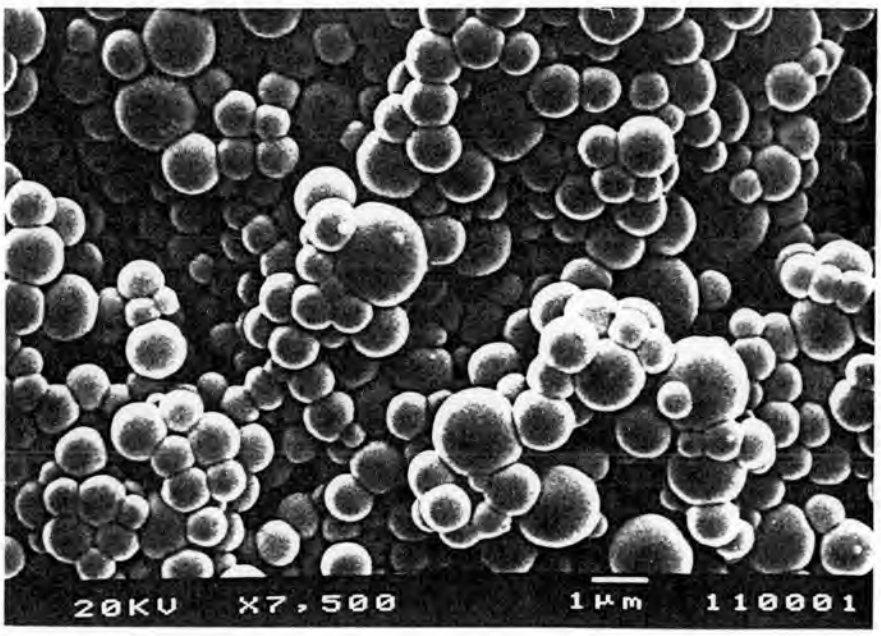

Figure 4.41 SEM micrograph of poly(styrene-*co*-methyl methacrylate) synthesized in 60/40 EtOH/H_2O controlled by 6 wt% PVP K-30

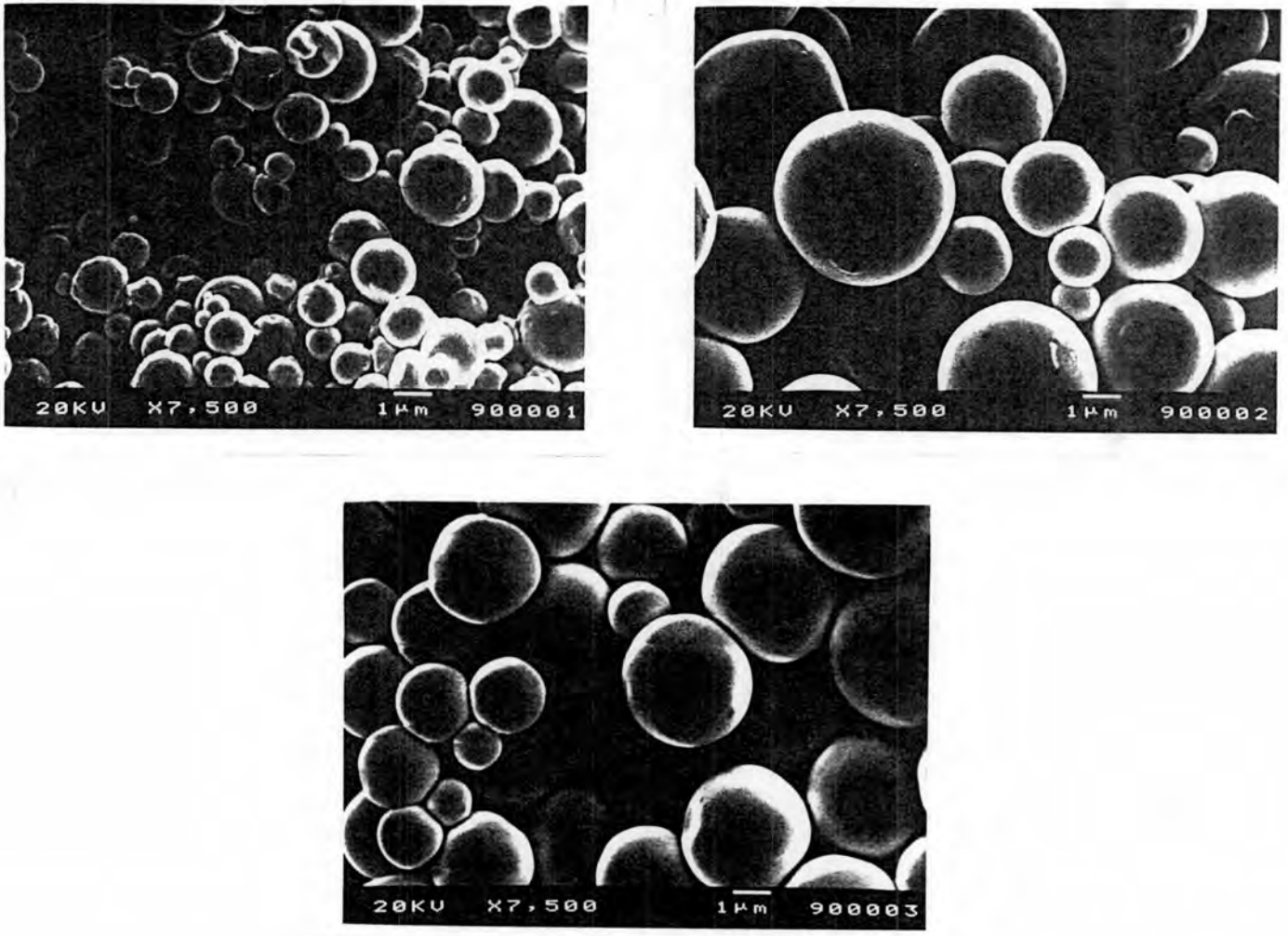

Figure 4.42 SEM micrographs for PSD measurement of poly(styrene-*co*-methyl methacrylate) synthesized in ethanol

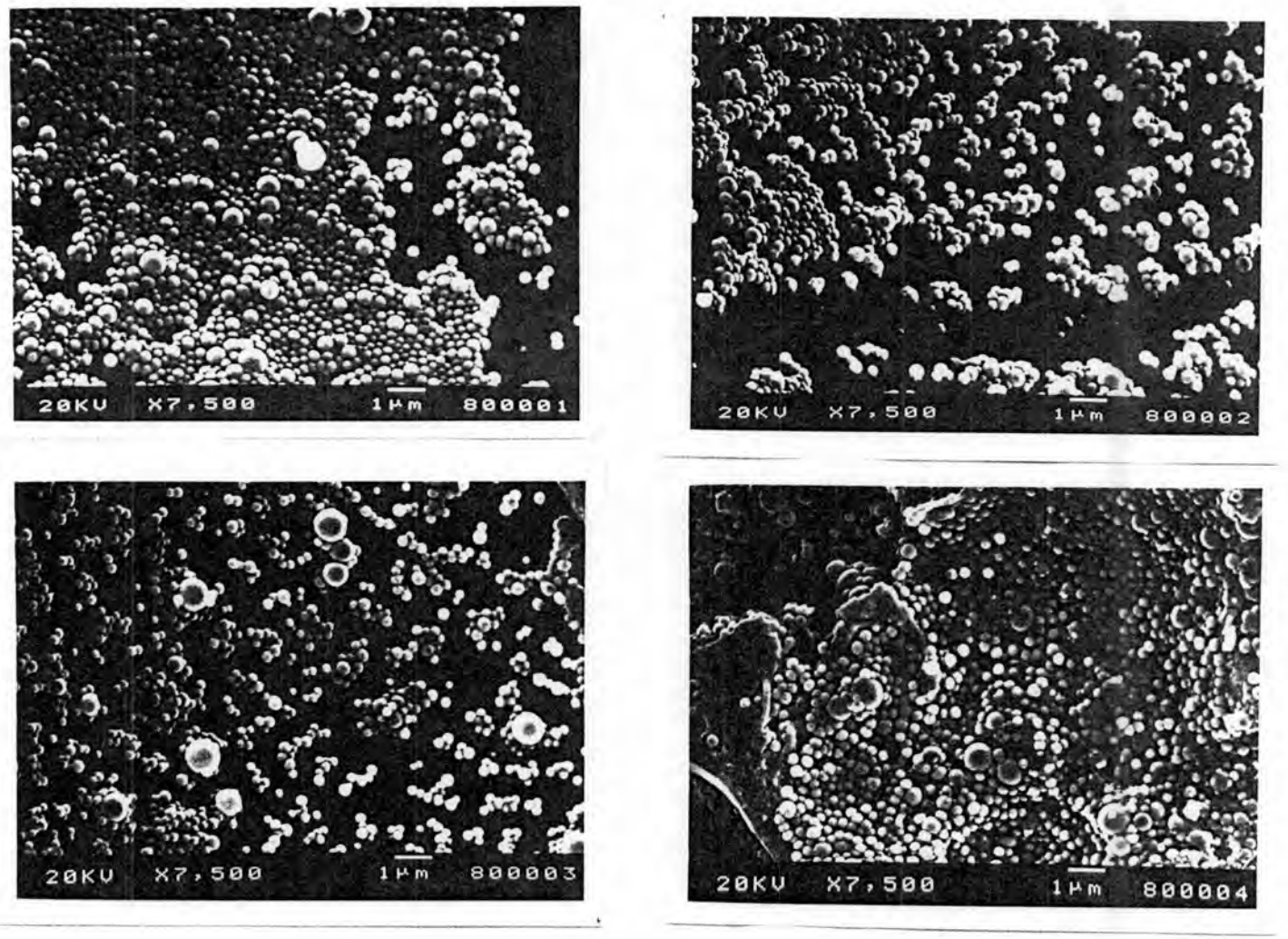

Figure 4.43 SEM micrographs for PSD measurement of poly(styrene-*co*-methyl methacrylate) synthesized in water

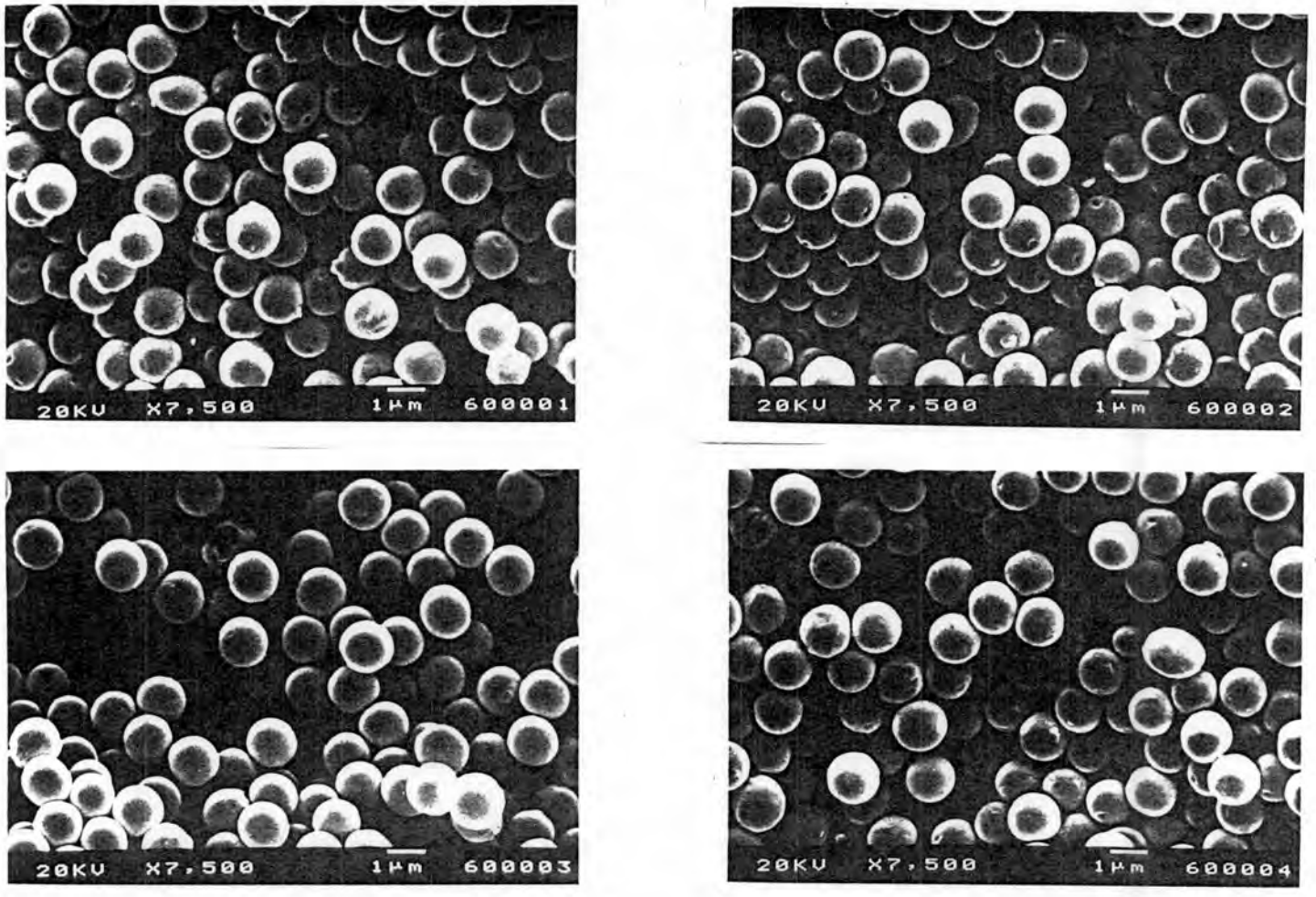

Figure 4.44 SEM micrographs for PSD measurement of poly(styrene-*co*-methyl methacrylate) synthesized in 90/10 EtOH/H_2O controlled by 6 wt% PVP K-30

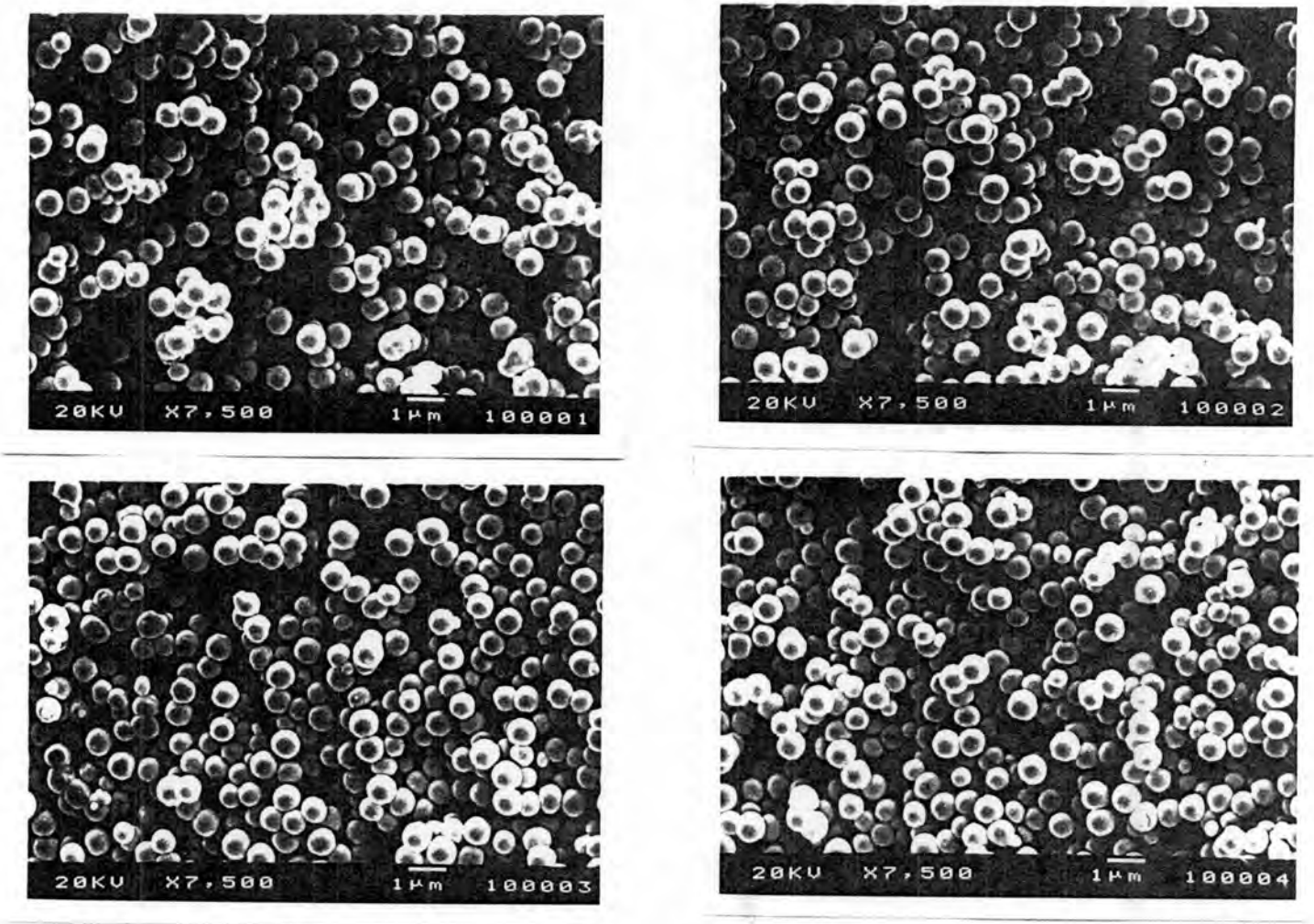

Figure 4.45 SEM micrographs for PSD measurement of poly(styrene-*co*-methyl methacrylate) synthesized in 80/20 EtOH/H_2O controlled by 6 wt% PVP K-30

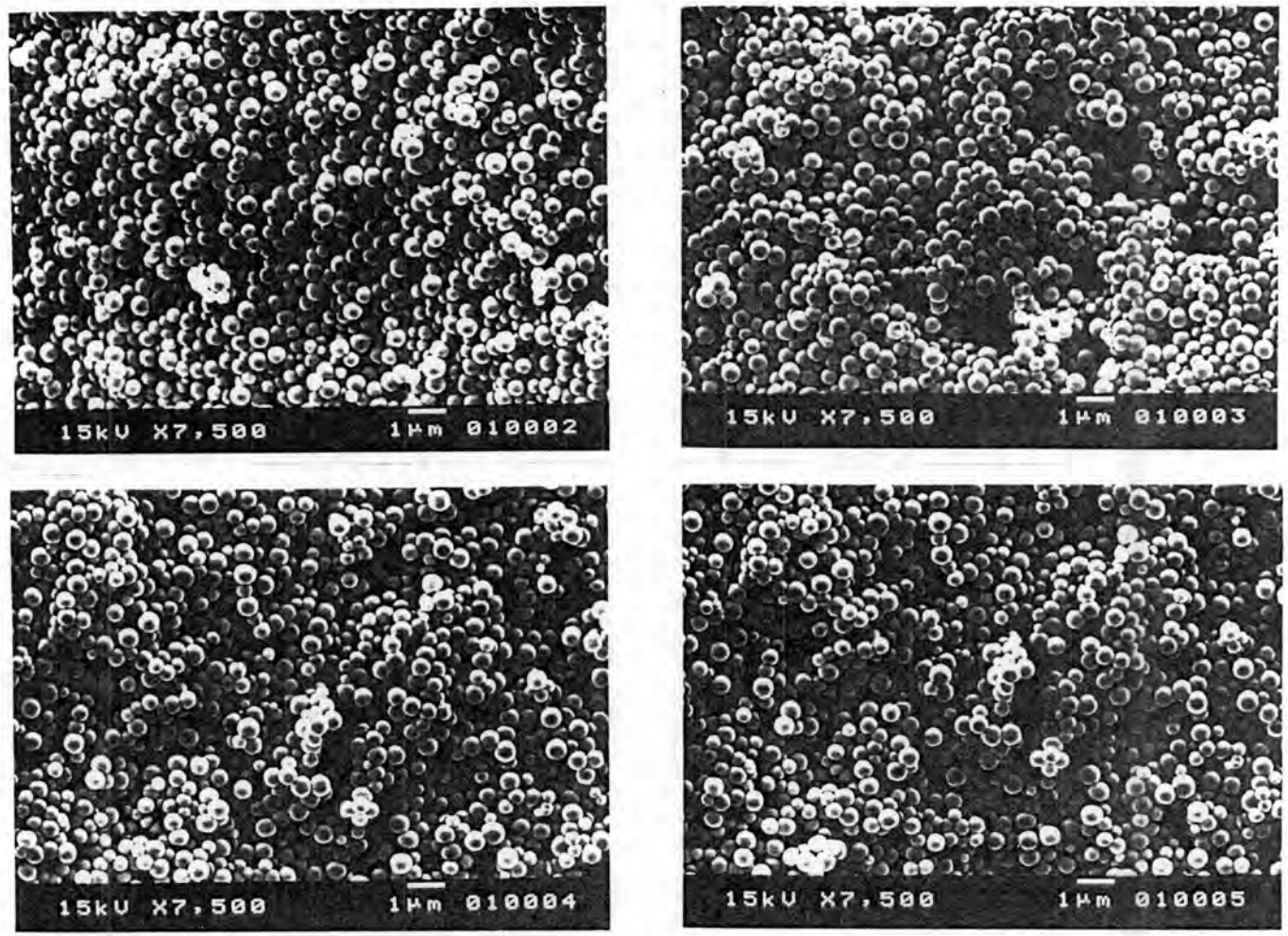

Figure 4.46 SEM micrographs for PSD measurement of poly(styrene-*co*-methyl methacrylate) synthesized in 70/30 EtOH/H_2O controlled by 6 wt% PVP K-30

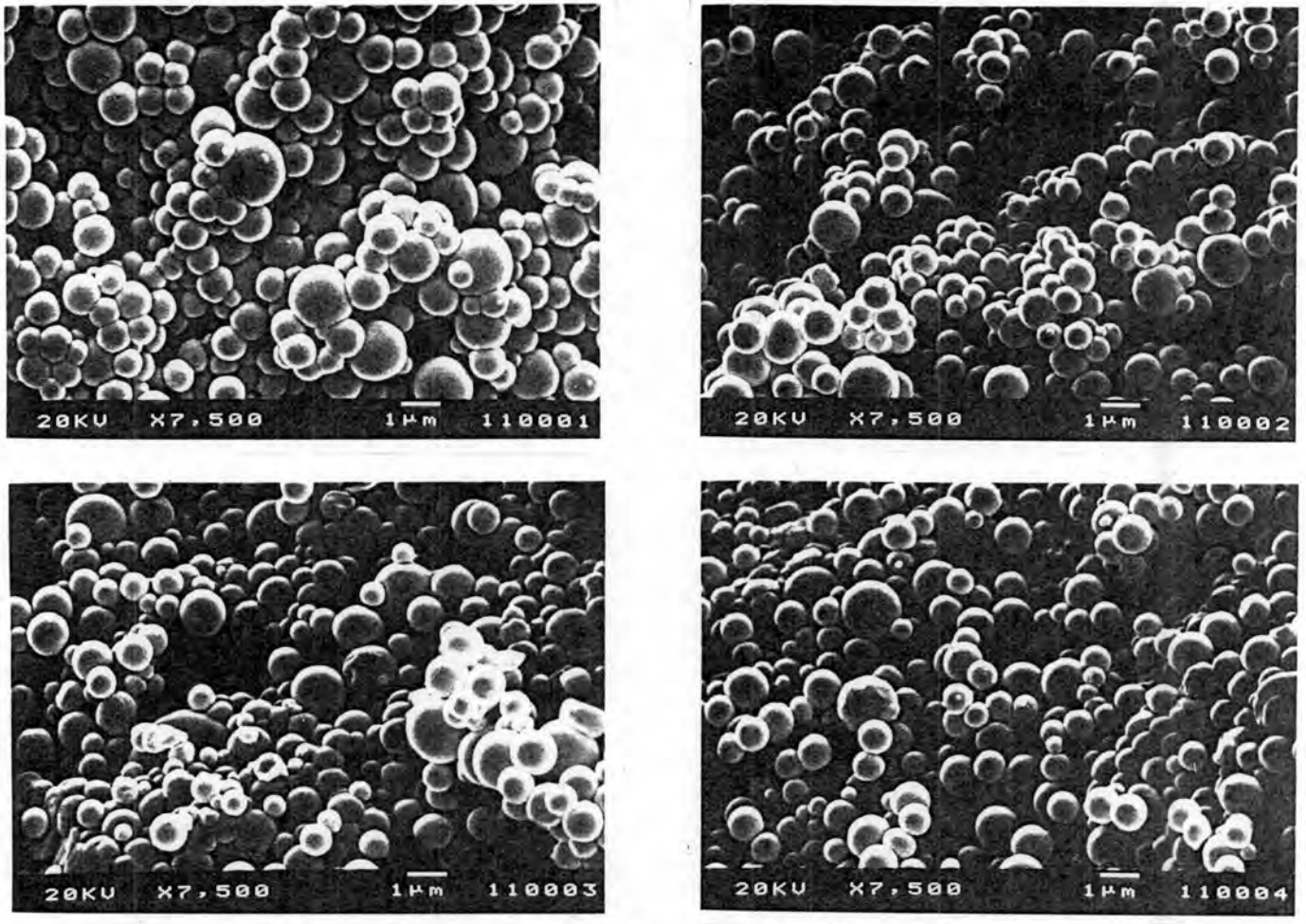

Figure 4.47 SEM micrographs for PSD measurement of poly(styrene-*co*-methyl methacrylate) synthesized in 60/40 EtOH/H_2O controlled by 6 wt% PVP K-30

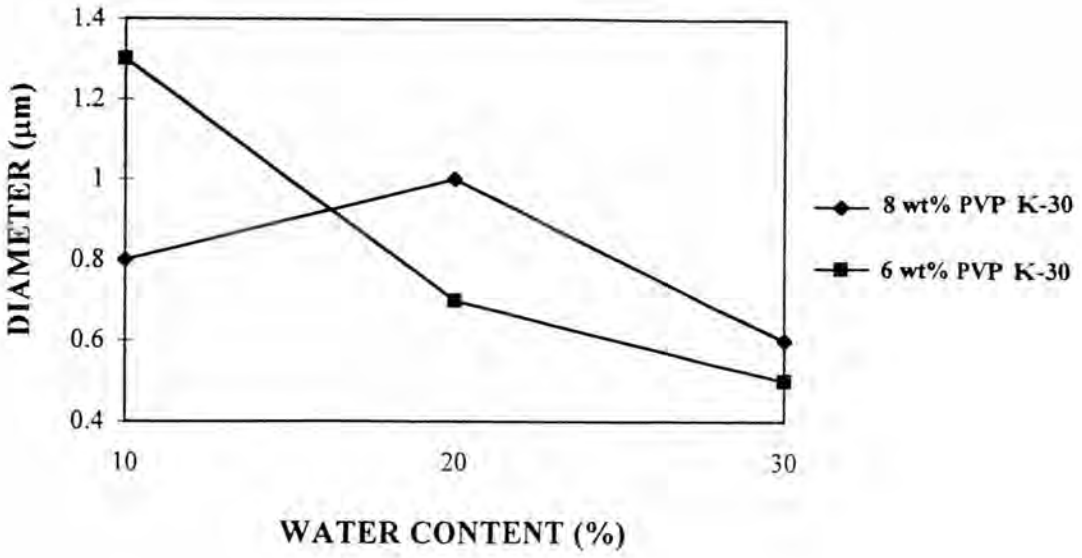

Figure 4.48 Effect of the solvency of medium on the particle size of poly(styrene-*co*-methyl methacrylate) controlled by 8 wt% and 6 wt% PVP K-30

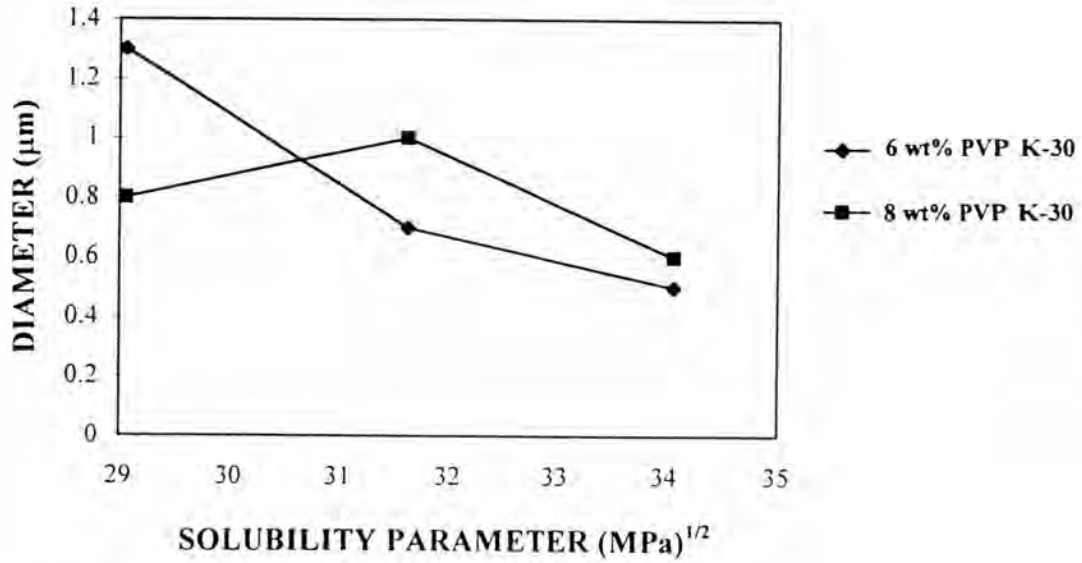

Figure 4.49 Effect of the average solubility parameter of the dispersion medium on the average particle size

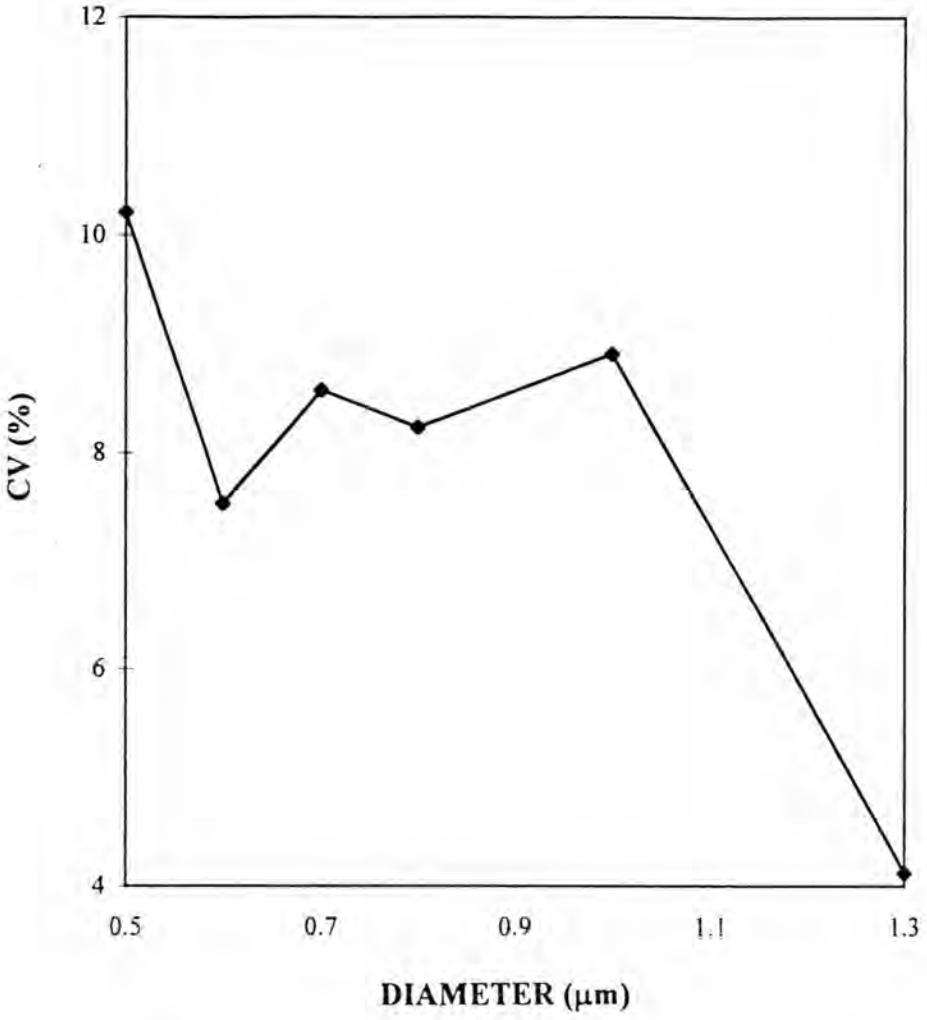

Figure 4.50 Relationship between the average particle size and CV for various ethanol/water ratios

Particle size distribution and relationship between average particle size and CV of poly(styrene-*co*-methyl methacrylate) microspheres are shown in Appendice D-b1 to D-b6 and Figure 4.50, respectively.

In conclusion, the environment for particle size is strongly influenced by increasing the solvency of the medium for the polymers in which the onset of particle formation is often retarded and the duration of particle formation is prolonged. These are correspondingly wider particle size distribution.

4.2.2 The Average Molecular Weights and Molecular Weight Distribution of Poly(Styrene-*co*-Methyl Methacrylate)

The effect of ethanol-to-water ratios on average molecular weights and molecular weight distribution are investigated. In this research, the PVP K-30 concentrations of 6 wt% and 8 wt% were used. In both cases, increasing the ethanol content from 70% to 90%, the average molecular weight increased as shown in Figures 4.51 and 4.52. At 60% ethanol, the average molecular weight increased rapidly and a very broad molecular weight distribution was produced ($\overline{M}_w/\overline{M}_n$ = 3.57 and 3.90) as shown in Figure 4.53. The GPC chromatographs of poly(styrene-*co*-methyl methacrylate) prepared in 60/40 ethanol/water in both cases (6 wt% and 8 wt%) are shown in Figures 4.54 and 4.55, respectively. This high MWD values could be observed when the gel effect is present. Besides, at 100% water, the average molecular weights of the copolymer is 56538 which is very much higher than that of 11265 in 100% ethanol. In water system (δ_{H2O} = 47.9 $(MPa)^{1/2}$) most of the styrene (δ_{STY} = 19 $(MPa)^{1/2}$) and methyl methacrylate monomer (δ_{MMA} = 18 $(MPa)^{1/2}$) quickly

diffused into the adjacent particle nucleus and sustained faster particle growth since the Tromsdorff effect is presented to result in an increase in molecular weights. Whereas in the ethanol case (δ_{EtOH} = 26.0 $(MPa)^{1/2}$), substantial quantities of monomer remain in the medium, and the slower growth of particles was observed resulted in the lower molecular weight.

However, the data obtained represents a significant solvent effect on the average molecular weights of the copolymer. The possible reason for the increased molecular weights is the copolymer particles remain for a longer period in a regime of oligomer capture and solid phase polymerization (49).

In this experiment, percent conversion of the polymerization of styrene and methyl methacrylate in 90/10 ethanol/water at the reaction time of 8 h was determined. It was found that the polymerization was carried out to a high conversion of 78%, and the molecular weight distribution (MWD) of the copolymer is 3.03. It shows that the overall molecular weight distributions for a high or complete conversion polymerization are quite broad (50).

Table 4.2 Effects of Ethanol/Water Ratio on Dispersion Copolymerization of Styrene and Methyl Methacrylate

No.	Ethanol/Water	$\overline{D}_n$ (μm)	CV (%)	SD (μm)	PSD	$\overline{M}_n$	$\overline{M}_w$	$\overline{M}_w/\overline{M}_n$
S1[a]	100/0	*	*	*	*	6413	11265	1.76
S2[a]	90/10	1.3	4.12	0.05	1.03	5839	15008	2.57
S3[a]	80/20	0.7	8.57	0.06	1.07	6001	13283	2.21
S4[a]	70/30	0.5	10.21	0.09	1.08	3222	4691	1.46
S5[a]	60/40	**	**	**	**	18807	67170	3.57
S6[a]	0/100	***	***	***	***	22518	56538	2.51
S7[b]	90/10	0.8	8.23	0.06	1.02	41652	126151	3.03
S8[b]	80/20	1.0	8.91	0.09	1.02	38637	93526	2.42
S9[b]	70/30	0.6	7.53	0.04	1.02	11619	37123	3.20
S10[b]	60/40	****	****	****	****	27426	106925	3.90

[a]Reaction temperature = 70°C, reaction time = 8 h [b]Reaction temperature = 60°C, reaction time = 10 h *,**,***,**** very broad PSD

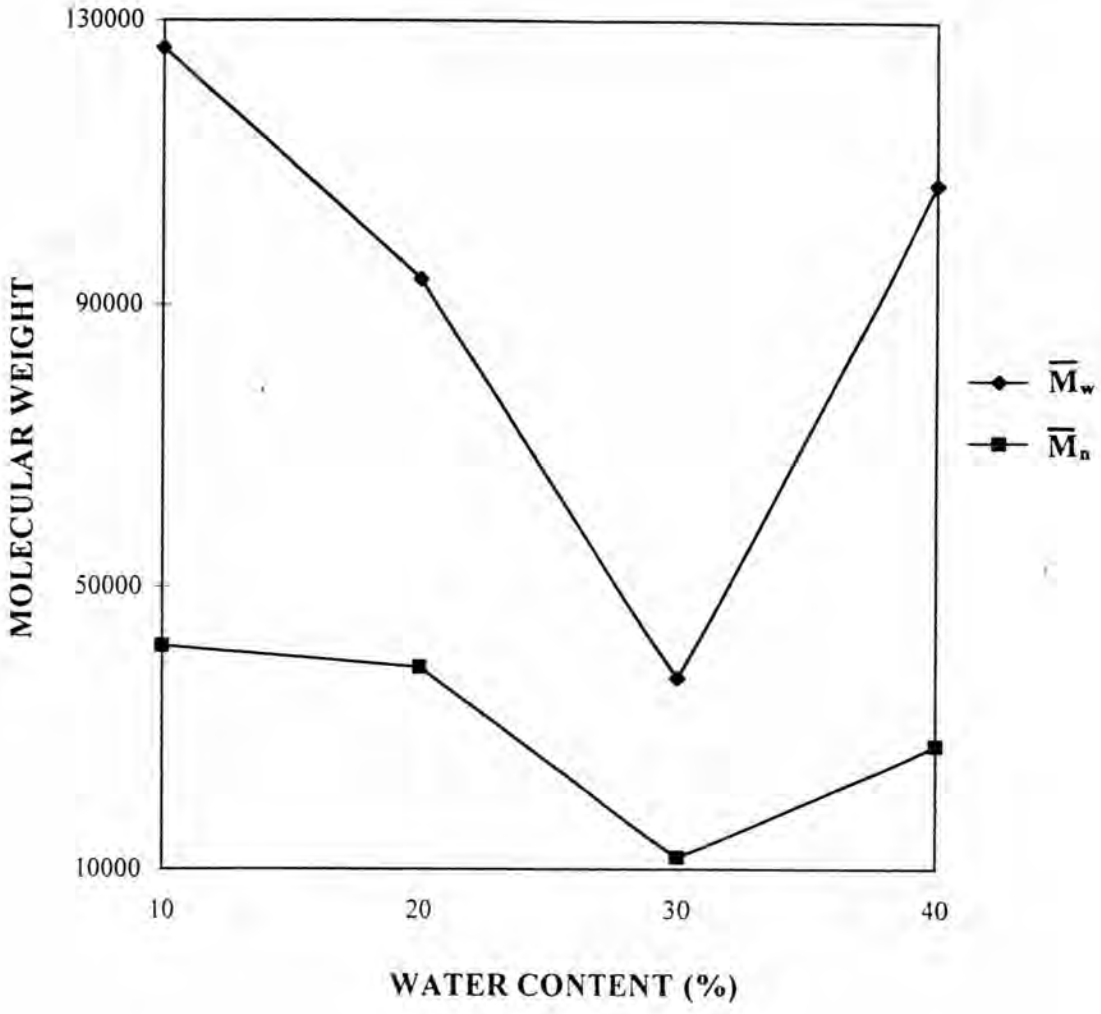

Figure 4.51 Effect of the solvency of medium on the average molecular weights of poly(styrene-*co*-methyl methacrylate) controlled by 8 wt% PVP K-30

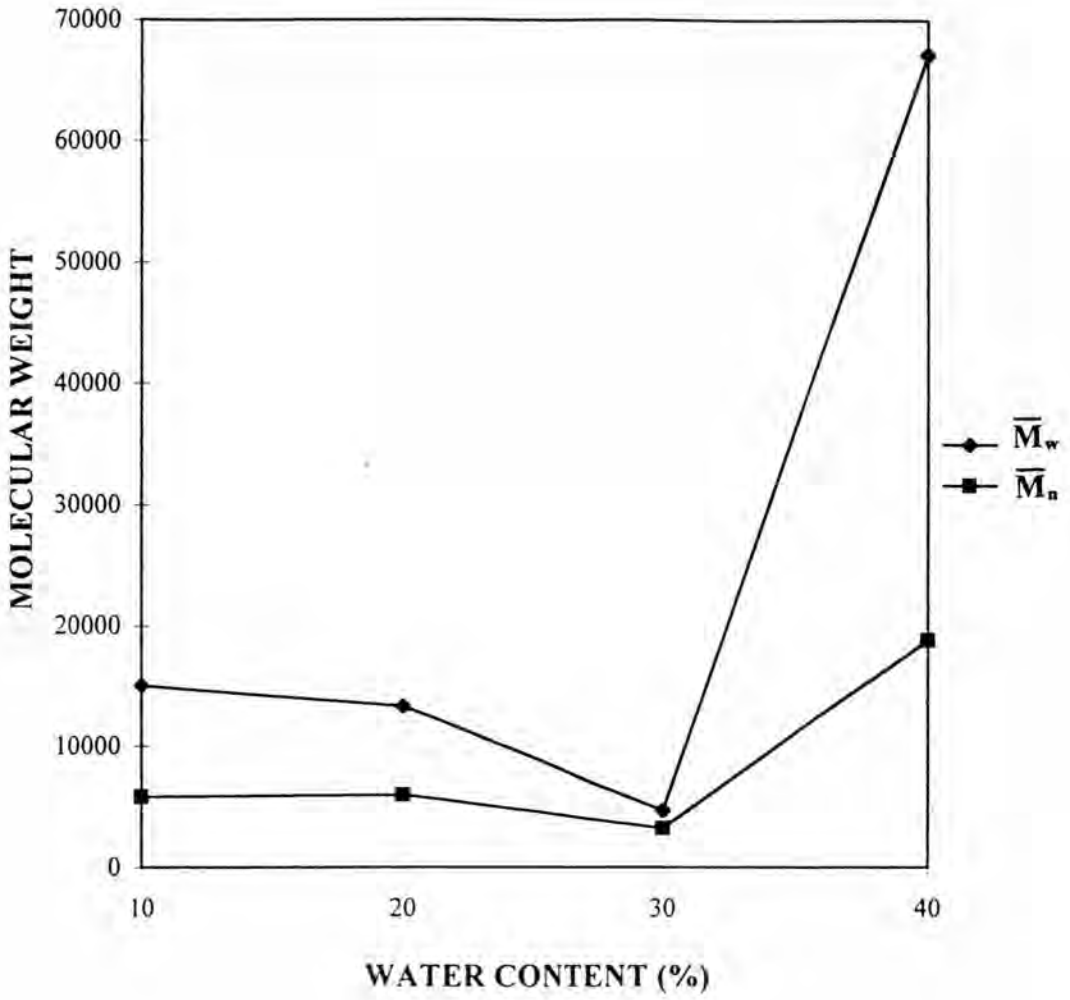

Figure 4.52 Effect of the solvency of medium on the average molecular weights of poly(styrene-*co*-methyl methacrylate) controlled by 6 wt% PVP K-30

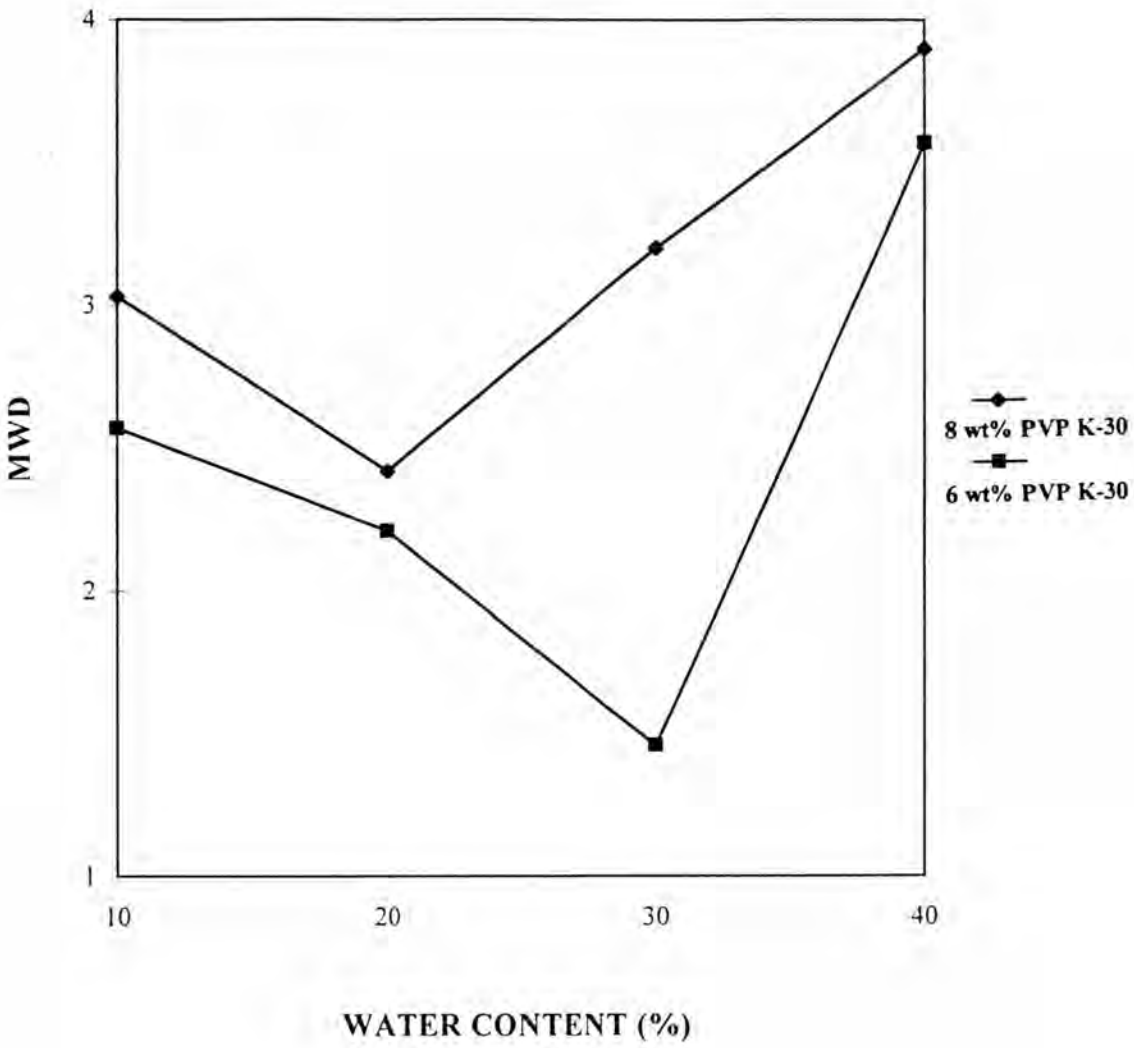

Figure 4.53 The curve of MWD of poly(styrene-*co*-methyl methacrylate) for various ethanol/water ratios in the presence of 8 wt% and 6 wt% PVP K-30

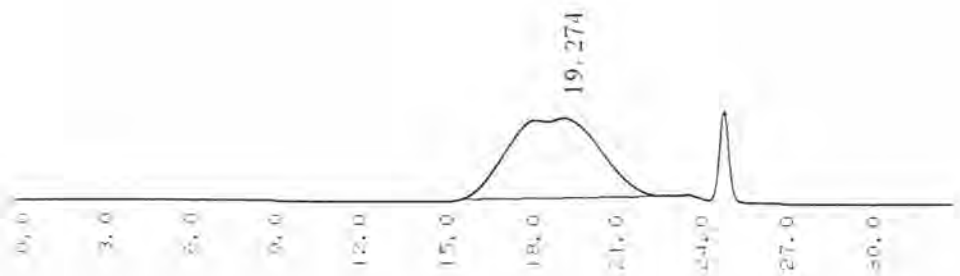

Peak information	Time (min)	Mol. size	Height
start	15.75	663521	32
top	19.274	28778	5040
end	22.75	1303	1

Number-A.M.W.	$\overline{M}_n$	=	18807	Weight-A.M.W. $\overline{M}_w$	=	67170
z-A.M.W.	$\overline{M}_z$	=	162445	Visc-A.M.W. $\overline{M}_v$	=	58793
Dispersity	$\overline{M}_w/\overline{M}_n$	=	3.57162	Dispersity $\overline{M}_z/\overline{M}_w$	=	2.41841
Dispersity	$\overline{M}_v/\overline{M}_n$	=	3.12619	I. Viscosity I. VISC	=	30.17179

Figure 4.54 The GPC chromatograph of the copolymer synthesized in ethanol/water ratios of 60/40 and 6 wt% PVP K-30

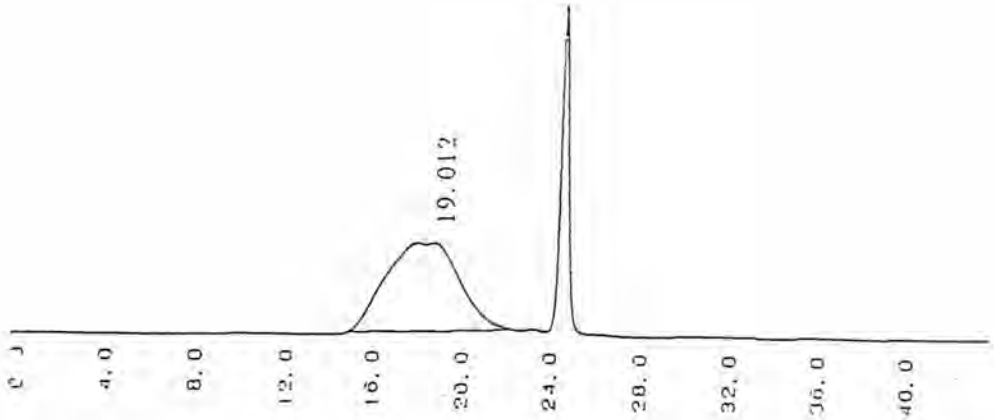

Peak information	Time (min)	Mol. size	Height
start	15.2	1082801	32
top	19.012	36351	5274
end	22.65	1424	1

Number-A.M.W.	$\overline{M}_n$	=	27426	Weight-A.M.W. $\overline{M}_w$	=	106925
z-A.M.W.	$\overline{M}_z$	=	269552	Visc-A.M.W. $\overline{M}_v$	=	92896
Dispersity	$\overline{M}_w/\overline{M}_n$	=	3.89872	Dispersity $\overline{M}_z/\overline{M}_w$	=	2.52095
Dispersity	$\overline{M}_v/\overline{M}_n$	=	3.38721	I. Viscosity I. VISC	=	42.71599

Figure 4.55 The GPC chromatograph of the copolymer synthesized in ethanol/water ratios of 60/40 and 8 wt% PVP K-30

4.3 The Effect of the Reaction Temperature on

4.3.1 The Particle Size and Particle Size Distribution of Poly(Styrene-*co*-Methyl Methacrylate)

The effect of reaction temperature on dispersion polymerization of styrene and methyl methacrylate was investigated. The dispersion polymerization was carried out in ethanol/water ratio of 70/30 with PVP K-30 concentration of 8 wt%.

Figures 4.56-4.59 show SEM photographs of microspheres and Figures 4.60-4.63 show SEM photographs of the copolymer particle size distribution. The copolymer particle size increased with increasing the reaction temperature in the range from 50°C to 70°C and then decreased with increasing temperature up to 80°C, as shown in Figure 4.64. However, the particle size distribution was narrower when increasing the polymerization temperature as shown in Figure 4.65.

Increasing the reaction temperature resulted in an increase in particle size of polymer because the critical chain length of precipitated oligomer chains was increased due to increasing in the solubility of the oligomer chain in the continuous phase at the higher reaction temperatures. Because of increasing the concentration of precipitated oligomer chains due to increases in both the decomposition rate constant of the initiator (k_d) and the propagation rate constant of the monomer (k_p), this could therefore lead to an increase in their aggregates. Finally, decrease in viscosity of the continuous phase and the adsorption rate of the matrix polymer are influenced by the increasing solubility of the matrix polymer increases. All of these reasons led to an increase in particle size of the polymer (51).

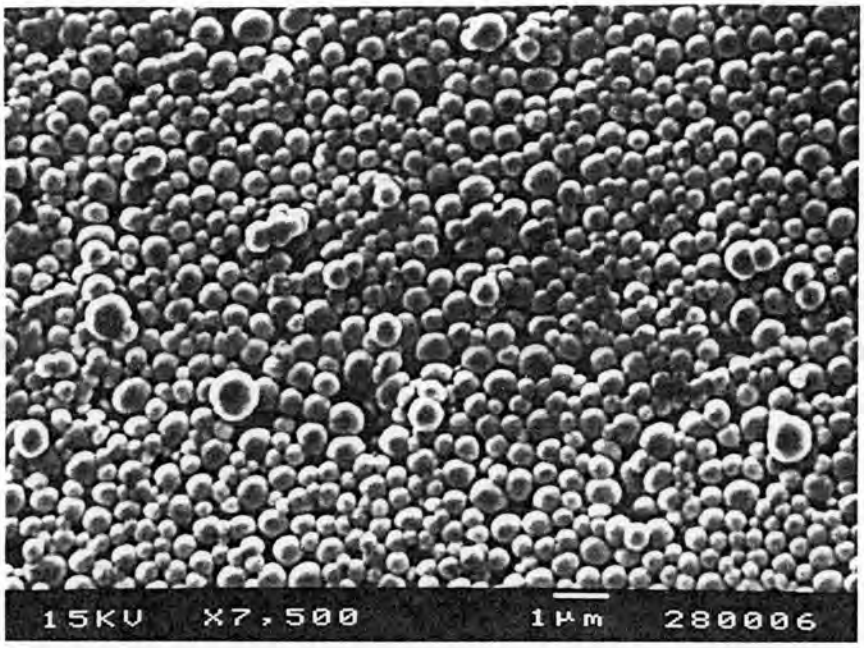

Figure 4.56 SEM micrograph of poly(styrene-*co*-methyl methacrylate) synthesized at 50°C reaction temperature

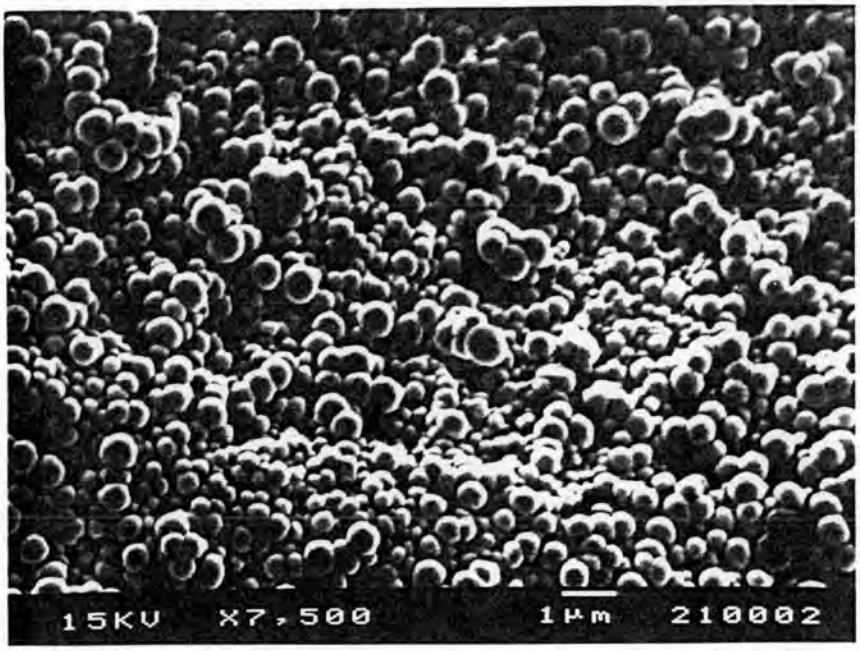

Figure 4.57 SEM micrograph of poly(styrene-*co*-methyl methacrylate) synthesized at 60°C reaction temperature

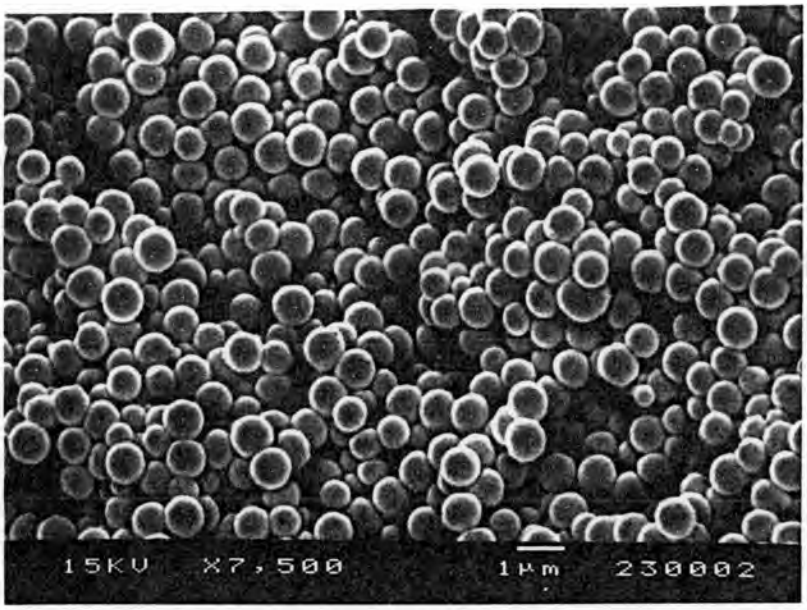

Figure 4.58 SEM micrograph of poly(styrene-*co*-methyl methacrylate) synthesized at 70°C reaction temperature

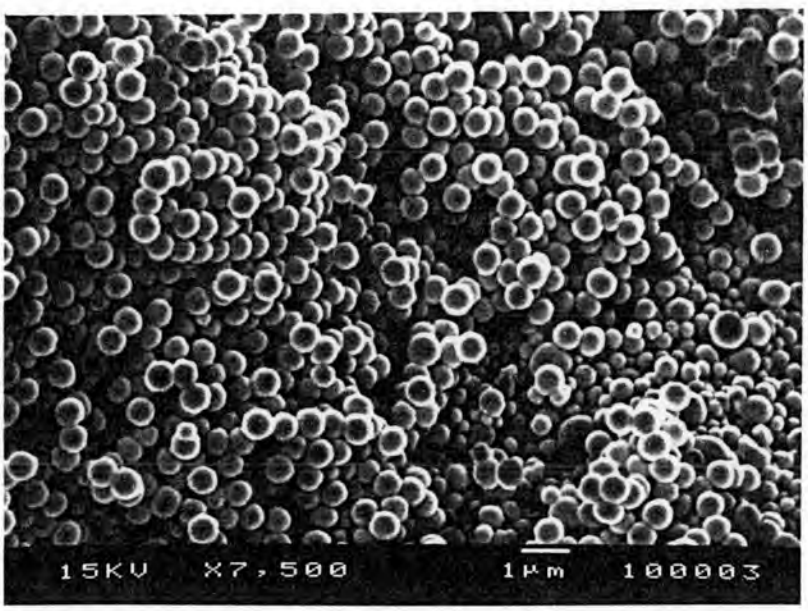

Figure 4.59 SEM micrograph of poly(styrene-*co*-methyl methacrylate) synthesized at 80°C reaction temperature

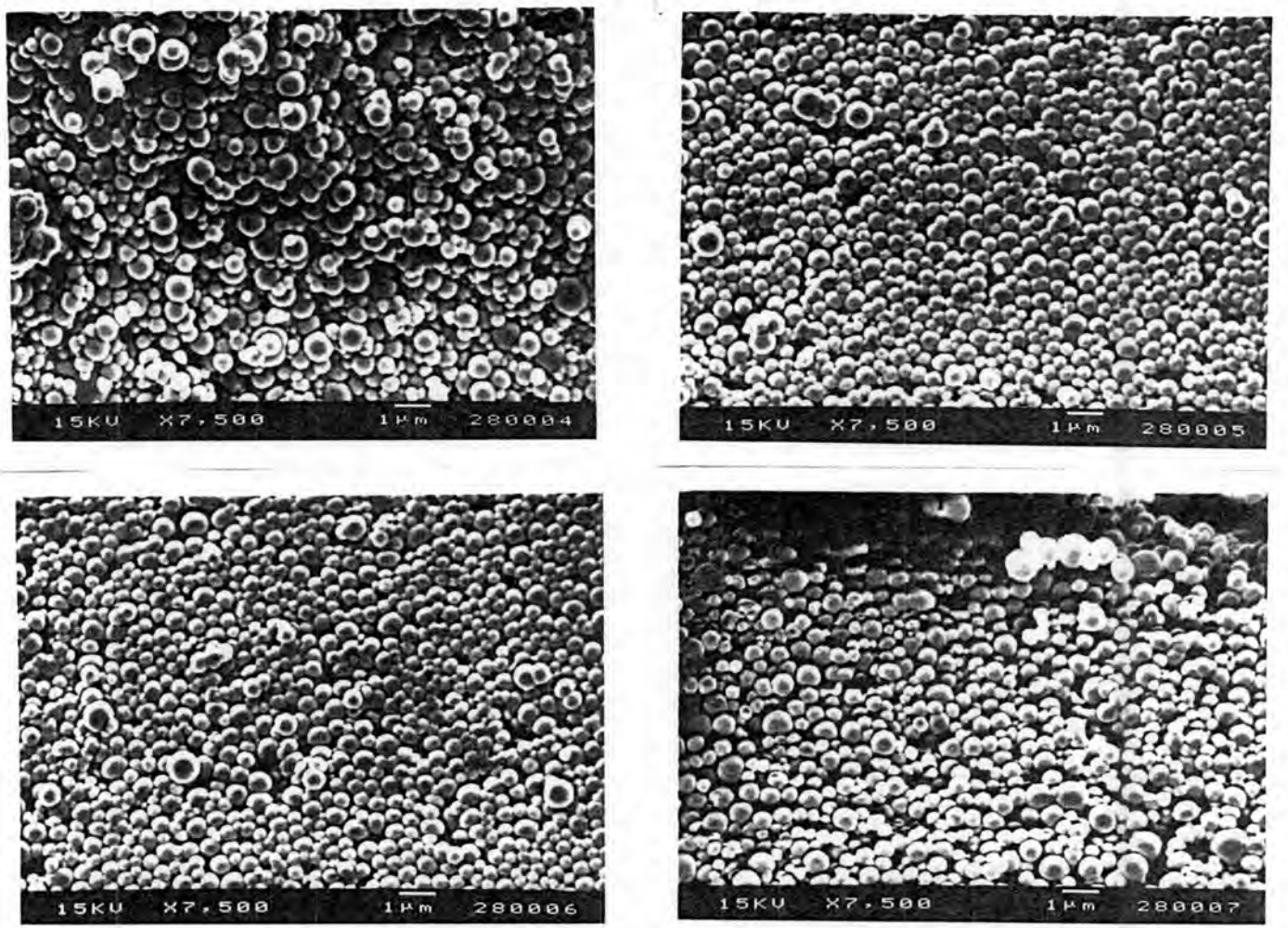

Figure 4.60 SEM micrographs for PSD measurement of poly(styrene-*co*-methyl methacrylate) synthesized at 50°C reaction temperature

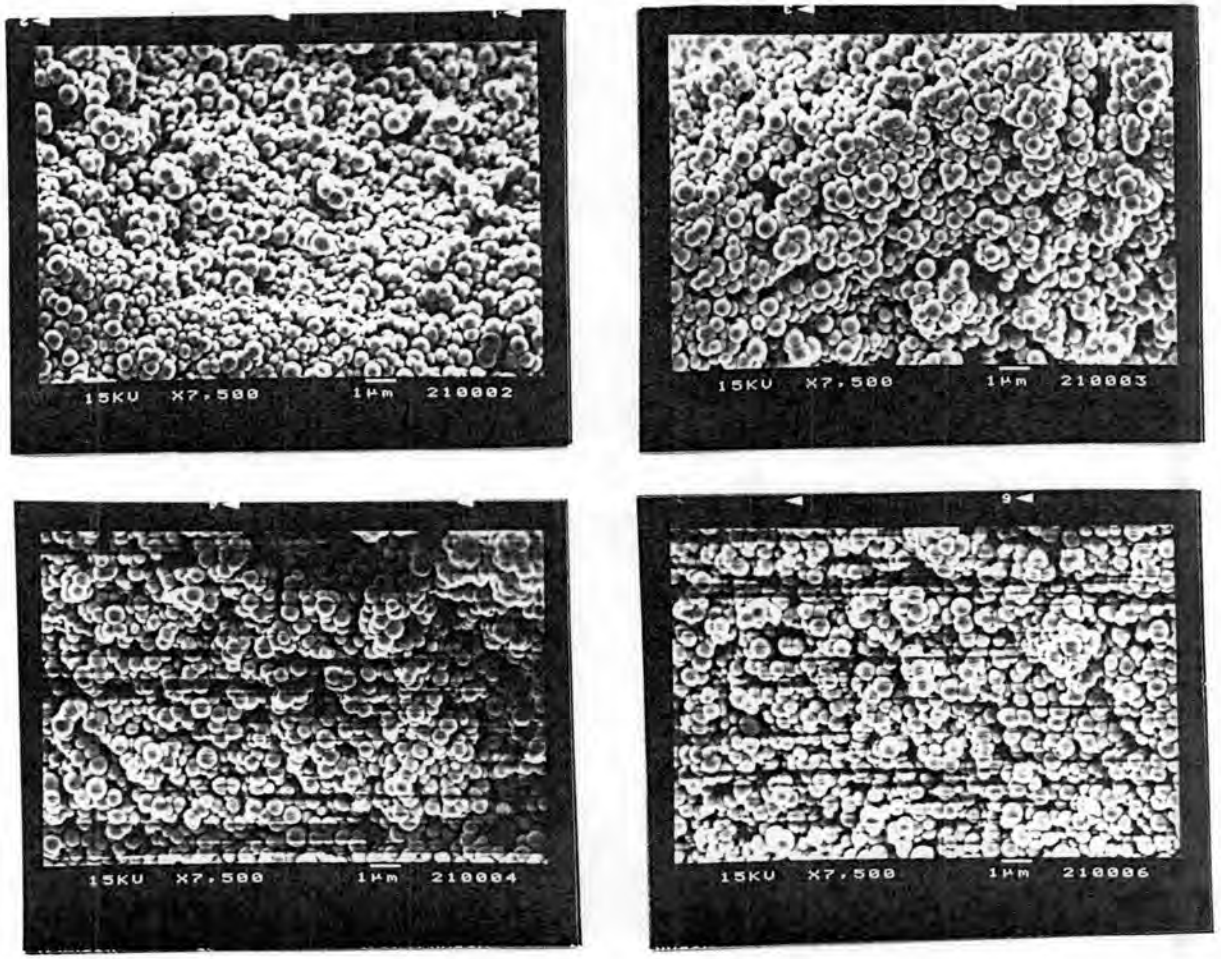

Figure 4.61 SEM micrographs for PSD measurement of poly(styrene-*co*-methyl methacrylate) synthesized at 60°C reaction temperature

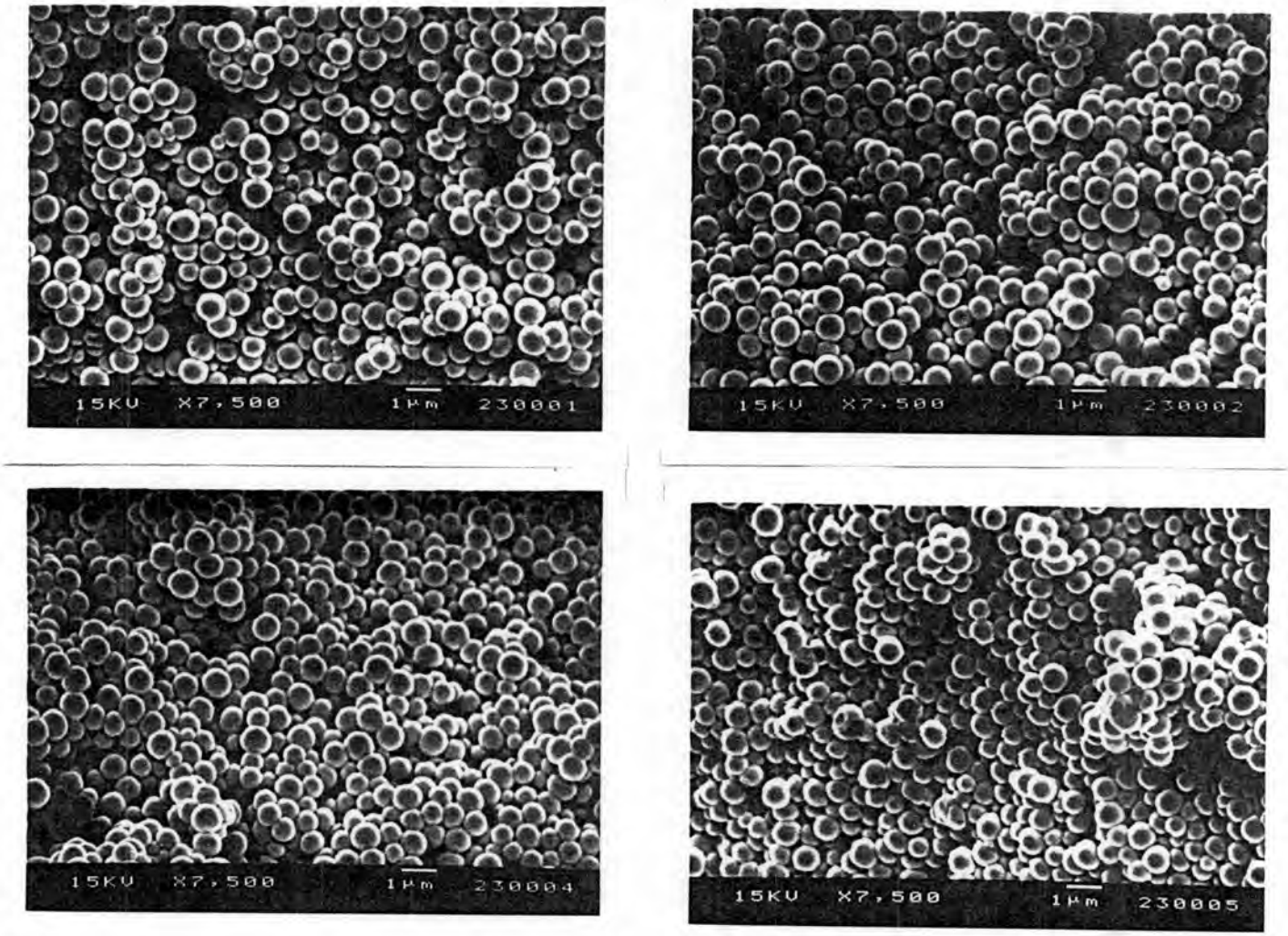

Figure 4.62 SEM micrographs for PSD measurement of poly(styrene-*co*-methyl methacrylate) synthesized at 70°C reaction temperature

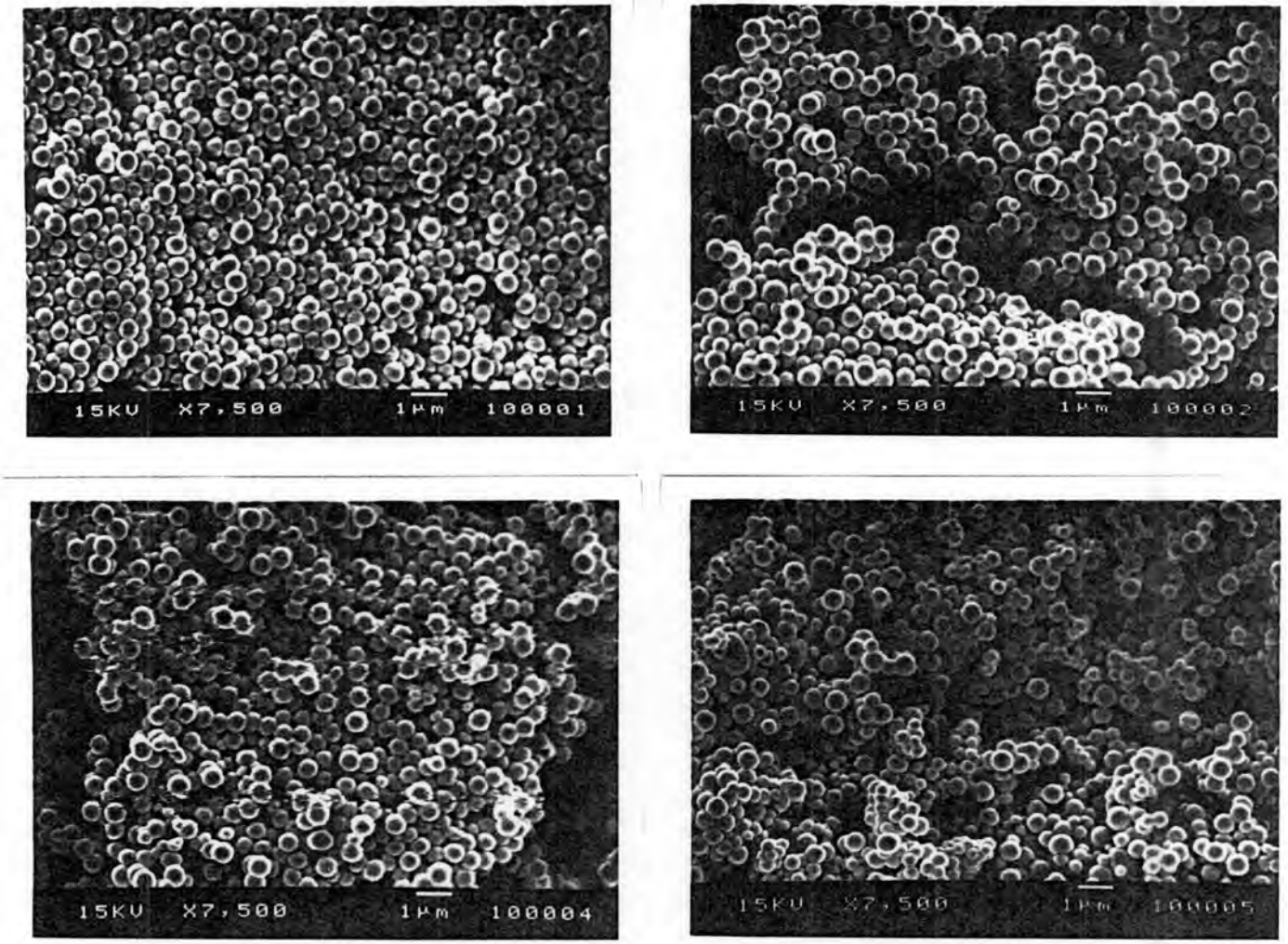

Figure 4.63 SEM micrographs for PSD measurement of poly(styrene-*co*-methyl methacrylate) synthesized at 80°C reaction temperature

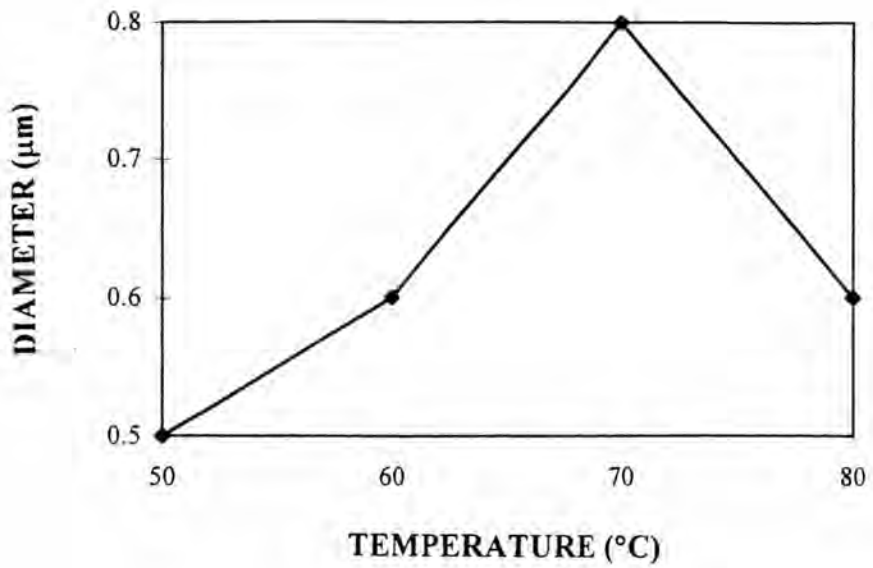

Figure 4.64 Effect of the reaction temperature on the particle sizes of poly(styrene-*co*-methyl methacrylate)

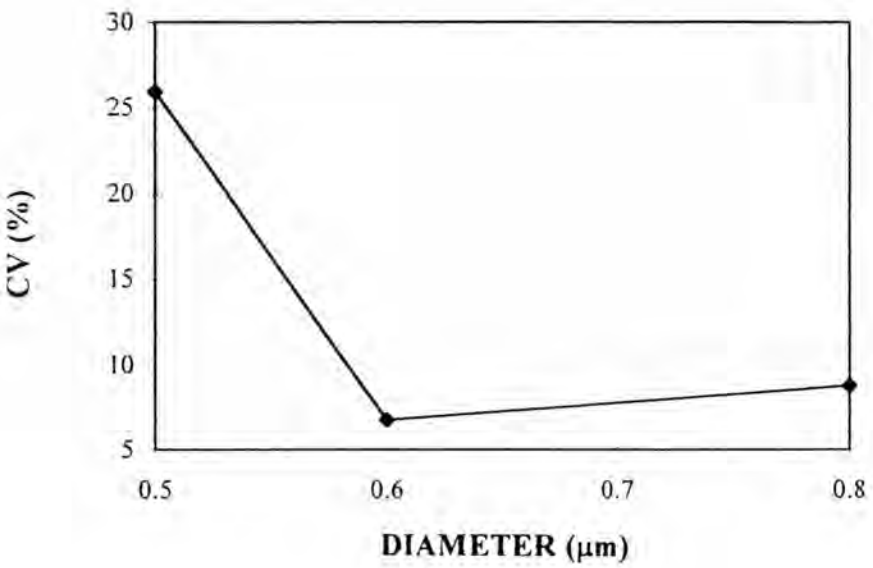

Figure 4.65 Relationship between the average particle size and CV of poly(styrene-*co*-methyl methacrylate) for various reaction temperatures

4.3.2 The Average Molecular Weights and Molecular Weight Distribution of Poly(Styrene-*co*-Methyl Methacrylate)

It is seen that the smallest particle size prepared at 50°C have the broadest size distribution. The variation in molecular weight of the copolymers with increasing the reaction temperature is shown in Figure 4.66. The experimental data show that the average molecular weights of the copolymer increase up to the synthesized reaction temperature of 70°C. Increasing the reaction temperature of 50°C to 60°C, the average molecular weights increased gradually and then increased rapidly with the reaction temperature of 70°C. The average molecular weights decreased rapidly when increasing the reaction temperature up to the reaction temperature of 80°C. Figure 4.67 shows the curve of molecular weight distribution of the copolymer. The narrowest molecular weight distribution ($\overline{M}_w/\overline{M}_n = 1.52$) in this research was produced at the reaction temperature of 70°C as shown in Figure 4.68 and Table 4.3.

With increasing the reaction temperature from 70°C to 80°C, the average molecular weights was decreased. This result can be discussed as below:

Initially, considering the kinetic chain length (ν) of a radical chain polymerization is defined as the average number of monomer units converted to polymer by a single initiating radical, is given in eq 4.18 (52).

$$\nu = \frac{k_p[M]}{2(fk_dk_t[I])^{1/2}} \qquad (4.18)$$

The variation of this ratio with the reaction temperature is given by

$$\ln \frac{k_p}{(k_d k_t)^{1/2}} = \ln \frac{A_p}{(A_d A_t)^{1/2}} - \frac{[E_p - (E_d/2) - (E_t/2)]}{RT} \quad (4.19)$$

Where the energy term $[E_p - (E_d/2) - (E_t/2)]$ is the composite or overall activation energy for the degree of polymerization ($E_{\overline{X}n}$). For termination, $\overline{X}_n$ is given in eq 4.20.

$$\ln \overline{X}_n = \ln \frac{A_p}{(A_d A_t)^{1/2}} + \ln \frac{[M]}{(f[I])^{1/2}} - \frac{E_{\overline{X}n}}{RT} \quad (4.20)$$

From $E_{\overline{X}n} = E_p - (E_d/2) - (E_t/2)$

where E_d = the activation energy for initiator decomposition

(E_d (AIBN) = 123.4 kJ/mole)

E_p = the activation energy for propagation

(~20-40 kJ/mole)

E_t = the activation energy for termination (~8-20 kJ/mole)

From above equation, $E_{\overline{X}n}$ is negative value and $\overline{X}_n$ decreases rapidly with increasing the reaction temperature, therefore, the average molecular weights decreases with increasing the reaction temperature. This explanation confirms the above result at the reaction temperature of 80°C. Besides, the rising temperature up to 80°C reduces the magnitude of the auto-acceleration effect. These reasons led to smaller chain length or size of the copolymer particles than the reaction temperature of 70°C.

At 50°C, the average molecular weights is higher than 80°C, it may be concluded that the rate of polymerization carried out at 50°C is lower than it would be

Table 4.3 Effects of Reaction Temperature on Dispersion Copolymerization of Styrene and Methyl Methacrylate[a]

No.	Temp (°C)	$\overline{D}_n$[b,c] (μm)	CV[d,c] (%)	SD[e,c] (μm)	PSD[f]	$\overline{M}_n$	$\overline{M}_w$	$\overline{M}_w/\overline{M}_n$
T1	50	0.5	25.94	0.13	1.19	10461	21714	2.08
T2	60	0.6	7.53	0.04	1.02	11619	37123	3.20
T3	70	0.8	8.77	0.07	1.02	82445	125050	1.52
T4	80	0.6	5.96	0.03	1.01	3676	9217	2.51

[a]Reaction time = 10 h

[b]Calculated diameter

[c]Determined by Scanning Electron Microscope

[d]Coefficient of variation of number-average size

[e]Standard Deviation [f]Particle size distribution

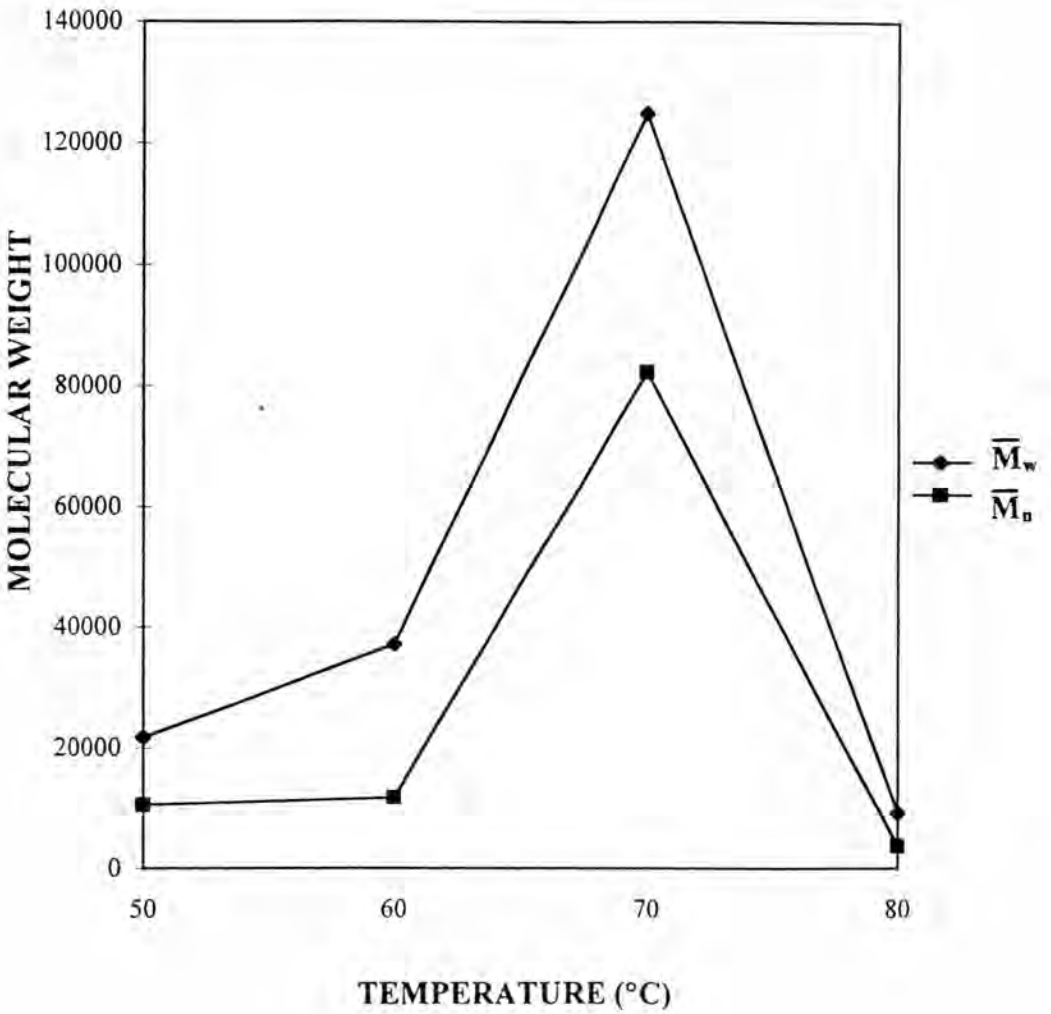

Figure 4.66 Effect of the reaction temperature on the average molecular weights of poly(styrene-*co*-methyl methacrylate)

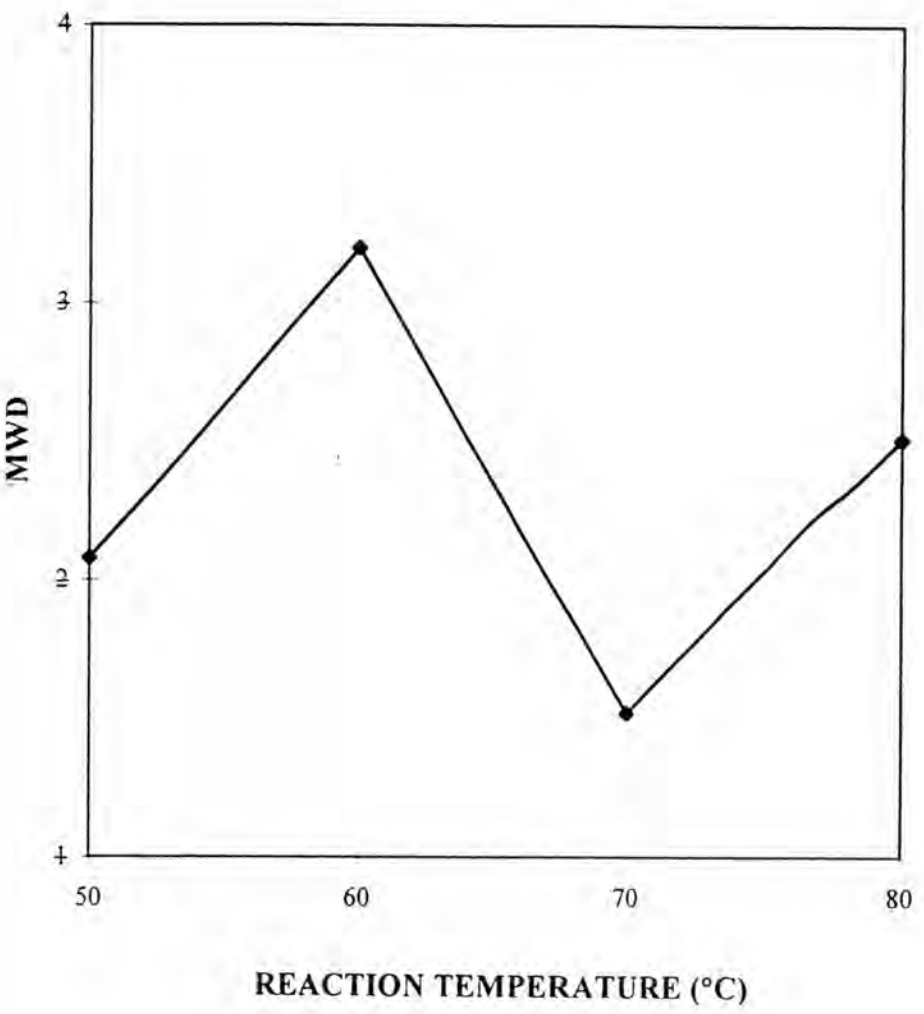

Figure 4.67 The curve of MWD of poly(styrene-*co*-methyl methacrylate) for various reaction temperatures

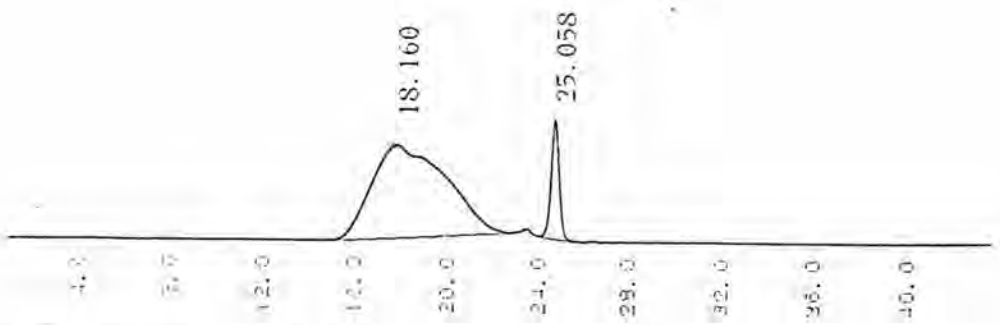

** CALCULATION REPORT **

CH	PKNO	TIME	AREA	HEIGHT	MK	IDNO	CONC
1	1	18.16	1222489	5560			87.3152
	2	25.058	177597	7148			12.6847
		TOTAL	1400086	12708			100

Peak information	Time (min)	Mol. size	Height
start	15.65	725314	29
top	18.16	77578	5508
end	19.05	35131	4755

Number-A.M.W.	$\overline{M}_n$	=	82445	Weight-A.M.W.	$\overline{M}_w$	=	125050
z-A.M.W.	$\overline{M}_Z$	=	196962	Visc-A.M.W.	$\overline{M}_v$	=	118242
Dispersity	$\overline{M}_w/\overline{M}_n$	=	1.51677	Dispersity	$\overline{M}_z/\overline{M}_w$	=	1.57506
Dispersity	$\overline{M}_v/\overline{M}_n$	=	1.43419	I. Viscosity	I. VISC	=	51.3121

Figure 4.68 The GPC chromatograph of the copolymer synthesized at 70°C

expected, that is, when considering the overall activation energy for the rate of polymerization in eq 4.21, the rate of polymerization for a temperature decrease by the overall activation energy (E_R) for most polymerizations initiated by thermal initiator decomposition is about 80-90 kJ/mole.

$$\ln R_p = \ln [A_p (A_d/A_t)]^{1/2} + \ln [(f[I]^{1/2}[M])] - \frac{E_R}{RT} \qquad (4.21)$$

The kinetic chain length is inversely dependent on the polymerization rate as given by

$$\nu = \frac{k_p^2[M]^2}{2k_t R_p} \qquad (4.22)$$

From above equation, decreasing of the rate of polymerization means an increase in the average molecular weights. In conclusion, at 80°C, the average molecular weight is lower than at 50°C, but the rate of polymerization is higher.

4.4 The Effect of the Agitation Rate on

4.4.1 The Particle Size and Particle Size Distribution of Poly(Styrene-*co*-Methyl Methacrylate)

In dispersion copolymerization, the mixture was polymerized with stirring in the reactor for 10 h. The rates of stirring were varied from 80 to 290 rpm. The sizes of copolymer particles are in the range of 0.6-0.8 μm. These results are presented in Table 4.4 and Figures 4.69-4.72. The particle size distribution of copolymer prepared with various agitation rate are shown in Figures 4.73-4.76. It was found that increasing the rates of mixing, the particle size of the copolymers decreases as shown in Figure 4.77. The smallest particle size obtained from the highest agitation rate gave the narrowest size distribution as shown in Figure 4.78. It is probably due to the free volume in the polymeric solution became smaller at increasing rates of mixing due to the system being more dynamic. The higher the agitation, the faster the chain diffusion and termination and the lower the molecular weight.

4.4.2 The Average Molecular Weights and Molecular Weight Distributions

The copolymer particles prepared with various agitation rates gave broad molecular weight distributions. The lowest average molecular weights with a narrowest molecular weight distribution is obtained at the agitation rate of 290 rpm as shown in Figures 4.79 and 4.80, respectively. As increasing the rates of mixing as high as 290 rpm, the shearing force exerted on the solution viscosity to permit faster segmental diffusion in the polymer solution increases, the average molecular weights of the copolymer is decreased, whereas a mild agitation of the reaction mixture, the copolymer with higher molecular weights is produced.

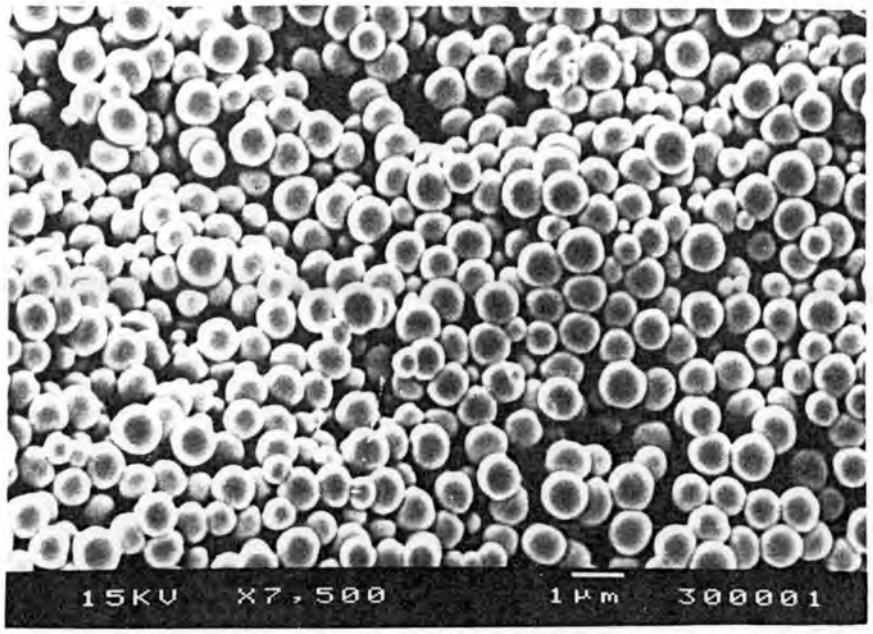

Figure 4.69 SEM micrograph of poly(styrene-*co*-methyl methacrylate) synthesized at an agitation rate of 80 rpm

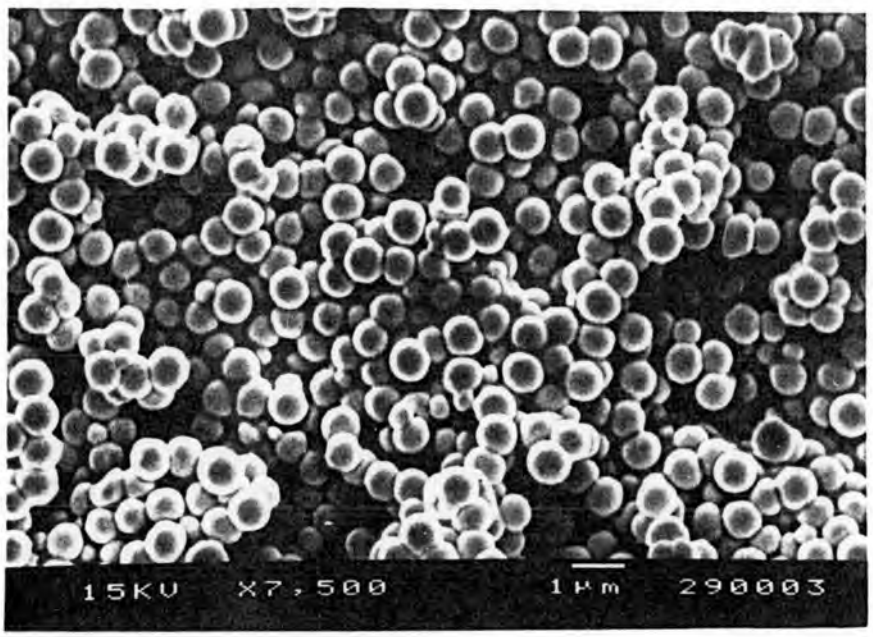

Figure 4.70 SEM micrograph of poly(styrene-*co*-methyl methacrylate) synthesized at an agitation rate of 150 rpm

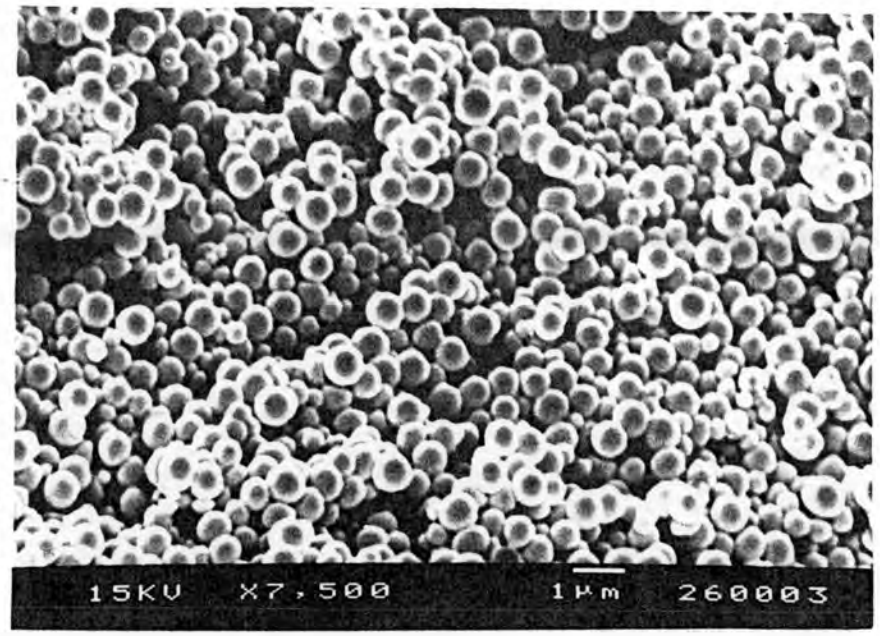

Figure 4.71 SEM micrograph of poly(styrene-*co*-methyl methacrylate) synthesized at an agitation rate of 200 rpm

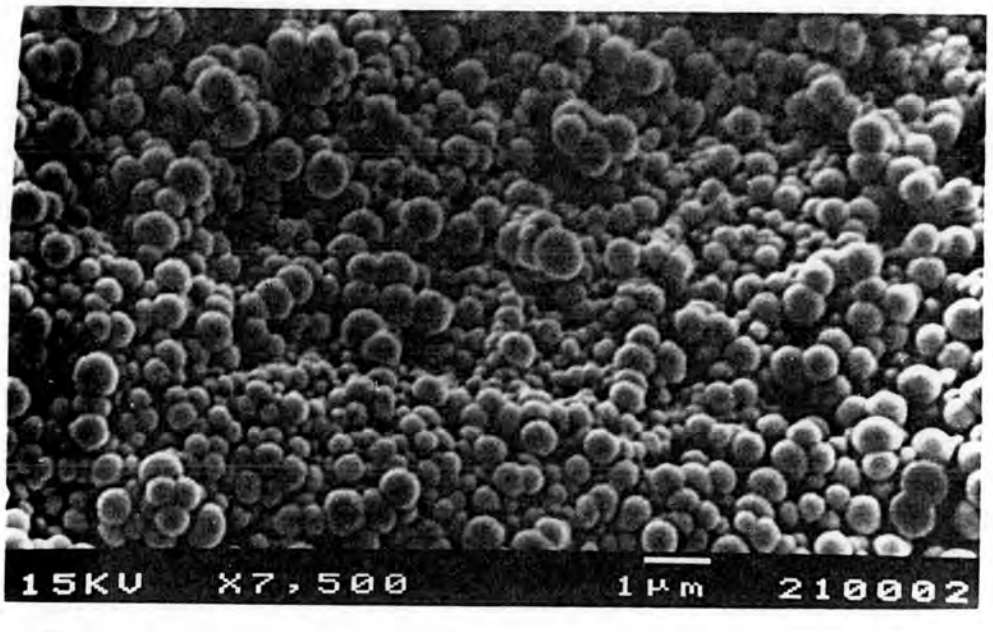

Figure 4.72 SEM micrograph of poly(styrene-*co*-methyl methacrylate) synthesized at an agitation rate of 290 rpm

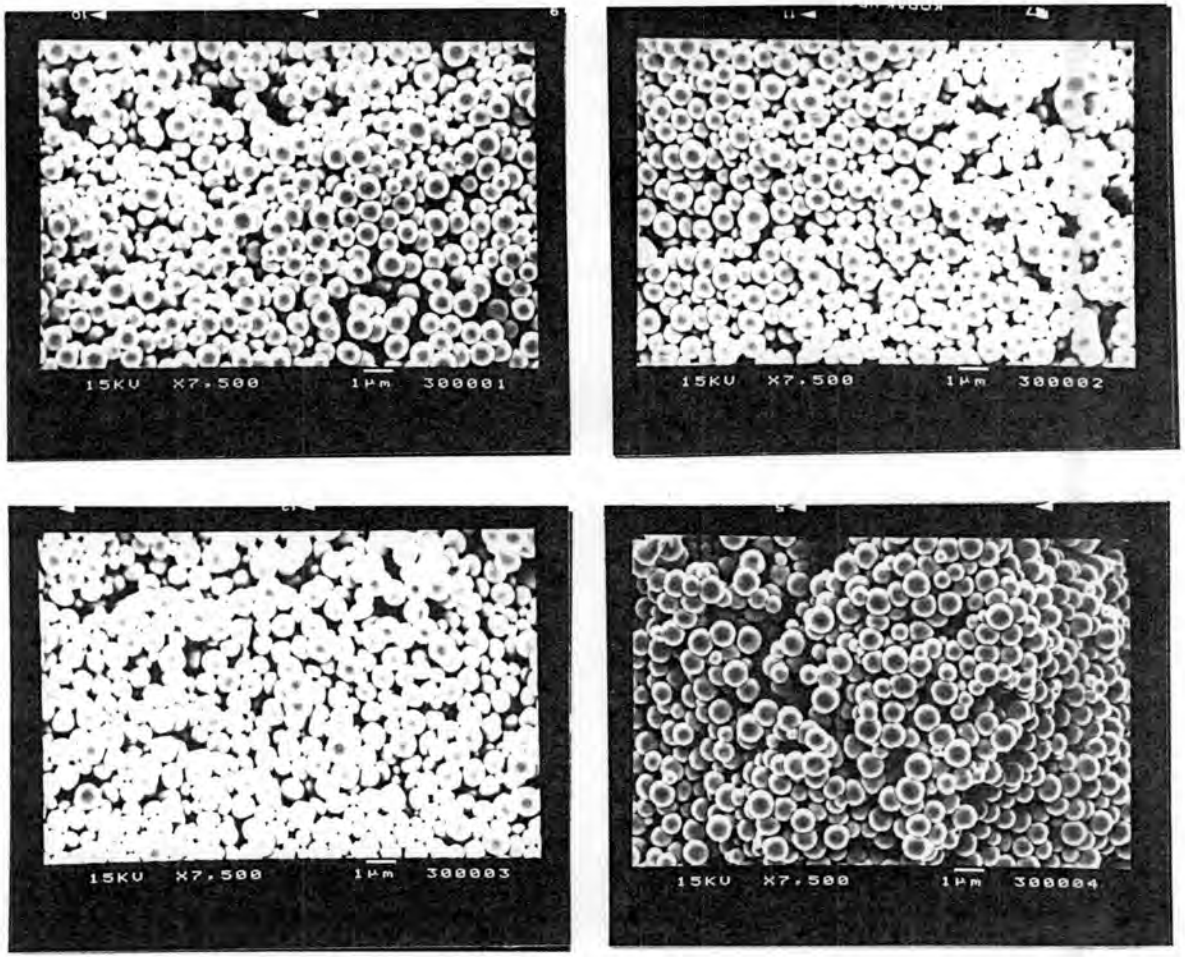

Figure 4.73 SEM micrographs for PSD measurement of poly(styrene-*co*-methyl methacrylate) synthesized at an agitation rate of 80 rpm

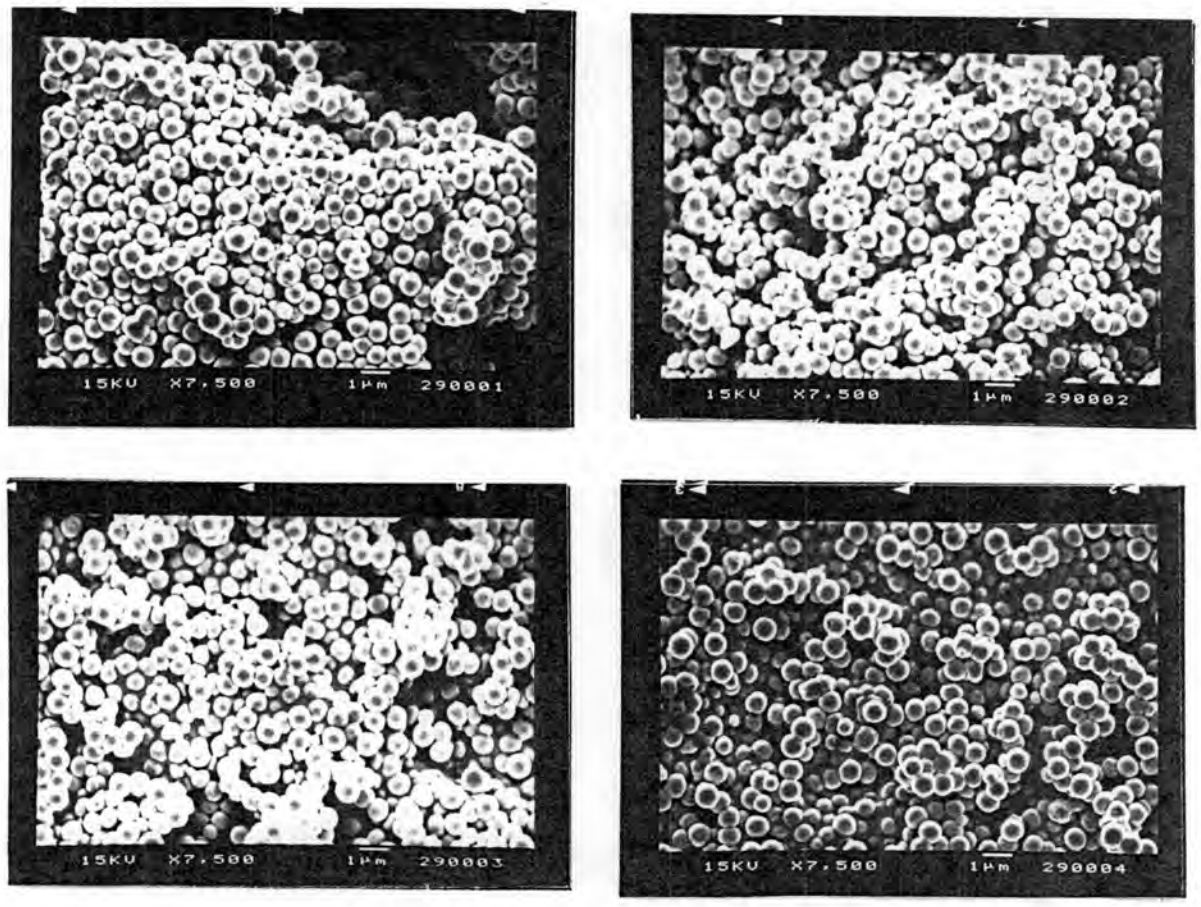

Figure 4.74 SEM micrographs for PSD measurement of poly(styrene-*co*-methyl methacrylate) synthesized at an agitation rate of 150 rpm

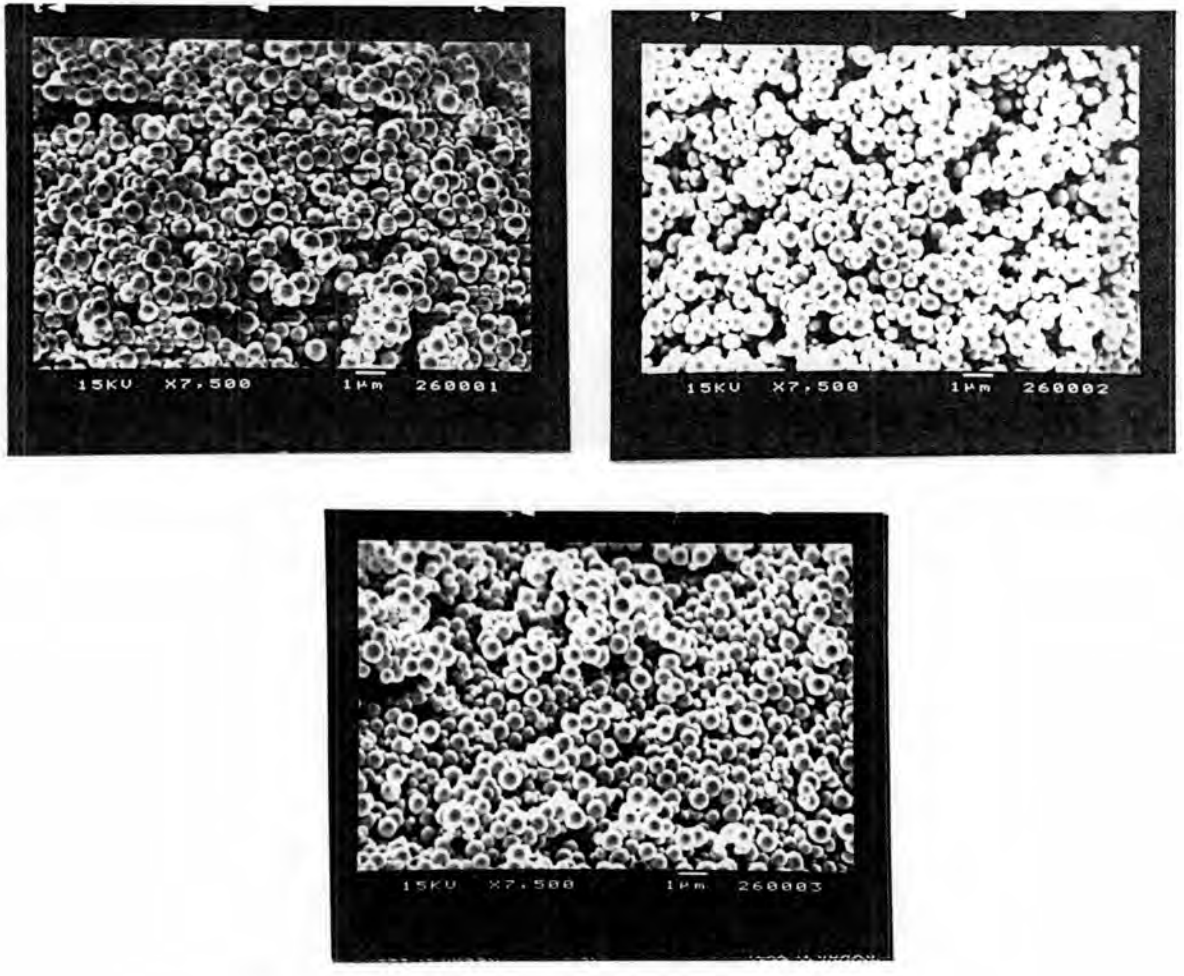

Figure 4.75 SEM micrographs for PSD measurement of poly(styrene-*co*-methyl methacrylate) synthesized at an agitation rate of 200 rpm

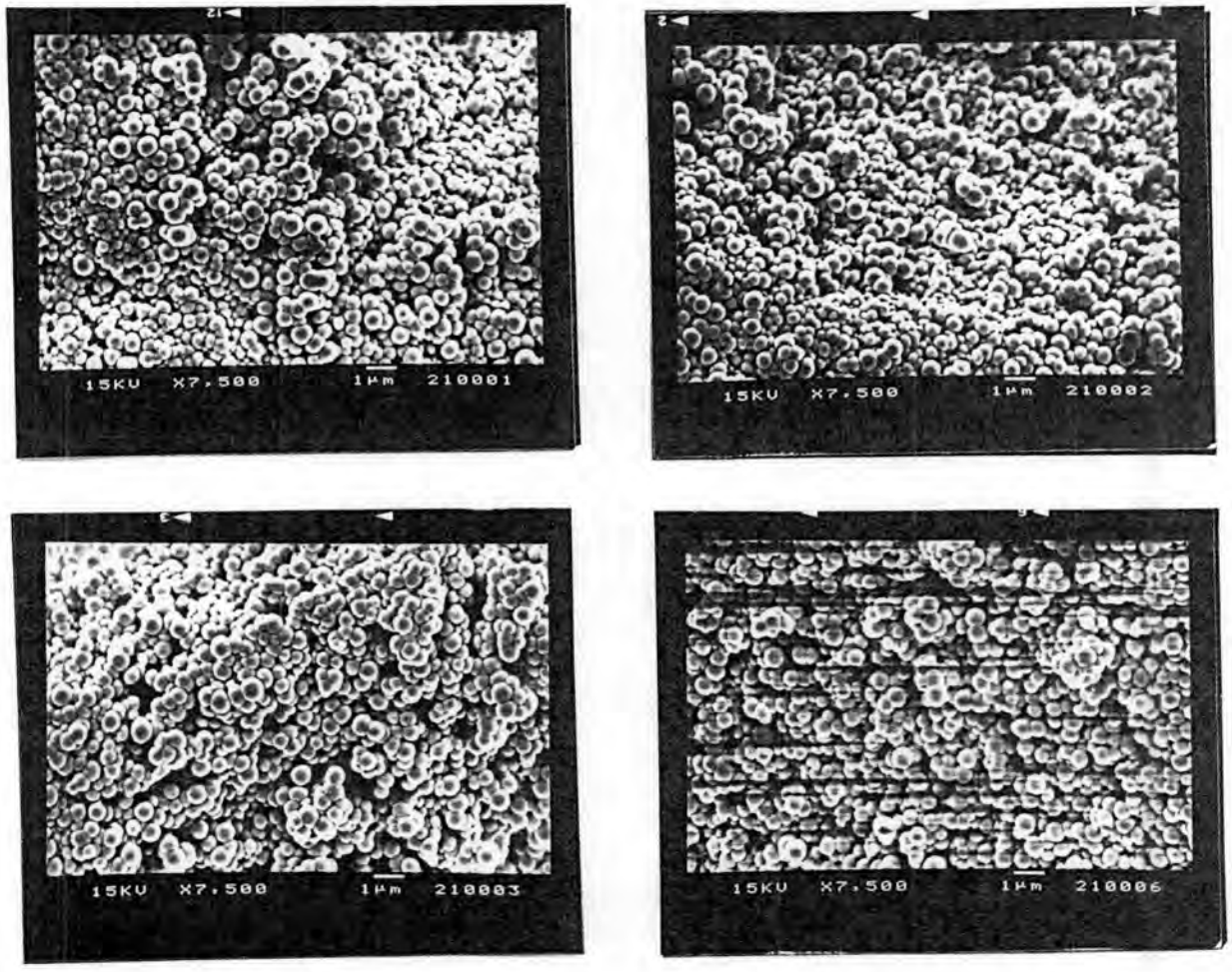

Figure 4.76 SEM micrographs for PSD measurement of poly(styrene-*co*-methyl methacrylate) synthesized at an agitation rate of 290 rpm

Table 4.4 Effects of Agitation Rate on Dispersion Copolymerization of Styrene and Methyl Methacrylate[a]

No.	Agitation Rate (rpm)	$\bar{D}_n$[b,c] (μm)	CV[d,c] (%)	SD[e,c] (μm)	PSD[f]	$\bar{M}_n$	$\bar{M}_w$	$\bar{M}_w/\bar{M}_n$
A1	80	0.8	8.72	0.07	1.02	35125	156218	4.45
A2	150	0.8	8.32	0.06	1.02	31336	143985	4.59
A3	200	0.7	9.86	0.07	1.03	34413	150799	4.38
A4	290	0.6	7.53	0.04	1.02	11619	37123	3.20

[a]Reaction temperature = 60°C, reaction time 10 h

[b]Calculated diameter

[c]Determined by Scanning Electron Microscope

[d]Coefficient of variation of number-average size

[e]Standard Deviation [f]Particle size distribution

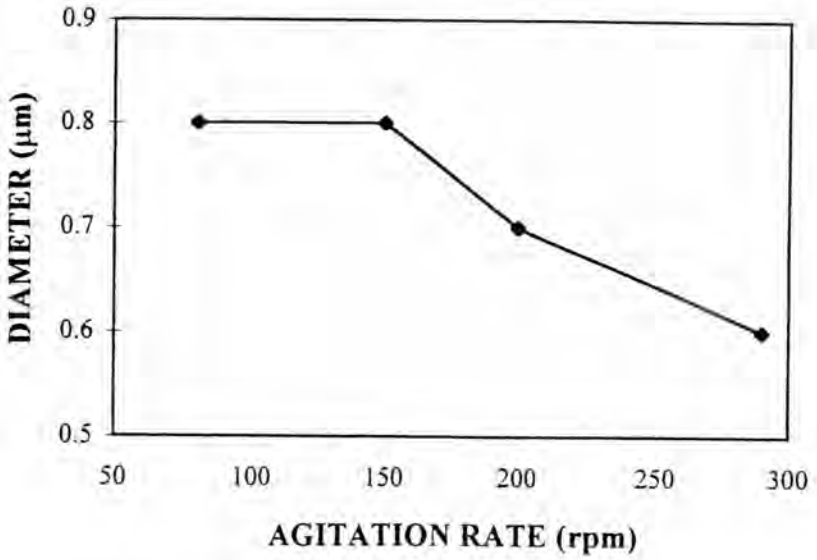

Figure 4.77 Effect of the agitation rate on the particle size of poly(styrene-*co*-methyl methacrylate)

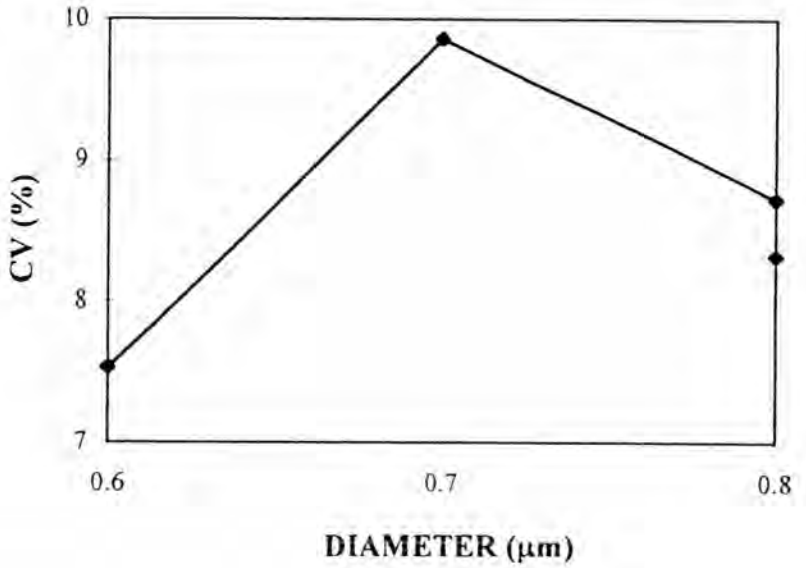

Figure 4.78 Relationship between the average particle size and CV of poly(styrene-*co*-methyl methacrylate) prepared with various agitation rates

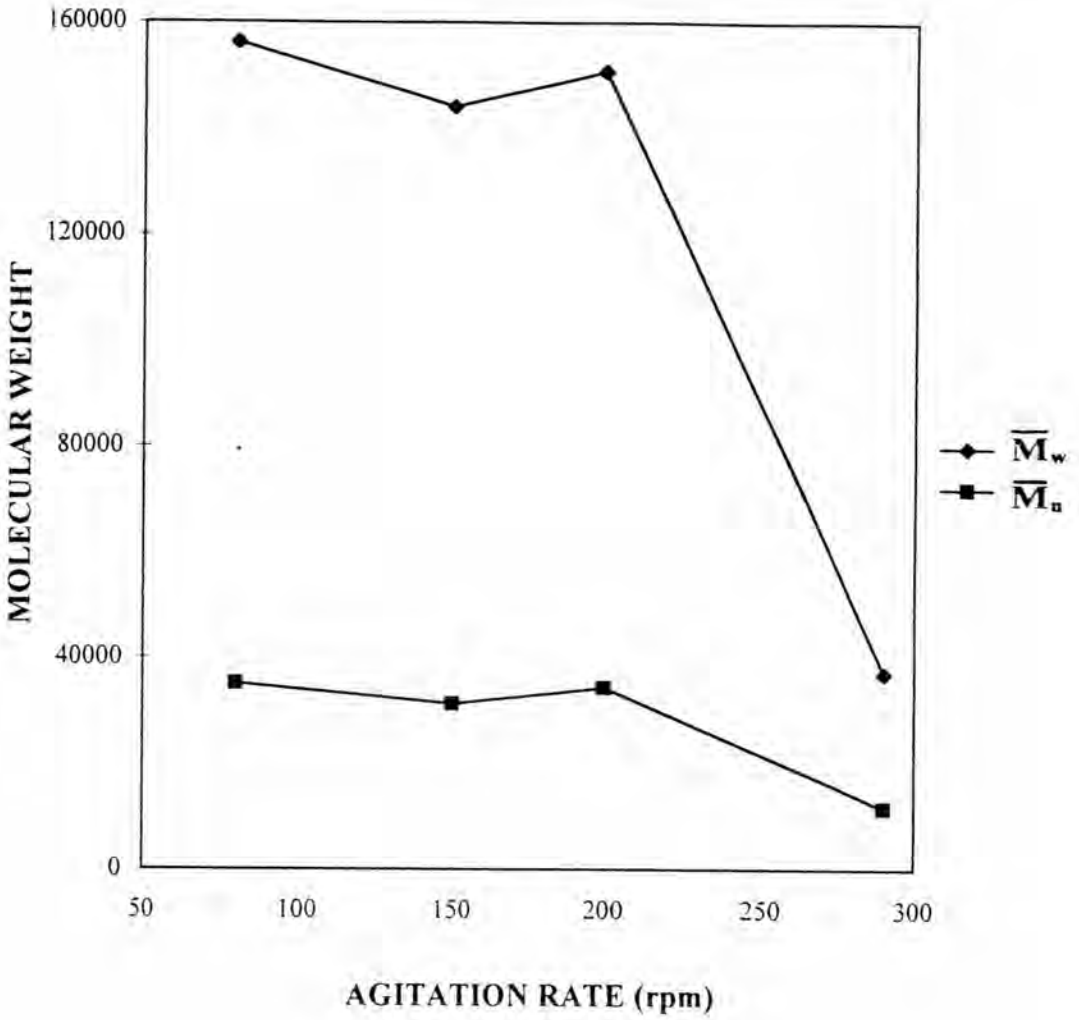

Figure 4.79 Effect of the agitation rate on the average molecular weights of poly(styrene-*co*-methyl methacrylate)

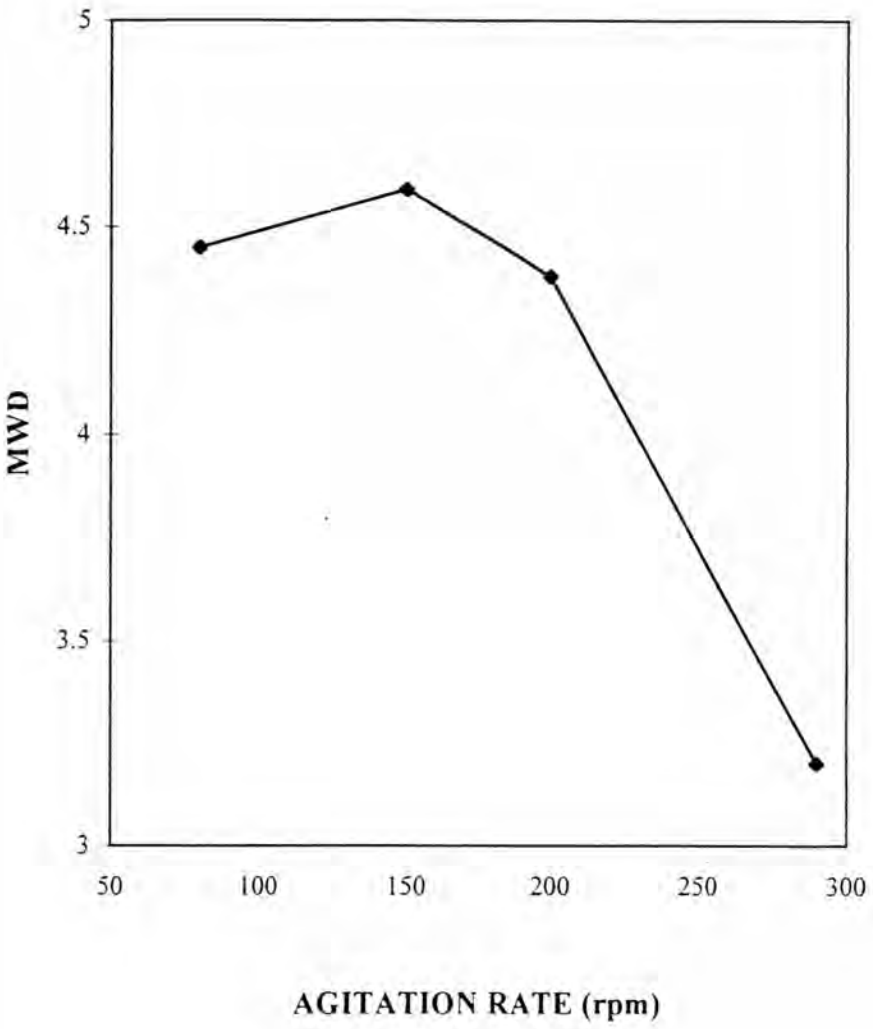

Figure 4.80 The curve of MWD of poly(styrene-*co*-methyl methacrylate) for various agitation rates

4.5 The Effect of the Reaction Time on

4.5.1 The Particle Size and Particle Size Distribution of Poly(Styrene-*co*-Methyl Methacrylate)

In this research, the reaction time is also investigated. The sizes of copolymer particles are in the range of 0.3-0.6 μm as shown in Figures 4.81-4.84. The particle size distribution of copolymer prepared with various reaction times are shown in Figures 4.85-4.88. The effect of the particle size on the reaction time is presented in Table 4.5 and Figure 4.89.

Increasing the reaction time, no new polymer nuclei are formed after the initial precipitation of polymer particles because they are inaccessible and the size distribution is very narrow as shown in Figure 4.90. Following the nucleation stage, subsequent polymerization is confined to further growth of the polymer particles formed initially. The predominant mode of polymerization is carried out by monomers being absorbed into the interior of the polymer particles. Besides, as soon as particles have been formed they began to capture some of the oligomer molecules before they can take part in forming new nuclei. As the size of the particles grow, this competing process becomes dominant and more or less rapidly reduces the rate of nucleation to negligible proportions Therefore, the special feature of polymerizing systems, involving growth of individual molecules, permits rapid attainment of steady-state conditions of nucleation. The chain-length or the size of particles of the polymer is therefore increased with increasing the reaction time. These larger-sized particles size gave also a narrower size distribution than smaller-sized ones.

The mechanism for particle formation and growth in the dispersion polymerization is presented in Figure 4.2 (53). At the start of the polymerization, monomer, matrix polymer, and initiator, is dissolved in a diluent (a). Upon heating with stirring, primary radicals, generated by decomposition of the initiator, grow in the continuous phase by the addition of monomer units to form growing oligomer chains with a reactive free radical at the end (b). At a critical chain length, the oligomers precipitate and aggregate with each other, concurrently, they adsorb the stabilizer and finally become stable particle nuclei (c). The stable particle nuclei capture the oligomer radicals and nuclei generated in the continuous phase and thus reduce the rate of particle formation. As long as enough stable particles are formed to capture all of the oligomer radicals and nuclei, no more new particles will be formed and the particle formation stage is complete. The existing particles continue to grow by capturing the nuclei, absorb monomer from the continuous phase and capturing the oligomer radicals which will either continue to grow inside the particles or terminate with other radicals (d). At the end of the polymerization, nuclei formation stops owing to the exhaustion of either the monomer or the radicals, only stable particles are finally observed (e).

In the formation of a stable polymer, the random grafting onto a soluble polymer is the simplest method for preparing a graft copolymer which is used as a stabilizer in dispersion systems. The formation of graft copolymer is dependent on the generation of a reactive radical site on the soluble polymer molecule by hydrogen abstraction or by radical addition to a double bond. Stages in the formation of random graft stabilizers is an important factor in the mechanism for particle formation as given in Section 4.1.2.

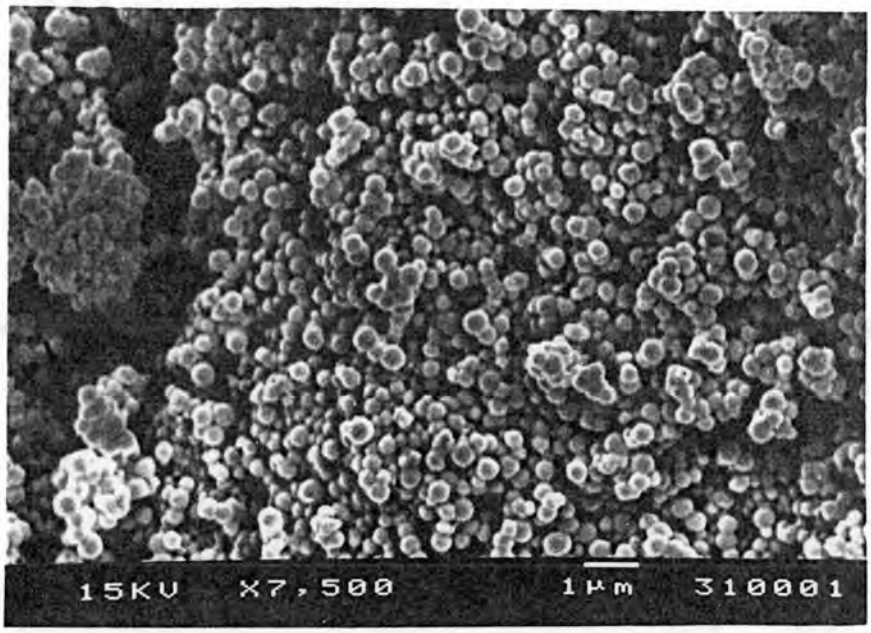

Figure 4.81 SEM micrograph of poly(styrene-*co*-methyl methacrylate) synthesized for 6 h reaction time

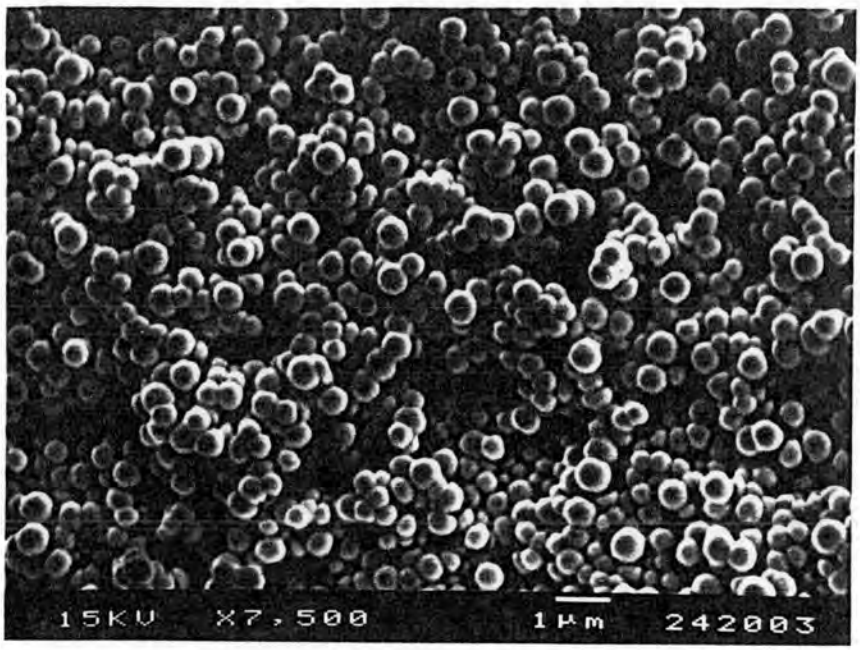

Figure 4.82 SEM micrograph of poly(styrene-*co*-methyl methacrylate) synthesized for 8 h reaction time

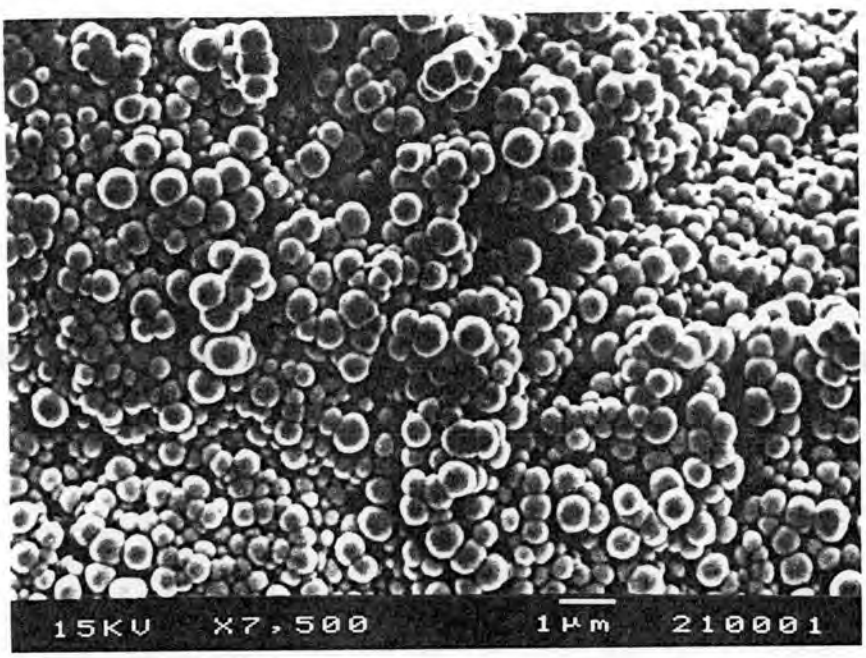

Figure 4.83 SEM micrograph of poly(styrene-*co*-methyl methacrylate) synthesized for 10 h reaction time

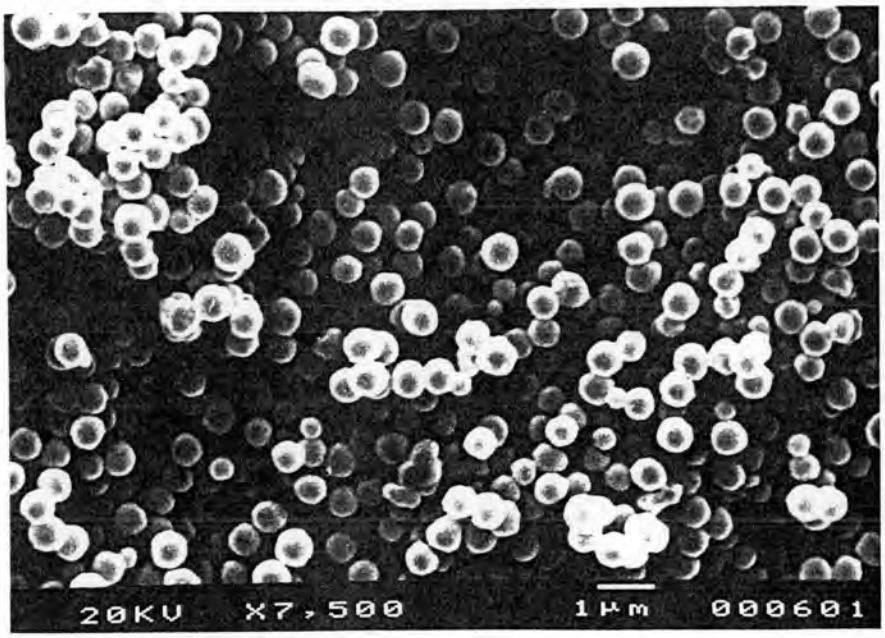

Figure 4.84 SEM micrograph of poly(styrene-*co*-methyl methacrylate) synthesized for 15 h reaction time

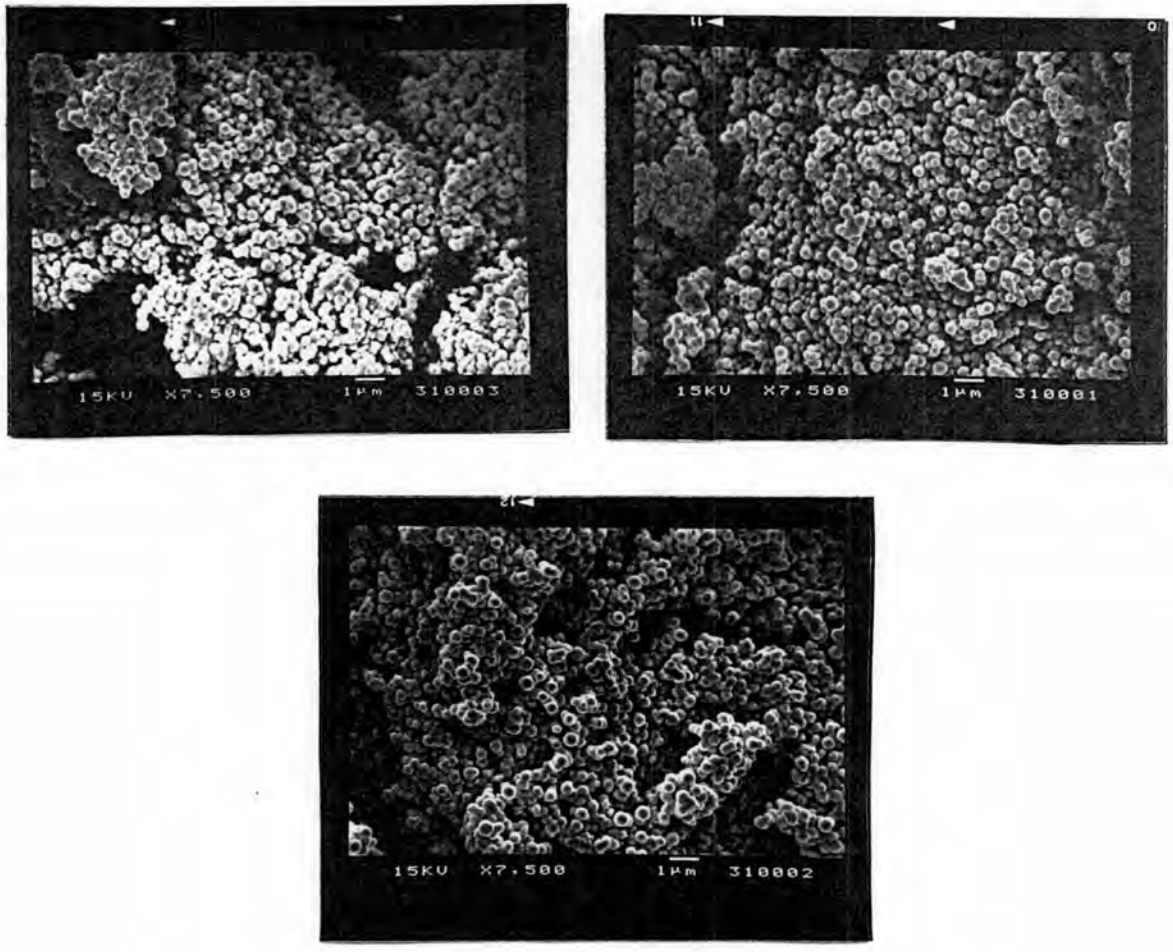

Figure 4.85 SEM micrographs for PSD measurement of poly(styrene-*co*-methyl methacrylate) synthesized for 6 h reaction time

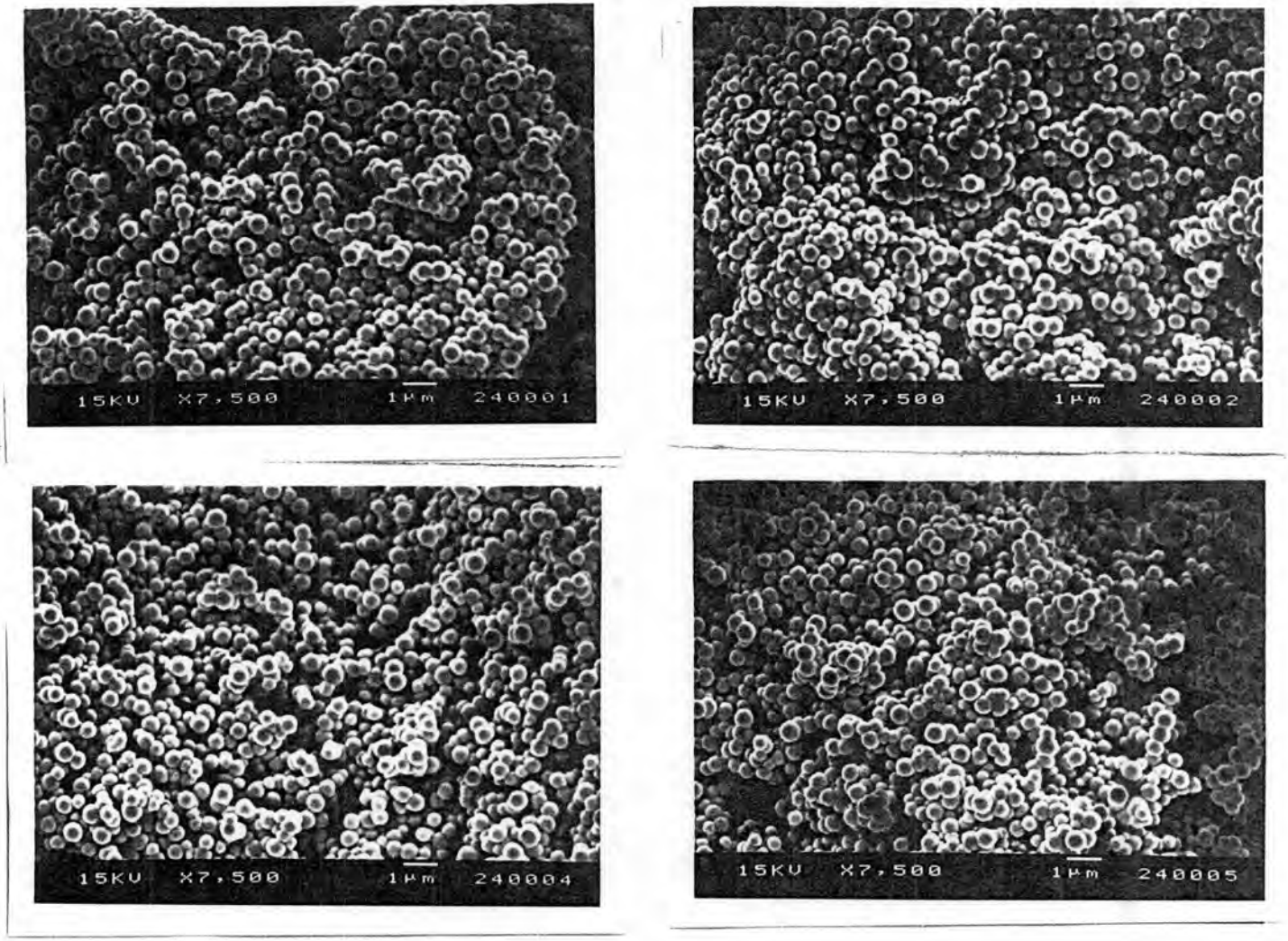

Figure 4.86 SEM micrographs for PSD measurement of poly(styrene-*co*-methyl methacrylate) synthesized for 8 h reaction time

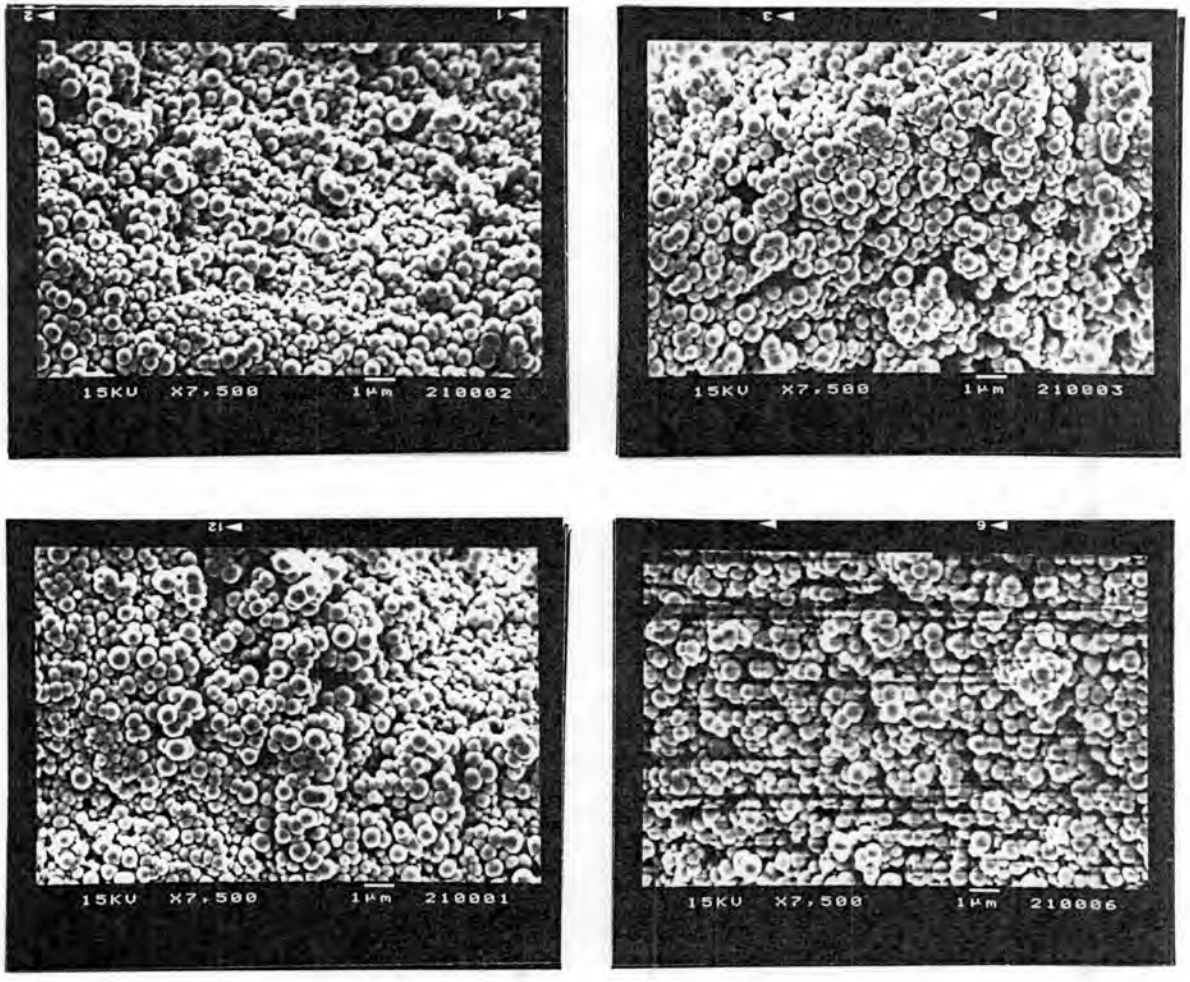

Figure 4.87 SEM micrographs for PSD measurement of poly(styrene-*co*-methyl methacrylate) synthesized for 10 h reaction time

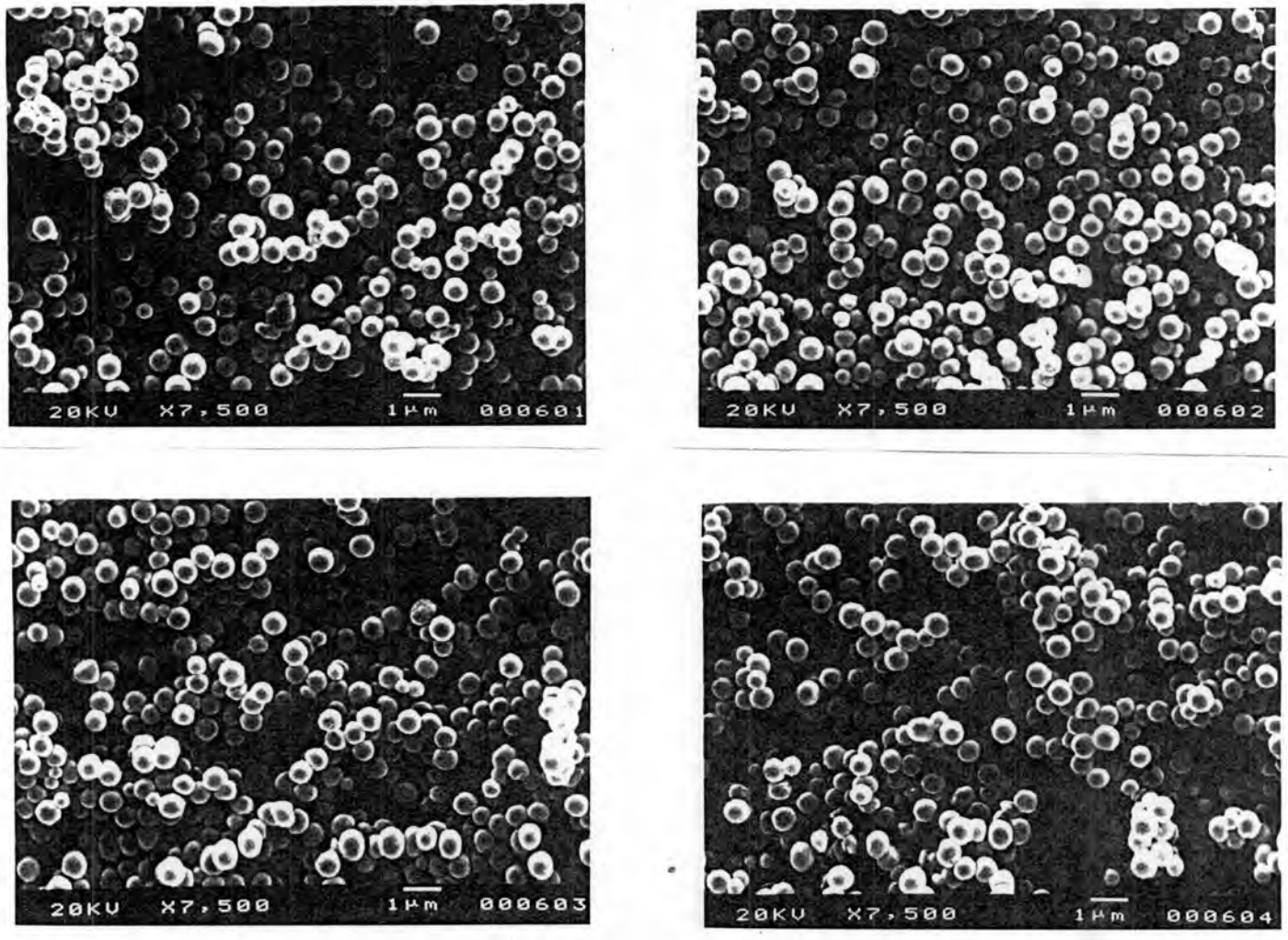

Figure 4.88 SEM micrographs for PSD measurement of poly(styrene-*co*-methyl methacrylate) synthesized for 15 h reaction time

Table 4.5 Effects of Reaction Time on Dispersion Copolymerization of Styrene and Methyl Methacrylate[a]

No.	Time (h)	$\bar{D}_n$[b,c] (μm)	CV[d,c] (%)	SD[e,c] (μm)	PSD[f]	$\bar{M}_n$	$\bar{M}_w$	$\bar{M}_w/\bar{M}_n$	F[g,h] (mole% STY)
T1	6	0.3	16.97	0.05	1.08	14099	28198	2.00	73.56
T2	8	0.4	14.09	0.06	1.07	19183	48559	2.53	81.99
T3	10	0.6	7.53	0.04	1.02	11619	37123	3.20	81.66
T4	15	0.6	8.33	0.05	1.05	112036	214032	1.91	79.18 (78.04)[i]

[a]Reaction temperature = 60°C

[b]Calculated diameter

[c]Determined by Scanning Electron Microscope

[d]Coefficient of variation of number-average size

[e]Standard Deviation [f]Particle size distribution

[g]Copolymer composition, determined by Nuclear Magnetic Resonance

[h]Known mole% styrene = 75 mole% [i]Determined by Elemental Analysis

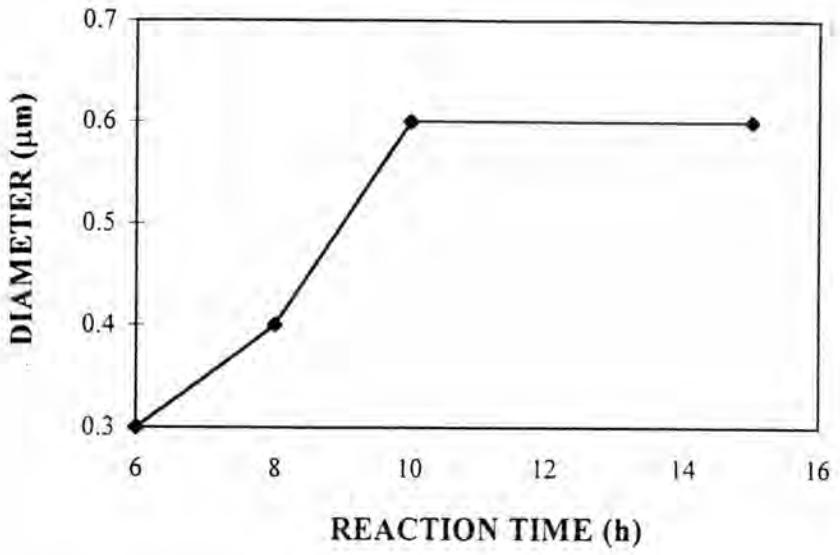

Figure 4.89 Effect of the reaction time on the particle size of poly(styrene-*co*-methyl methacrylate)

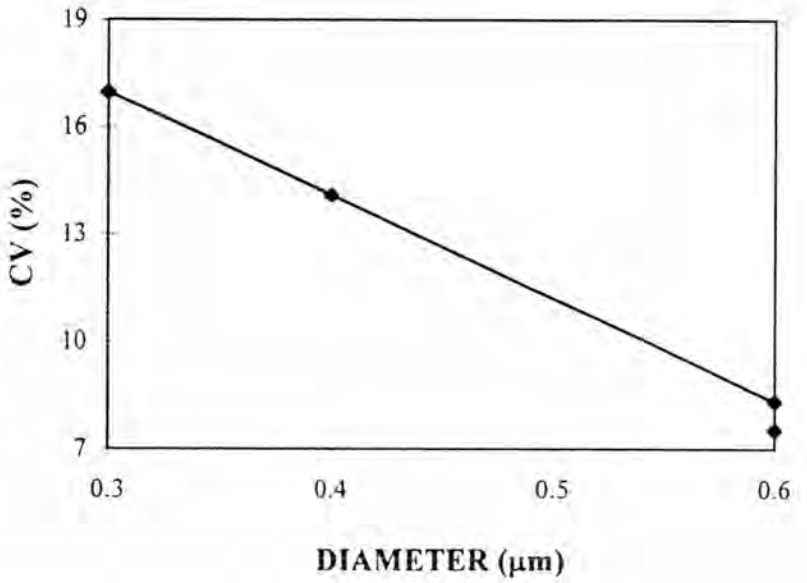

Figure 4.90 Relationship between the average particle size and CV of poly(styrene-*co*-methyl methacrylate) prepared with various reaction times

4.5.2 The Average Molecular Weights and Molecular Weight Distribution of Poly(Styrene-*co*-Methyl Methacrylate)

As the polymerization progresses, the critical chain length of oligomer radical is increased and the growth of the copolymer particles is increased as above mentioned. The average molecular weights is gradually increasing, the complete of the polymerization or high conversion gave larger particle sizes with the higher average molecular weights as given in Figure 4.91. The average molecular weights is increased from 28198 to 214032 as the polymerization proceedes from 6 to 15 h. The molecular weight distribution is in the range of 1.91-3.20 as shown in Figure 4.92.

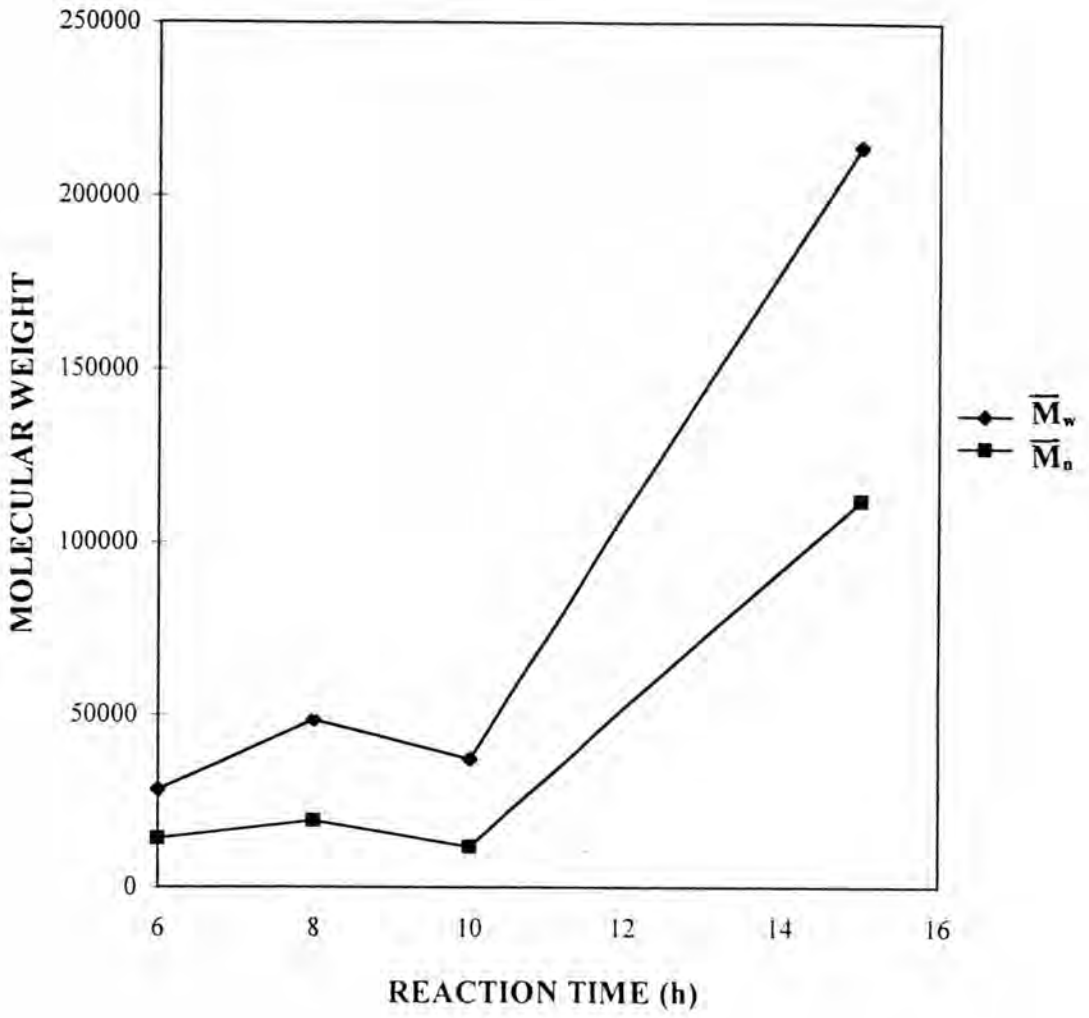

Figure 4.91 Effect of the reaction time on the average molecular weights of poly(styrene-*co*-methyl methacrylate)

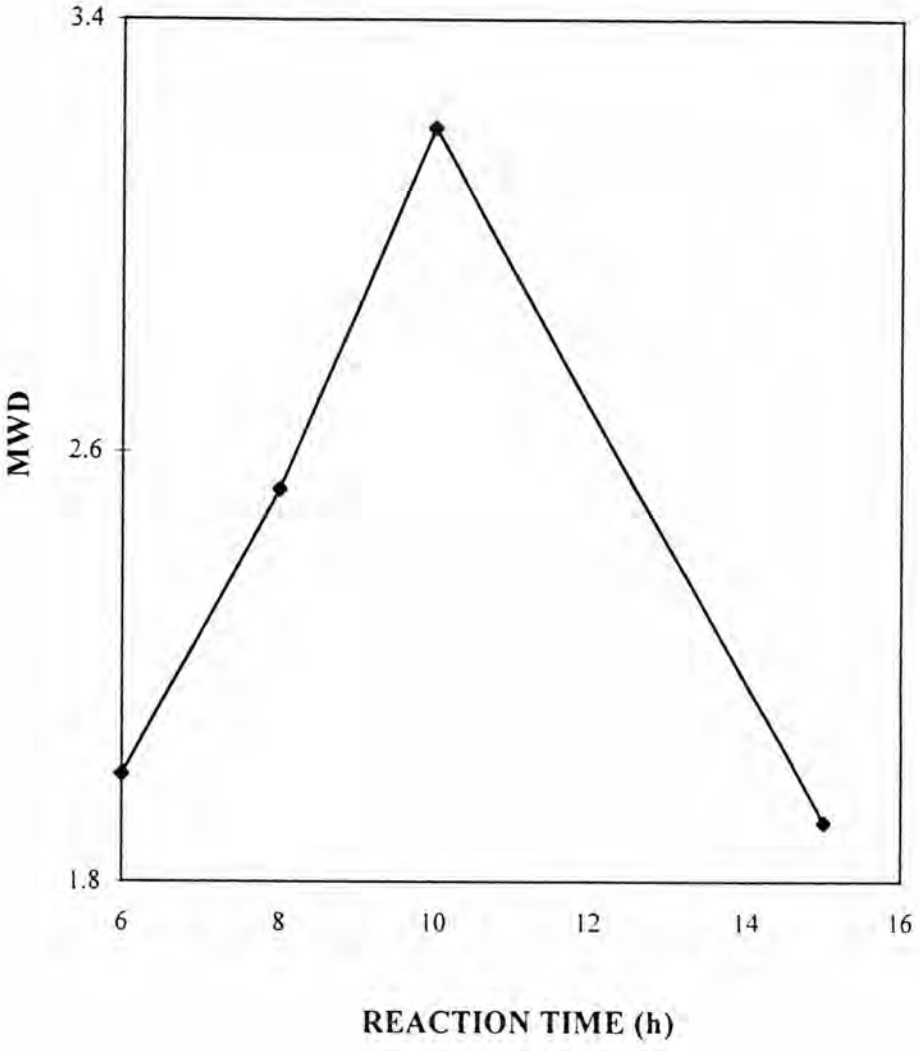

Figure 4.92 The curve of MWD of poly(styrene-*co*-methyl methacrylate) for various reaction times

4.6 The Effect of the Feed Ratio of Styrene/Methyl Methacrylate on

4.6.1 The Particle Size and Particle Size Distribution of Poly(Styrene-*co*-Methyl Methacrylate)

In this group of experiment, the feed ratio of styrene/methyl methacrylate was varied, the matrix polymer concentration and other conditions remained constant. The copolymer particles were prepared with different styrene/methyl methacrylate ratios of 100/0, 75/25, 50/50, 25/75, and 0/100.

Figures 4.93-4.97 show SEM photographs of the copolymer prepared from the above conditions. Figures 4.98-4.102 show SEM photographs of the particle size distribution of the copolymer and the homopolymers. Varying the feed ratios of styrene/methyl methacrylate, the smallest particle size (0.3 μm) was obtained for homopolymer of polystyrene and the very large particle size (11.82 μm) with the larger broad size distribution was obtained for homopolymer of poly(methyl methacrylate), which is the characteristic of the more polar monomers such as MMA. The solvent mixture of 70/30 ethanol/water (δ_pEtOH = 8.8, $\delta_p H_2O$ = 16.0 $(MPa)^{1/2}$) is a good solvent for methyl methacrylate monomer (δ = 18.0 $(MPa)^{1/2}$) with a $\Delta\delta$ ($\delta_p H_2O$-δMMA) value of about 2 units, the critical chain length of oligomer radical chains disentangle to render the very concentrated monomer to give the very long resulting the very large particle size of poly(methyl methacrylate). For polystyrene, 70/30 ethanol/water is a rather poor solvent for styrene monomer (δ_pSTY = 1.0 $(MPa)^{1/2}$) with a $\Delta\delta$ (δ_pEtOH-δ_pSTY) value of about 7.8 units, the critical chain length of oligomer radical chains is shorter than that of methyl methacrylate resulting in the smallest particle sizes.

In the range of 25% styrene to 100% styrene, the particle sizes so obtained are in the size range of 0.7-0.3 μm. With increasing the mole percent of the styrene feed from 25% to 100%, the particle sizes were found as shown in Figure 4.103. The curve of particle size distribution is given in Figure 4.104.

It is probably due to different monomer interactions with the matrix polymer, PVP. During the particle nucleation, in-situ grafting of the matrix polymer involving abstraction of hydrogen from the PVP molecule to create free radical sites (PVP•) can accept monomers. Styrene monomer is adsorbed much stronger on the free radical-PVP molecule than is the methyl methacrylate monomer, as the styrene monomer is a stronger electron donor for the PVP matrix and there were more styrene radicals than methyl methacrylate radicals in the reaction mixture (the reactivities of styrene and methyl methacrylate in radical copolymerization are 0.52 and 0.46, respectively) (54). Besides, the reactivity of styrene monomer toward the poly(methyl methacrylate) radical ($1/r_{STY} = 2.2$) is higher than the reactivity of methyl methacrylate monomer toward the polystyrene radical ($1/r_{MMA} = 1.9$), leading to a larger particle size. More styrene radicals than methyl methacrylate radicals are in the reaction mixture leading to a higher styrene content in the copolymer composition as shown in Table 4.6.

Considering the structure of styrene monomer, it shows that the phenyl substituent increases the reactivity of monomer attrack toward PVP radical. Monomer reactivities corresponds to the order of increased resonance stabilization by the particular substituent of the radical formed from the monomer (55). Substituents composed of unsaturated linkages are most effective in stabilizing the radicals because

of the loosely held π-electrons, which are available for resonance stabilization such as in case of styrene monomer as given below:

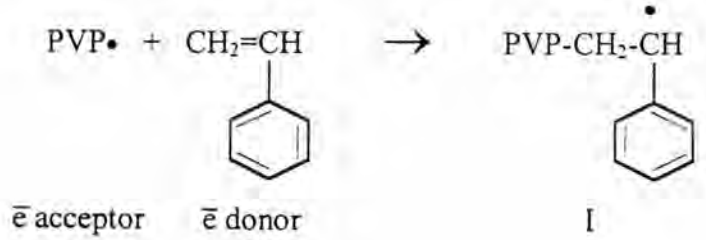

(4.23)

Resonance stabilization of structure I can occur as follows :

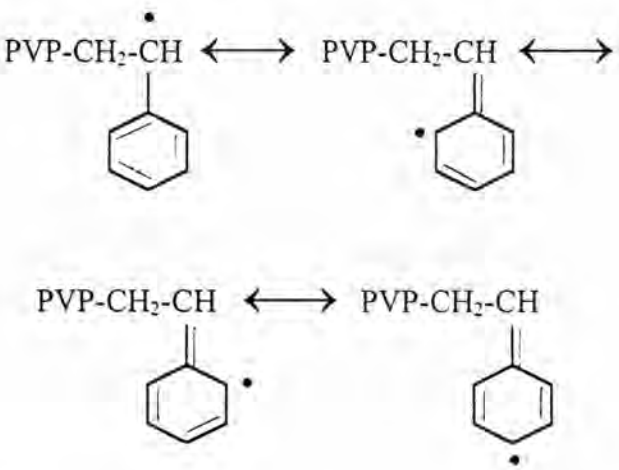

(4.24)

The phenyl substituent is able to stabilize the propagating radicals by delocalizing the radical over two or more atoms. Due to this resonance effect the overall activation energy of the monomer and its polymer radicals is low. Hence, the stage of aggregation of oligomer radical chains is in a short time range after the faster stabilized particles. Therefore, the number of aggregated oligomer chains in each particle is smaller to result in a smaller particle size.

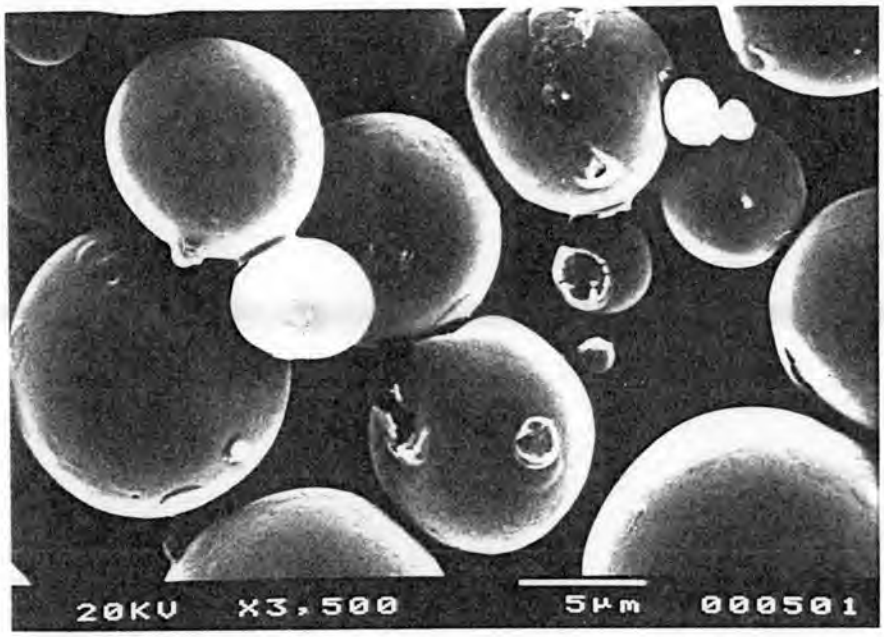

Figure 4.93 SEM micrograph of poly(methyl methacrylate) prepared by dispersion polymerization

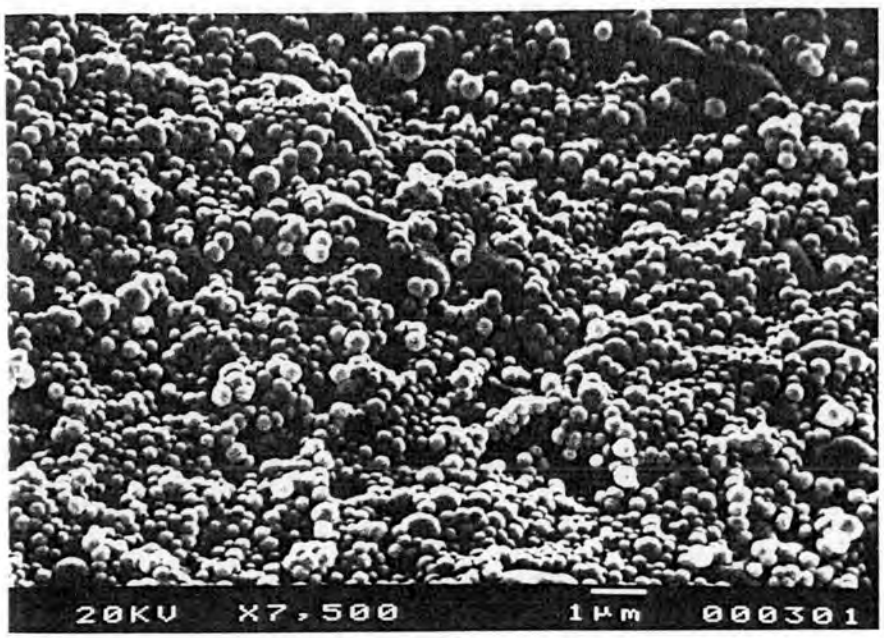

Figure 4.94 SEM micrograph of polystyrene prepared by dispersion polymerization

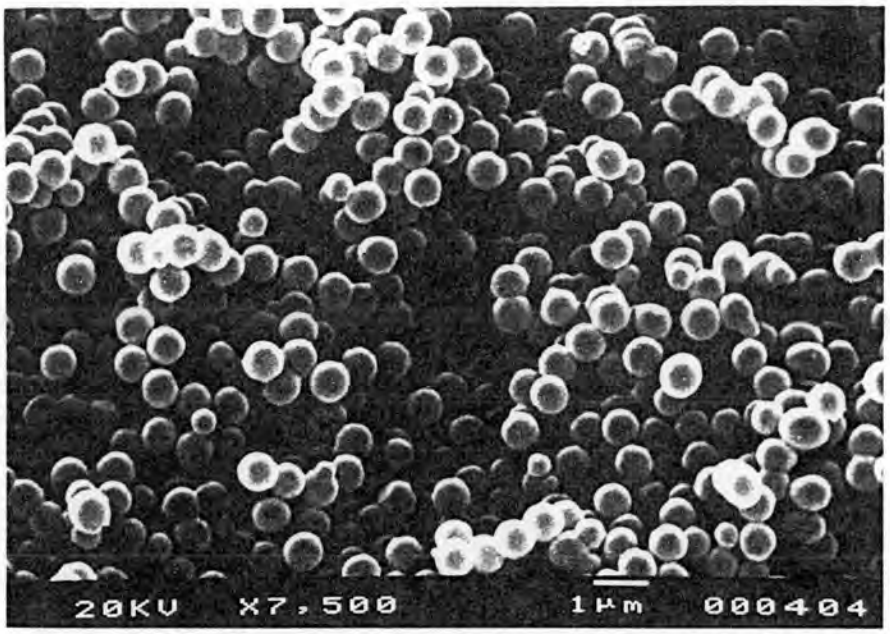

Figure 4.95 SEM micrograph of poly(styrene-*co*-methyl methacrylate) composed of 25% styrene

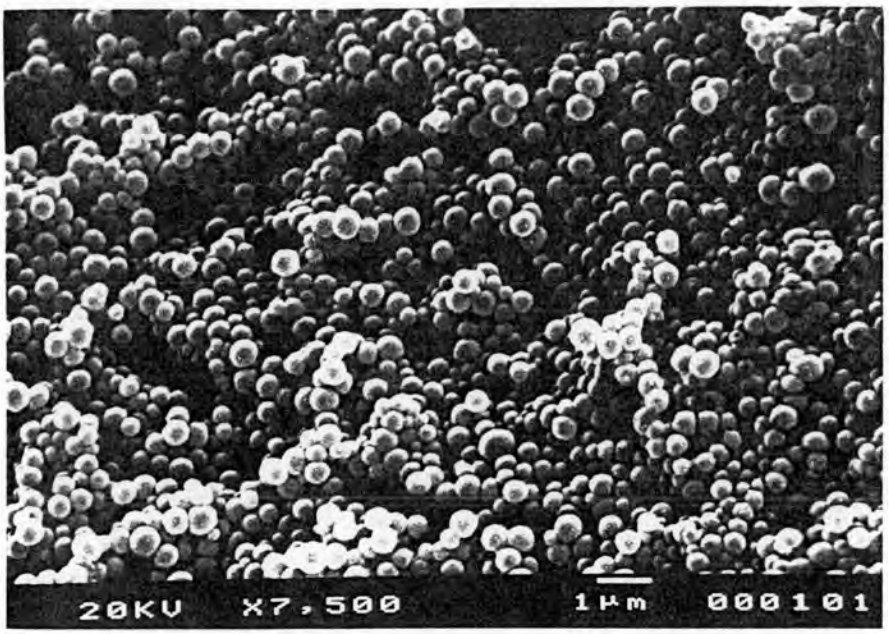

Figure 4.96 SEM micrograph of poly(styrene-*co*-methyl methacrylate) composed of 50% styrene

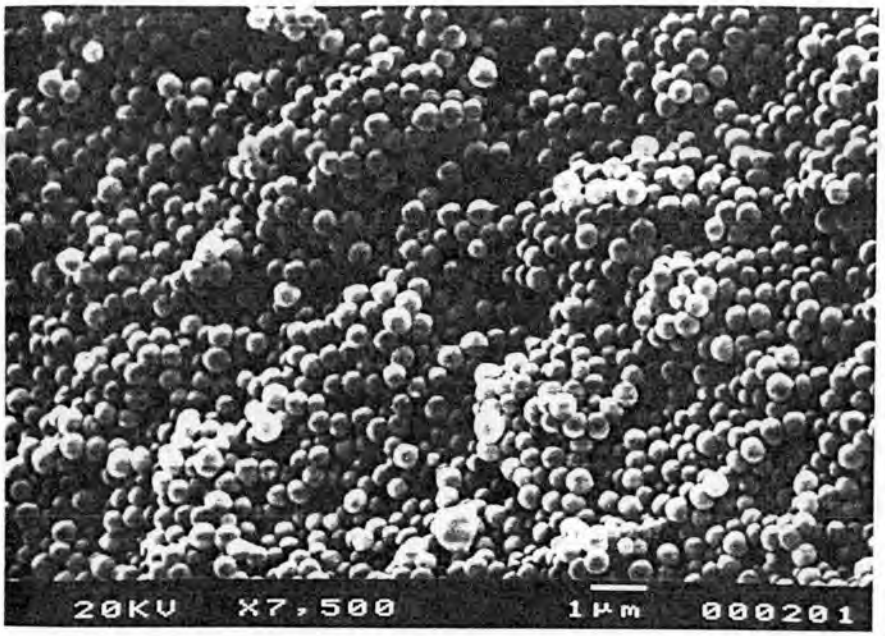

Figure 4.97 SEM micrograph of poly(styrene-*co*-methyl methacrylate) composed of 75% styrene

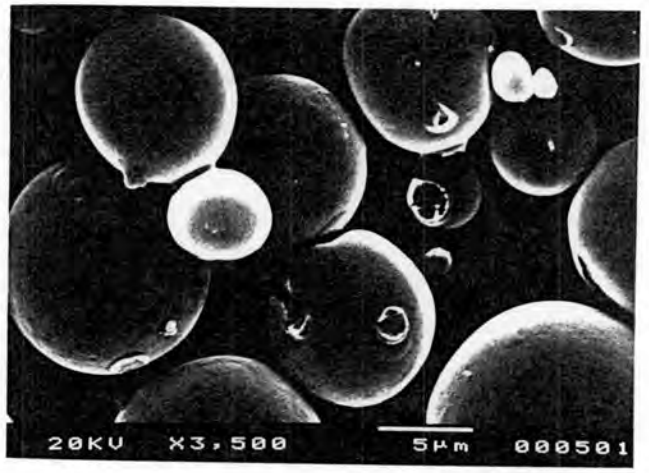

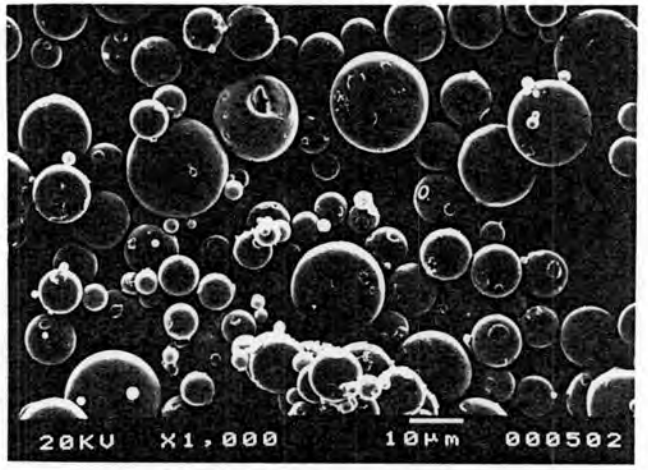

Figure 4.98 SEM micrographs for PSD measurement of poly(methyl methacrylate) prepared by dispersion polymerization

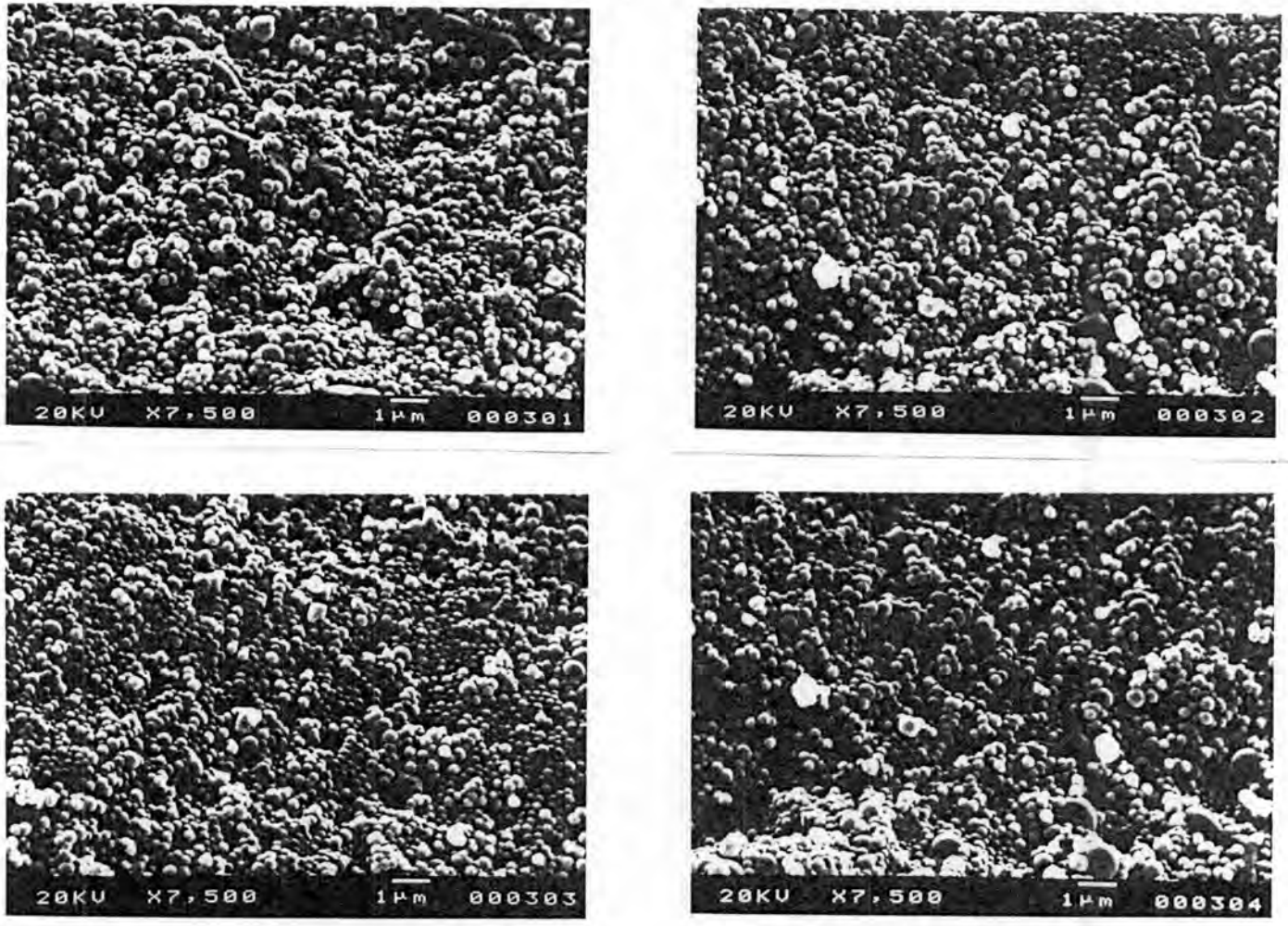

Figure 4.99 SEM micrographs for PSD measurement of polystyrene prepared by dispersion polymerization

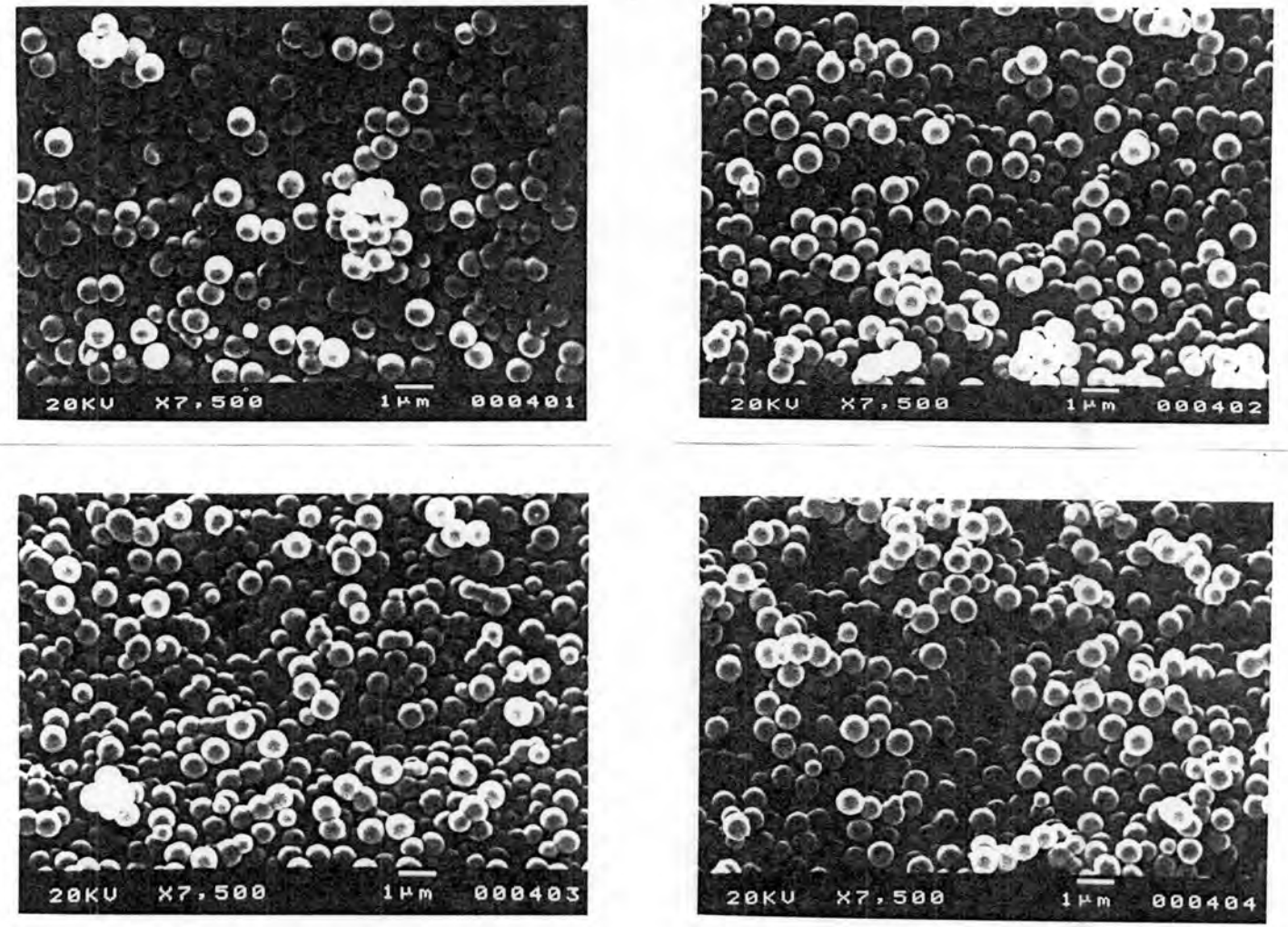

Figure 4.100 SEM micrographs for PSD measurement of poly(styrene-*co*-methyl methacrylate) composed of 25% styrene

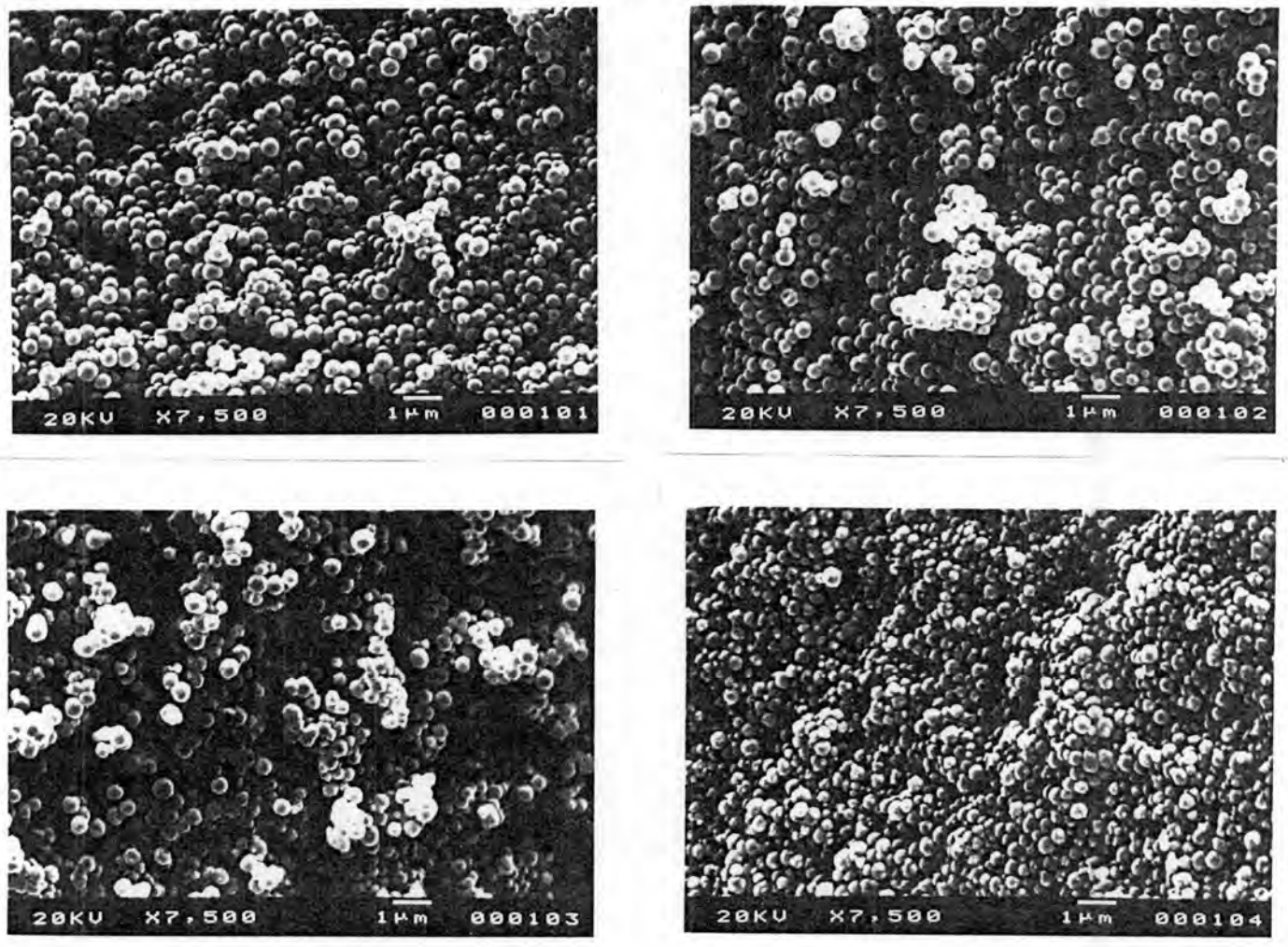

Figure 4.101 SEM micrographs for PSD measurement of poly(styrene-*co*-methyl methacrylate) composed of 50% styrene

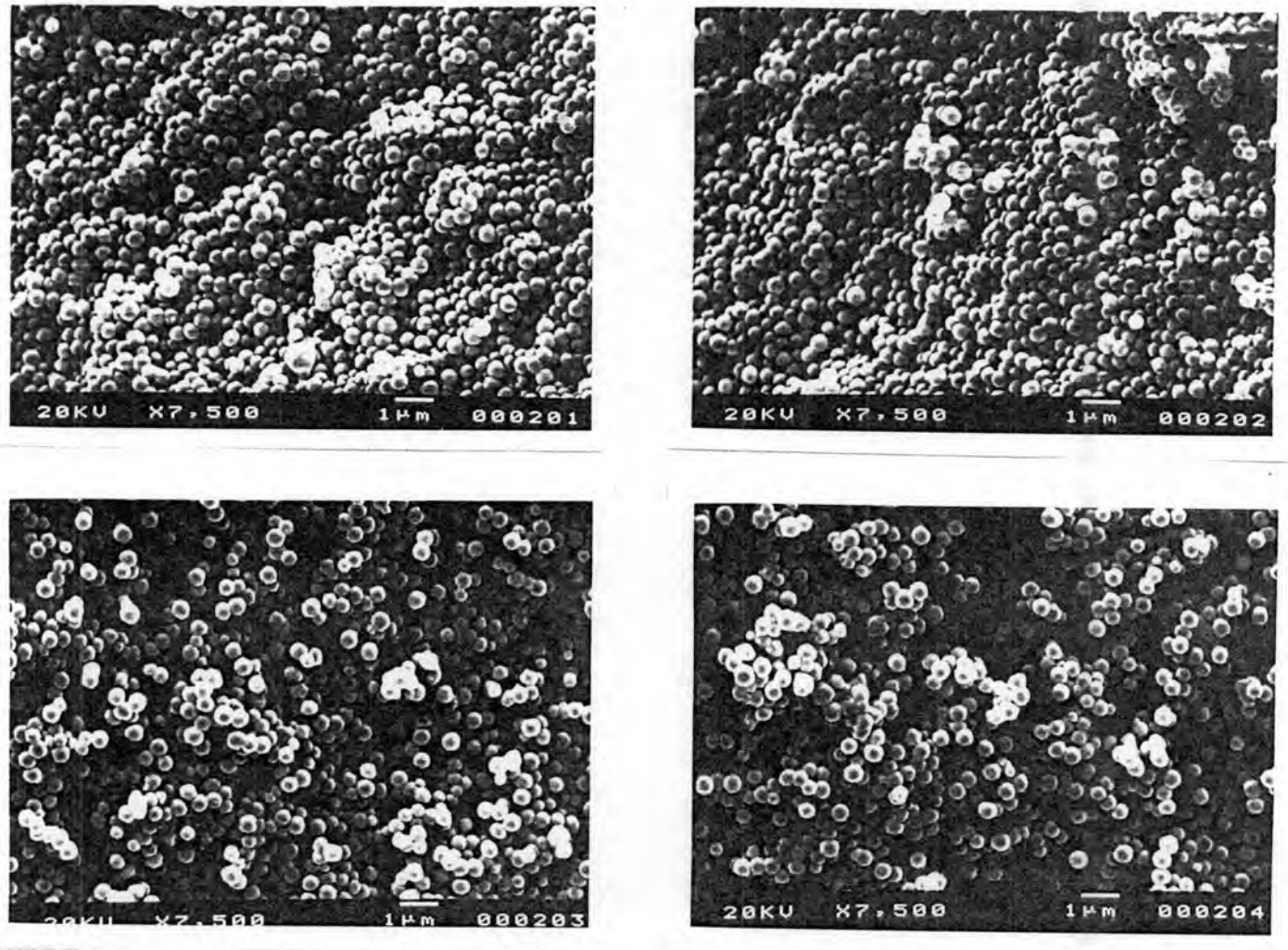

Figure 4.102 SEM micrographs for PSD measurement of poly(styrene-*co*-methyl methacrylate) composed of 75% styrene

Table 4.6 Effects of Styrene Feed on Dispersion Copolymerization of Styrene and Methyl Methacrylate[a]

No.	Styrene (mole%)	$\overline{D}_n$[b,c] (μm)	CV[d,c] (%)	SD[e,c] (μm)	PSD[f]	$\overline{M}_n$	$\overline{M}_w$	$\overline{M}_w/\overline{M}_n$	F[g] (mole% STY)
F1	0	*	*	*	*	-	-	-	0[h]
F2	25	0.7	2.86	0.02	0.99	16278	41078	2.52	42.15
F3	50	0.4	15	0.06	1.17	4097	7916	1.93	55.85
F4	75	0.4	12.5	0.05	1.1	8044	18901	2.35	80.18
F5	100	0.3	20	0.06	1.15	6757	18779	2.78	94.02

[a]Reaction temperature 60°C, reaction time 10 h

[b]Calculated diameter

[c]Determined by Scanning Electron Microscope

[d]Coefficient of variation of number-average size [e]Standard Deviation [f]Particle size distribution

[g]Copolymer composition, determined by Elemental Analysis [h]100.51 mole% methyl methacrylate *Very broad PSD

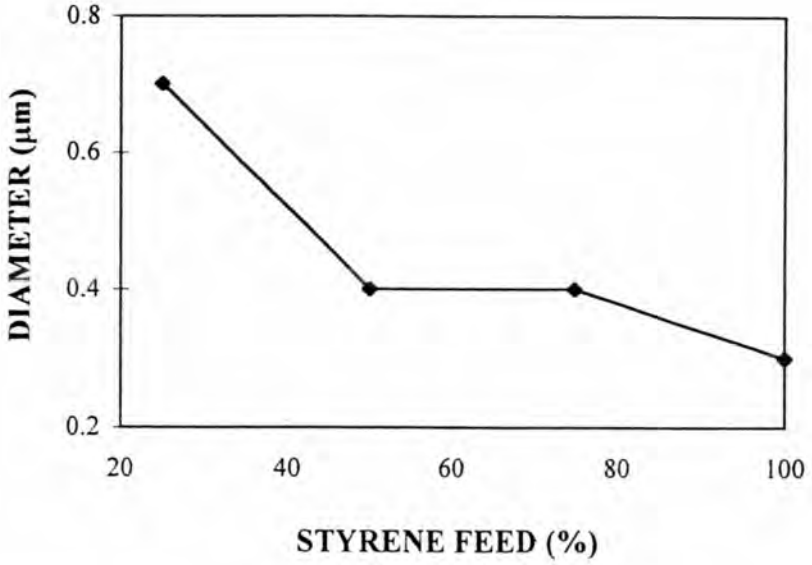

Figure 4.103 Effect of the feed ratio of styrene/methyl methacrylate on the particle size of poly(styrene-*co*-methyl methacrylate)

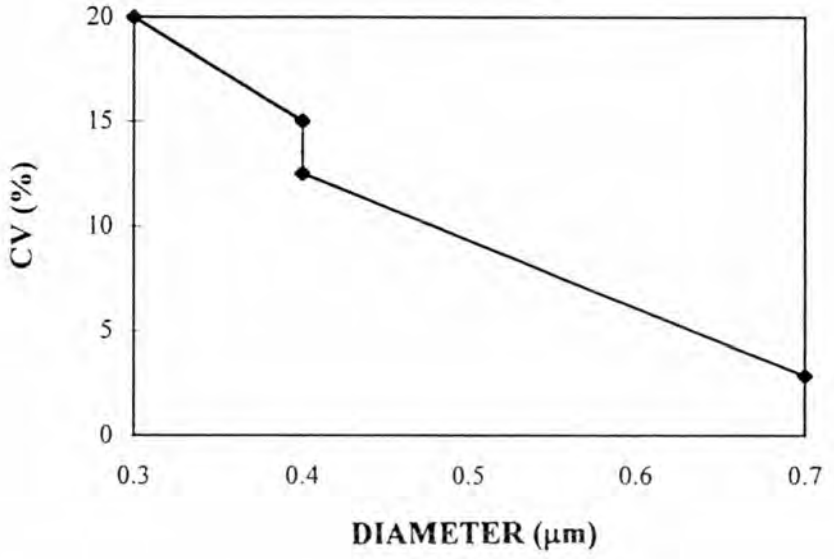

Figure 4.104 Relationship between the average particle size and CV for various feed ratios of styrene/methyl methacrylate

At a higher styrene content, the copolymer particles have a broader size distribution. It can be seen that the relatively small-sized particles have a broader size distribution than the corresponding large-sized particles.

In the case of poly(methyl methacrylate), the gel formation during polymerization under an isothermal reaction condition can be discussed as below:

The overall rate of dispersion polymerization can be given as an approximated expression :

$$R_p = \alpha C_m k_p (v R_i / k_t)^{1/2} \qquad (4.25)$$

where C_m = the overall monomer concentration in the dispersion polymerization

v = volume fraction

The larger increases in the $k_p/k_t^{1/2}$ ratio that accompany the gel effect lead to greater increases in the sizes of the polymers being produced as the polymerization proceeds (56).

4.6.2 The Average Molecular Weights and Molecular Weight Distribution of Poly(Styrene-*co*-Methyl Methacrylate)

For the feed ratios of styrene/methyl methacrylate, the weight average molecular weights of the copolymers are in the range of 18,000-40,000 as shown in Figure 4.105 and the curve of molecular weight distribution is given in Figure 4.106. It can be seen that increasing the styrene feed, the copolymer with a lower average molecular weights is produced except the copolymer prepared at the styrene feed of 50

mole%. Increasing the styrene feed, strong adsorption of the styrene monomer on the PVP matrix is increased, the rate of adsorption of PVP matrix is thus relatively high. This leads to a shorter chain length of the polymer to give the lower average molecular weights.

When the methyl methacrylate content was as high as 75 mole%, the gel effect might possibly occur and increases in chain lengths together with the overall higher molecular weights of the copolymers could be obtained.

The gel effect has been shown to result from a decrease in the termination rate as the viscosity of the polymerization medium increases. Although diffusion of monomer is still possible within the increasingly viscous medium, the diffusion of the much larger growing polymer radicals is considerably retarded and makes them much less likely to terminate with each other. Although the preparation of polymer growth continuous largely unhindered under these conditions, the termination rate is considerably reduced. The quantity $k_p/k_t^{1/2}$ in eq 4.25 therefore increases, with a resulting increase in the overall rate of polymerization. For the same reason there is a corresponding increase in the chain length or the sizes of poly(methyl methacrylate) with increasing conversion. The diminution of termination rate in the polymerization of methyl methacrylate has been similarly ascribed to hindered radical-radical termination due to the formation of tightly-coiled macroradicals (57).

Besides, the wide distribution of particle sizes has been shown to result from the monomers used are frequently solvents for their own polymers, the overall solvency of the continuous phase for polymer changes as monomer is consumed in the polymerization. Consequently, the conditions for precipitation of polymer formed in

solution change throughout the polymerization. In addition, the degree of association of the graft copolymer dispersant with the dispersed polymer, and hence its effectiveness as a dispersion matrix polymer is reduced by the increased solubility of its 'anchoring' component. These two factors together lead to polymer dispersions of an undesirably wide distribution of particle sizes (58).

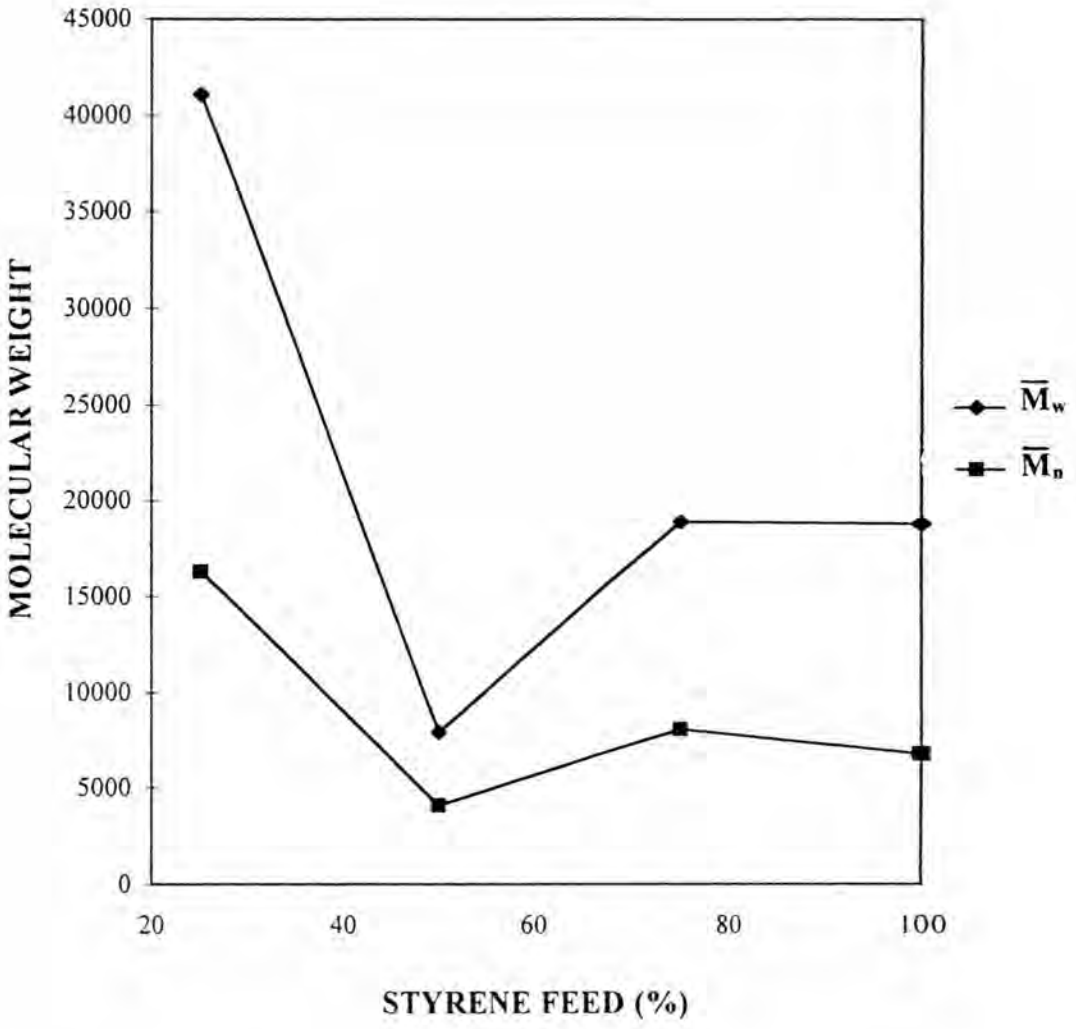

Figure 4.105 Effect of the feed ratio of styrene/methyl methacrylate on the average molecular weights of poly(styrene-*co*-methyl methacrylate)

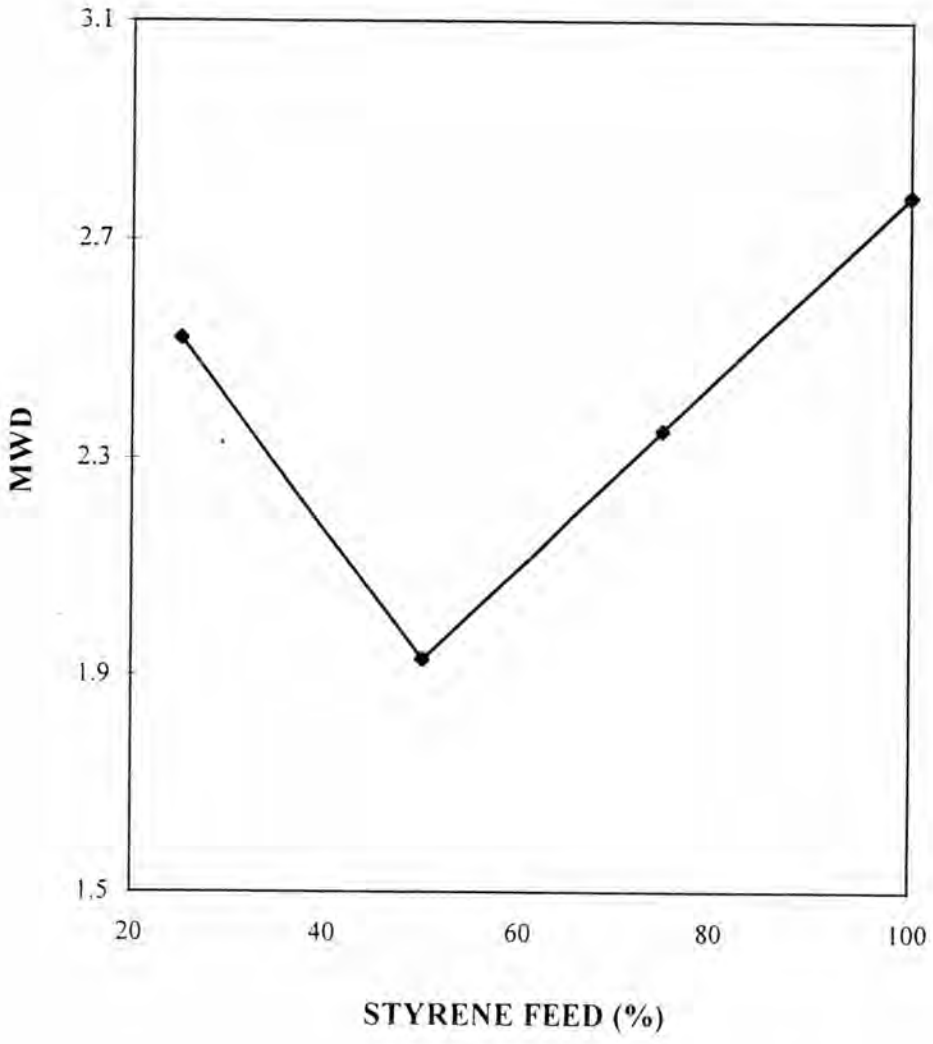

Figure 4.106 The curve of MWD of poly(styrene-*co*-methyl methacrylate) for various feed ratios of styrene/methyl methacrylate

4.7 Particle Growth and Conversion

Copolymer particle growth was studied by dispersion polymerization in 90/10 ethanol/water. In a typical dispersion polymerization producing polymer which is very insoluble in the diluent, the stage of particle formation is normally completed very quickly, within a few seconds or tens of seconds after the start of reaction (33).

During the growth stage of the reaction, the stabilized particles become so efficient at scavenging unstabilized smaller particles that new nuclei are captured almost immediately, before they have a chance to become stabilized themselves. All the evidence from electron micrographs indicates that very few particles form after the stage of particle formation unless the solvency of the medium is drastically altered or substantial amounts of additional dispersant are added. The number of particles therefore, remains virtually unchanged throughout the remaining course of the polymerization, unless some form of aggregation intervenes, as may happen if the total particle surface formed outruns the amount of dispersant available. The growing particles may also swell with monomer and capture growing oligomer radicals from solution (efficiently if the particle density is high enough), leading to solid phase polymerization of much higher molecular weight that terminated in solution (59).

In this research, the investigation of the particle growth is based upon measurements of particle size and its distribution during the reaction taken after the polymerization time of 0.6, 0.73, 1, 2, 4, 6, 8 and 10 h. The SEM photographs indicating the particle growth are given in Figure 4.107 and the SEM photographs of particle size distribution are shown in Figures 4.108-4.115. The conversion was measured by charging the reaction mixture at 0.33, 0.47, 1, 2, 4, 6, 8, and 10 h

reaction time. Figure 4.118 shows conversion (p) versus reaction time (t) for the system in 90/10 ethanol/water at 70°C reaction temperature. The particle growth of particle during the conversion is presented as the relationship between particle volume (V_p) and conversion (p) (1, 2, 4, 6, 8, and 10 h). Particle growth curve as a function of reaction time is shown in Figure 4.119. The particle volume was calculated from the diameter of the particles measured by a scanning electron microscope.

Table 4.7 shows the data obtained from the investigation of the particle growth and conversion. It can be seen that the sizes of copolymer particles are increased gradually with conversion as the polymerization progresses. Within 19 min of the beginning of the reaction, oxygen suppresses the polymerization of monomers. The oxygen reacts with the initiating radicals and converts them to either non-radical species or radicals of reactivity too low to undergo propagation. At the reaction time of 20 min (0.33 h), the polymerization occured only 0.1%. At 28 min (0.47 h), the polymerization was increased to only 3%. During the reaction time of 0.6 h to 0.73 h, the particle growth was constant. There might be some retardant in the reaction system that slows down the particle growth. However, in this case, the polymerization occurs but at a slower rate (from 3.44% at 0.6 h to 5.12% at 0.73 h). The retarder was less effective and it took only a portion of the radicals. Within the polymerization time of 10 h, the conversion was increased from 9% at 1 h to 78% at 10 h. Dispersion polymerization of 1 h, the average size of the particles was 0.7 μm and was increased to 1.3 μm at the reaction time of 8 h.

From these above results, it can be explained that increasing the reaction time is to allow the polymerization to proceed. The particles formed for the a short reaction

time were soft and were relatively irregular sphere with an indent half-circle at the edge like a cherry. During polymerization, the particle growth is increased gradually and the rate of polymerization is increased slowly within 1 h, after this time, it is increased rapidly until the reaction time reaches at 8 h. The particle growth has partly been described in the section of reaction time.

When a narrow size distribution of the particles is observed, it indicates that the initial nuclei are formed within a very short reaction time and its subsequent growth takes place without the formation of new nuclei and without agglomeration of particles, that is, the formation rate of the particles must fall to a negligible level after the early stages of the polymerization. It seems that when enough particles have been formed, the formation of new particles is inhibited. The reason is that nearly all the oligomeric radicals formed within the free volume in the continuous phase are captured by the existing particles before they can form new nuclei, and they continue to propagate within the particles (60).

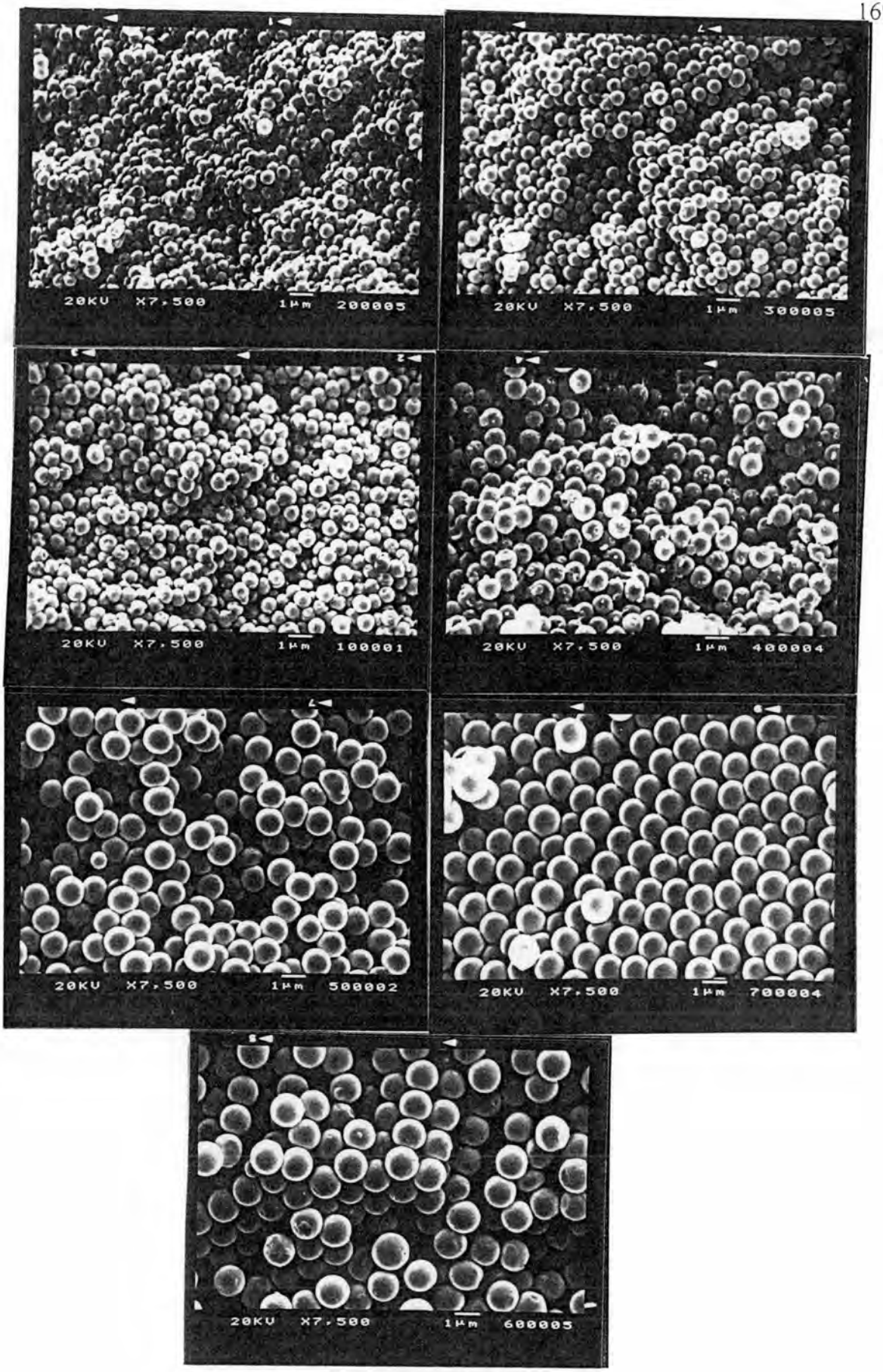

Figure 4.107 SEM micrographs of the particle growth of poly(styrene-*co*-methyl methacrylate)

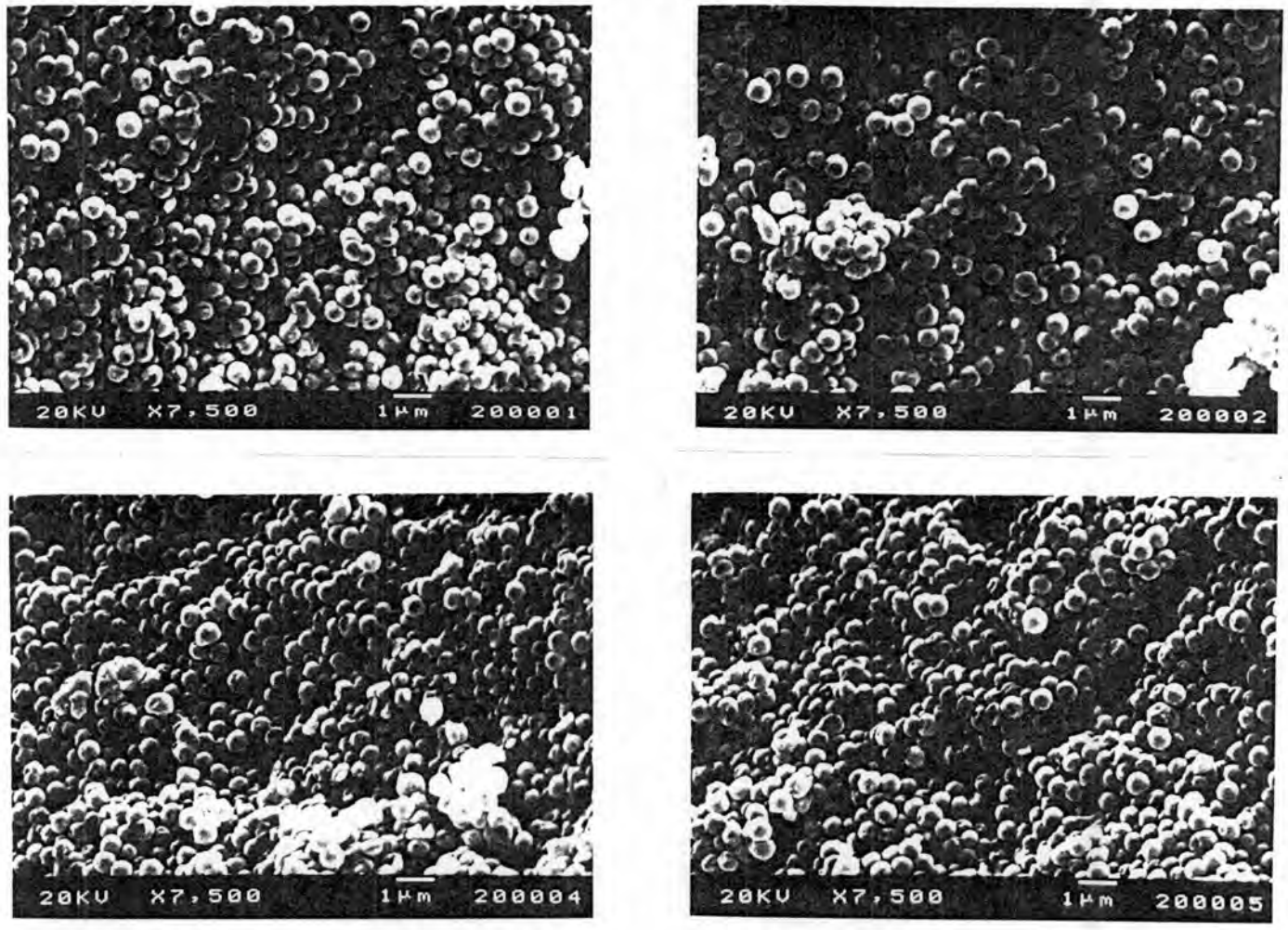

Figure 4.108 SEM micrographs for PSD measurement of poly(styrene-*co*-methyl methacrylate) synthesized for 0.6 h reaction time

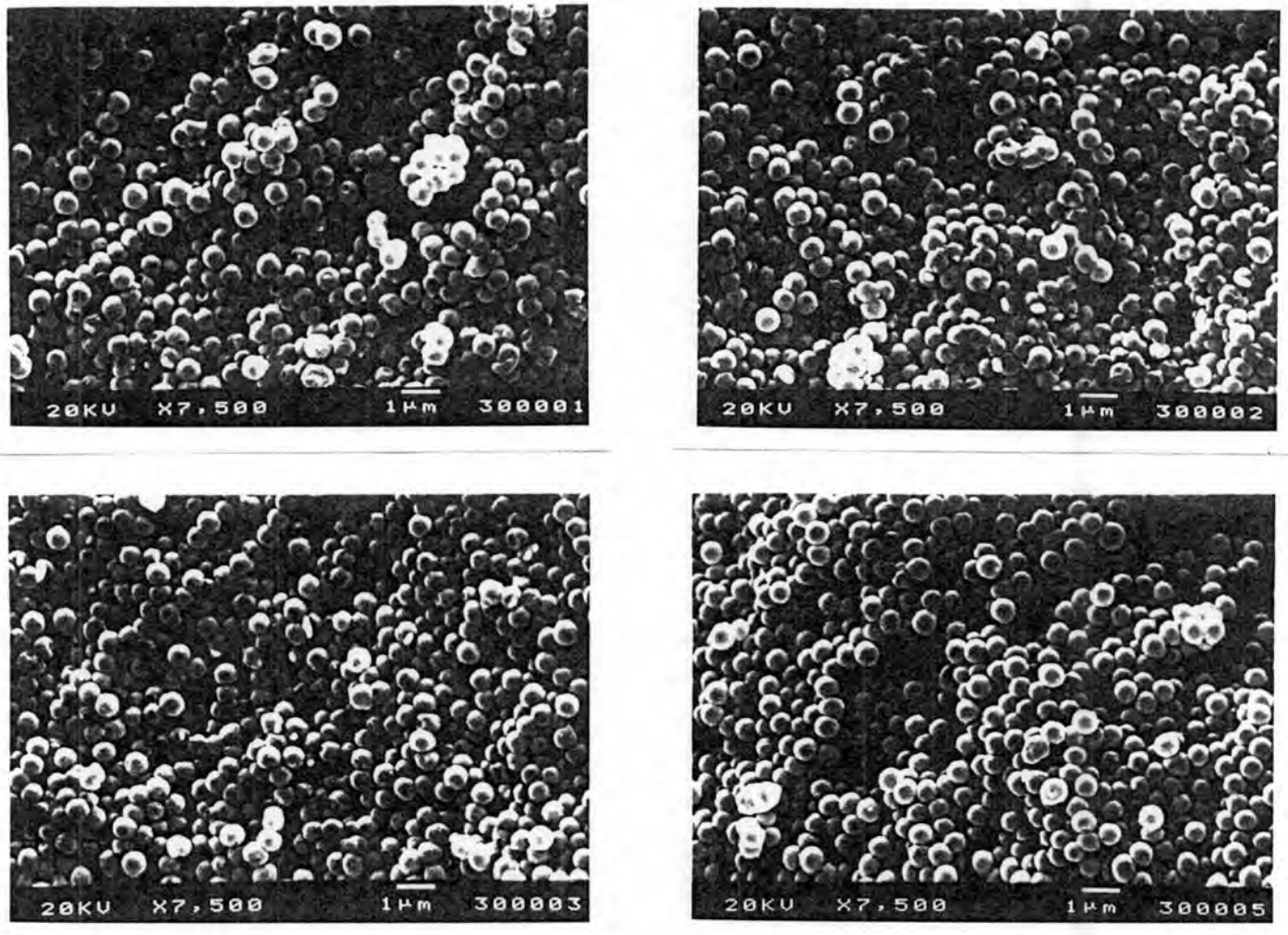

Figure 4.109 SEM micrographs for PSD measurement of poly(styrene-*co*-methyl methacrylate) synthesized for 0.73 h reaction time

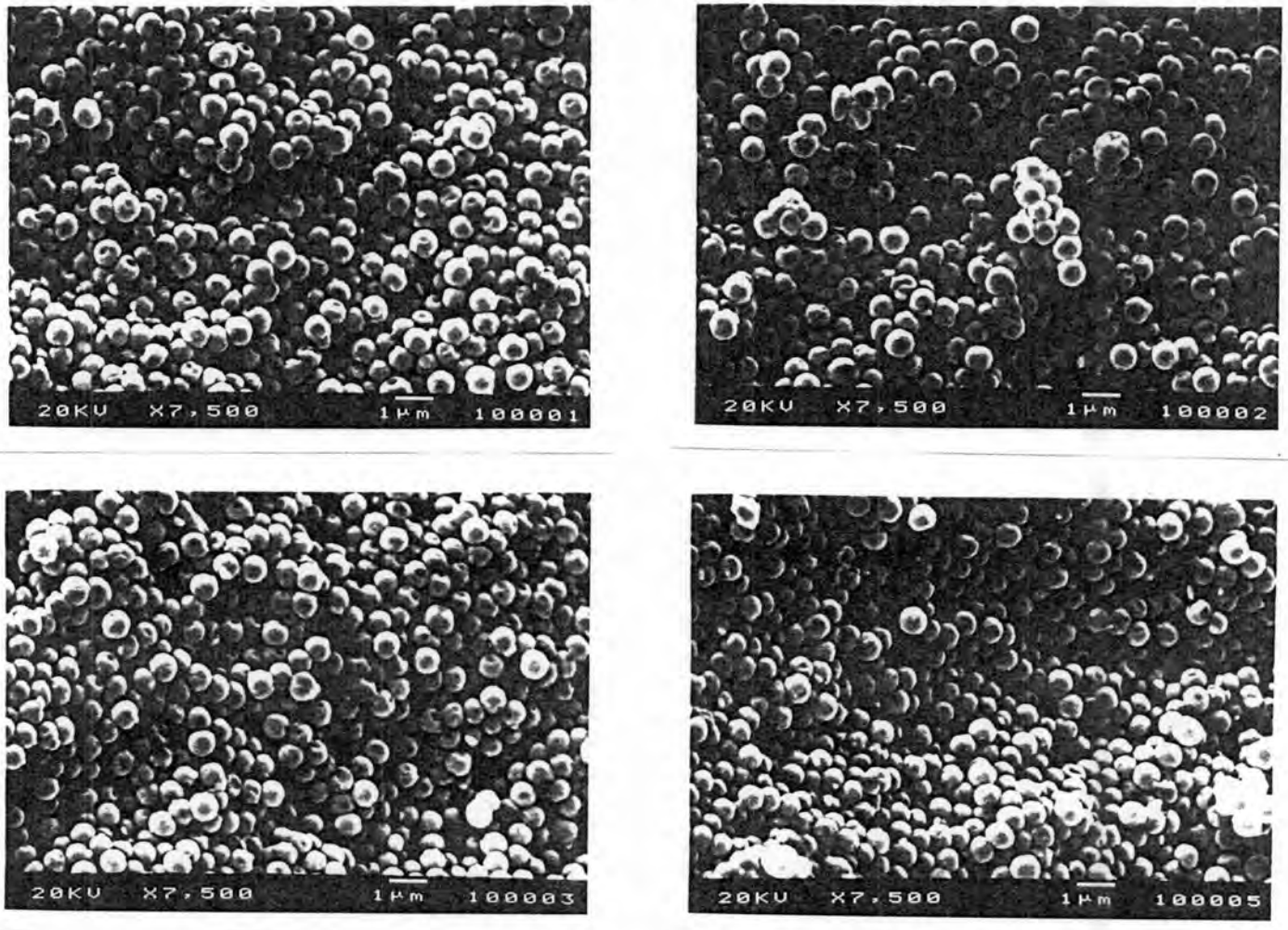

Figure 4.110 SEM micrographs for PSD measurement of poly(styrene-*co*-methyl methacrylate) synthesized for 1 h reaction time

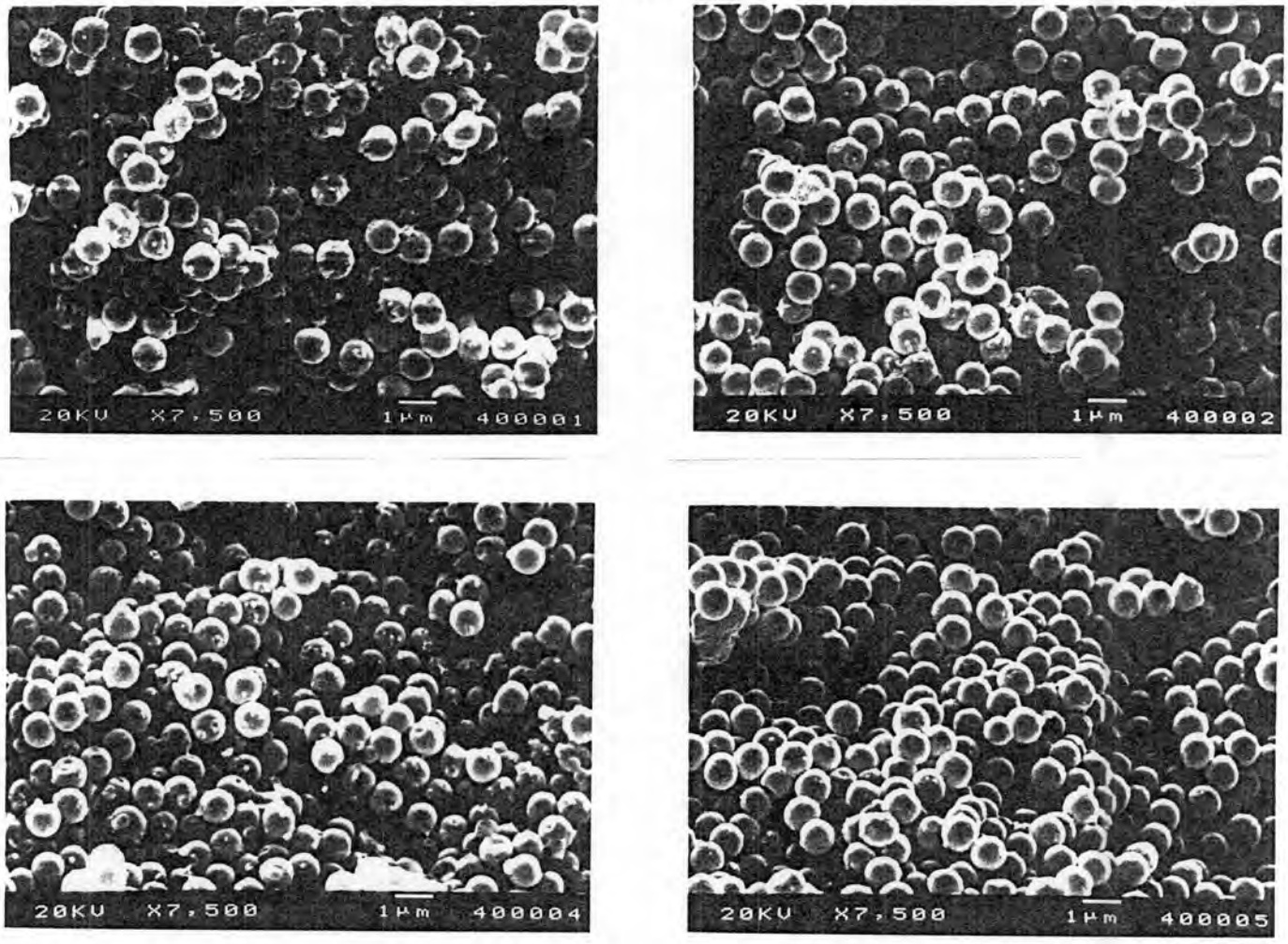

Figure 4.111 SEM micrographs for PSD measurement of poly(styrene-*co*-methyl methacrylate) synthesized for 2 h reaction time

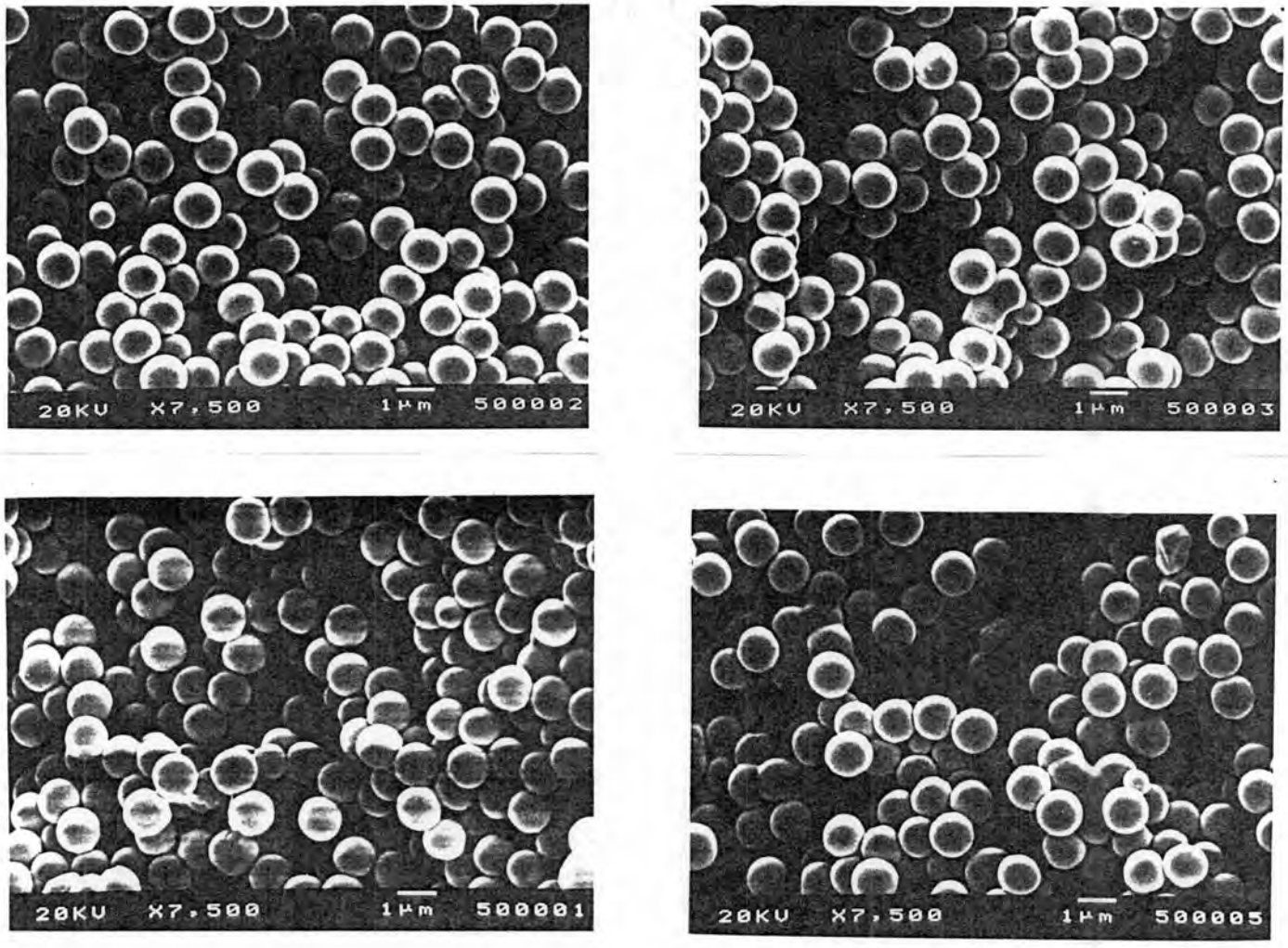

Figure 4.112 SEM micrographs for PSD measurement of poly(styrene-*co*-methyl methacrylate) synthesized for 4 h reaction time

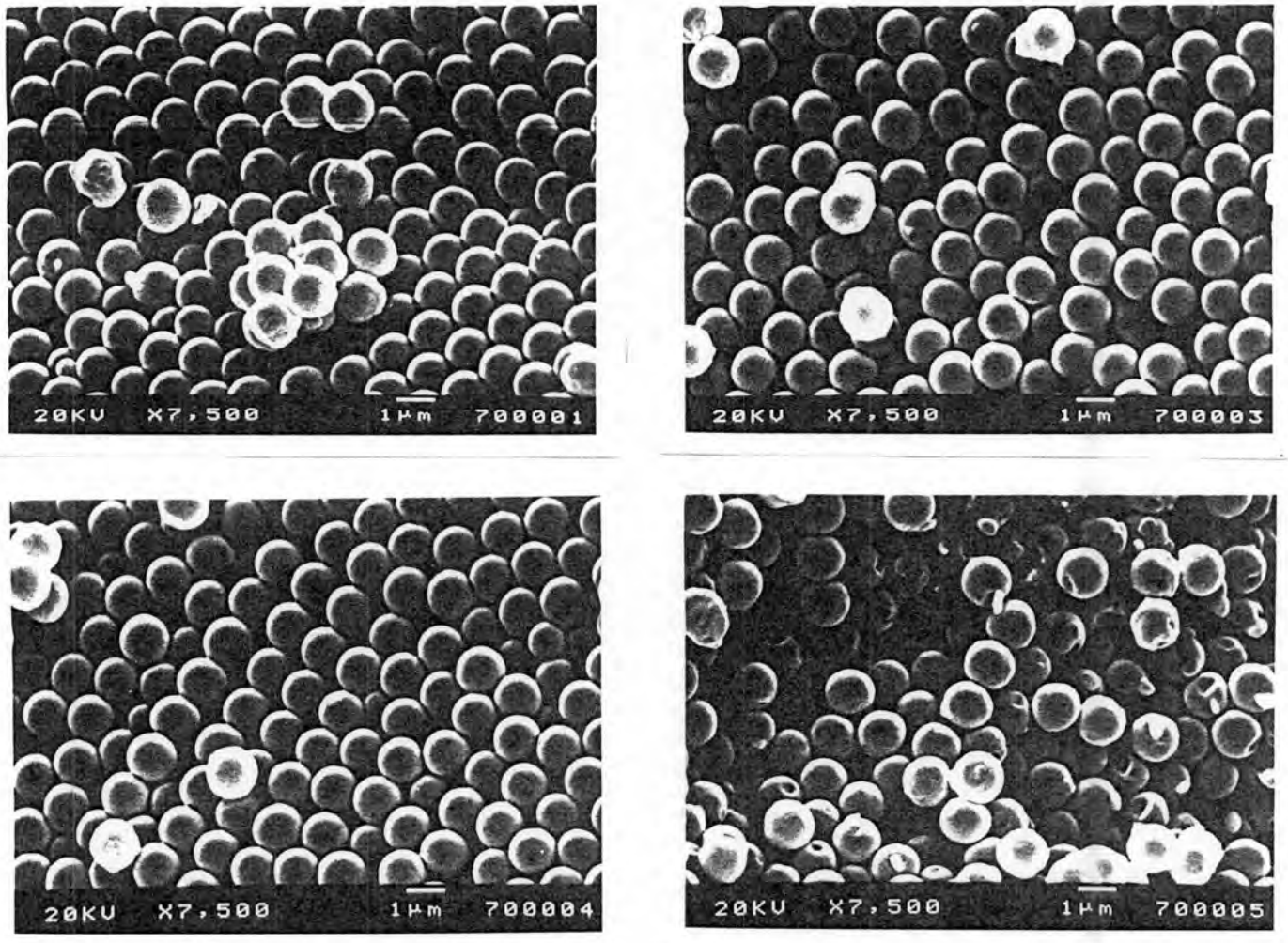

Figure 4.113 SEM micrographs for PSD measurement of poly(styrene-*co*-methyl methacrylate) synthesized for 6 h reaction time

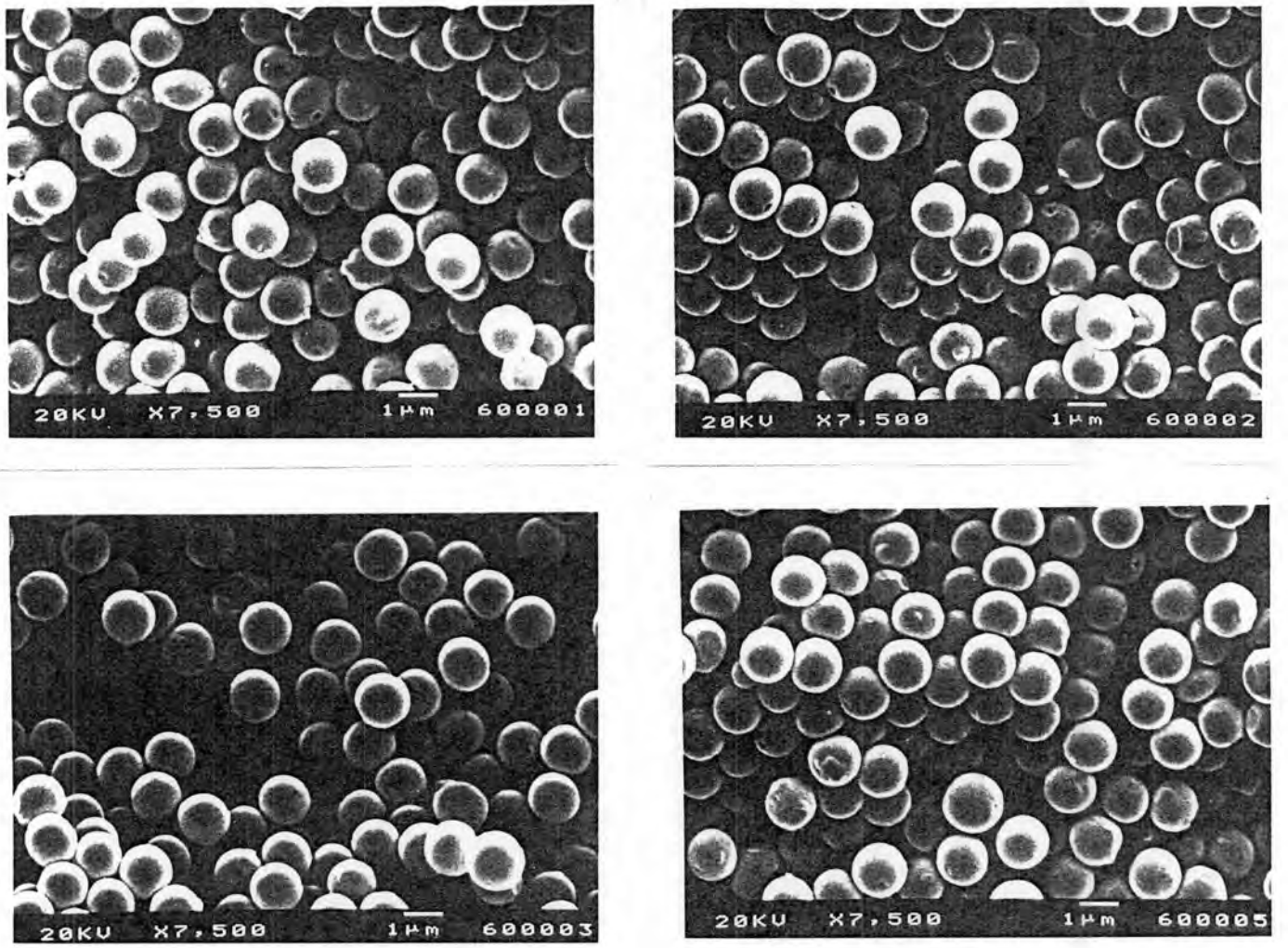

Figure 4.114 SEM micrographs for PSD measurement of poly(styrene-*co*-methyl methacrylate) synthesized for 8 h reaction time

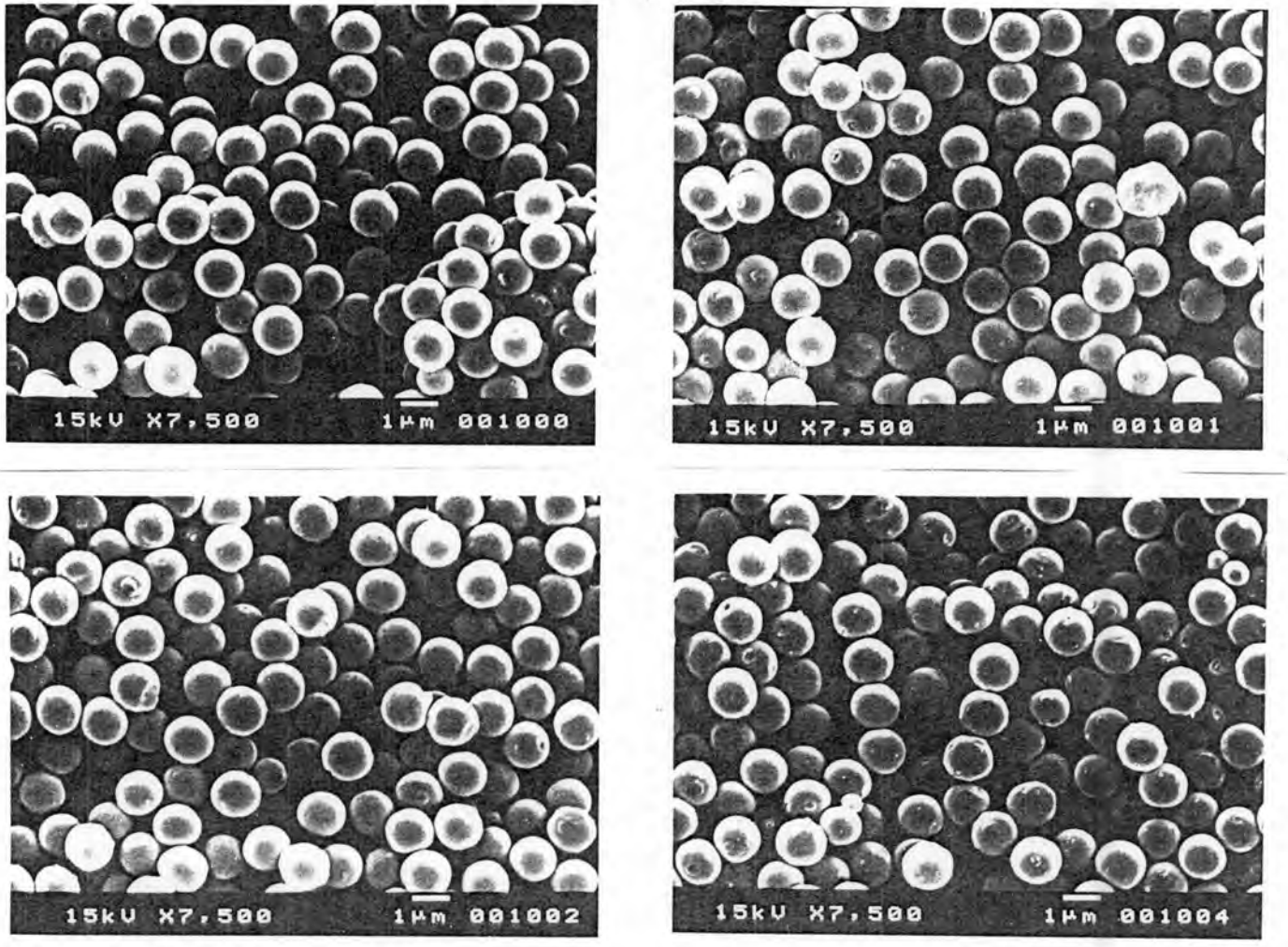

Figure 4.115 SEM micrograph for PSD measurement of poly(styrene-*co*-methyl methacrylate) synthesized for 10 h reaction time

Table 4.7 Investigation of the Particle Growth of Poly(Styrene-*co*-Methyl Methacrylate)and Conversion

Time (h)	$\bar{D}_n$ (μm)	CV (%)	SD	PSD	% Conversion (p)
0.33	*	-	-	-	0.1
0.47	*	-	-	-	2.95
0.6	0.6	8.33	0.05	1.08	3.44
0.73	0.6	10.6	0.06	1.02	5.12
1	0.7	8.03	0.06	1.07	9.39
2	0.9	5.21	0.05	1.02	27.46
4	1.2	4.13	0.05	0.99	45.48
6	1.3	3.08	0.04	1.02	62.22
8	1.3	4.12	0.05	1.03	74.86
10	1.3	3.32	0.04	1.02	77.73

*could not be measured by SEM, because the product was too little to be measured.

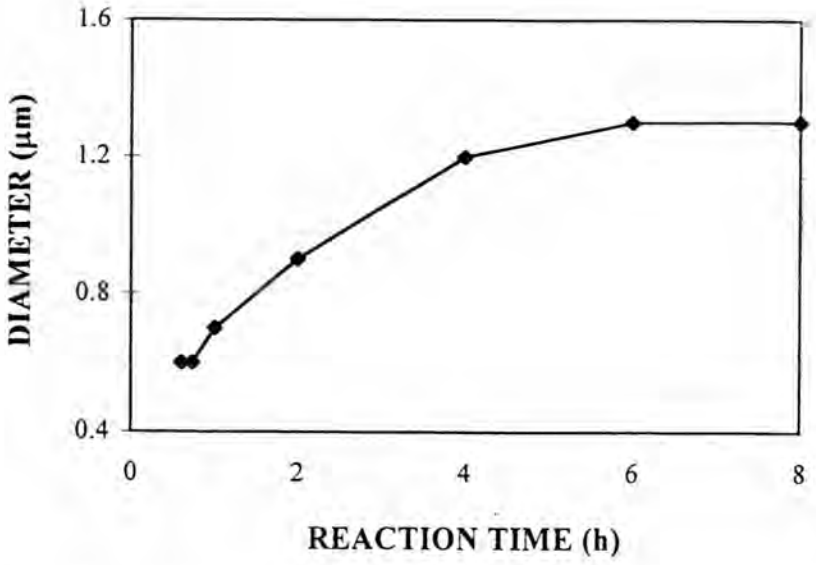

Figure 4.116 Average particle size as a function of reaction time

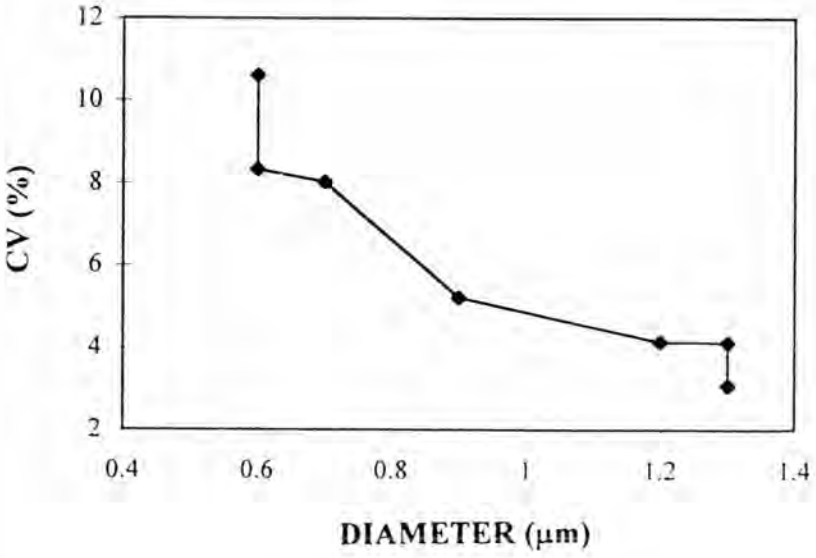

Figure 4.117 Relationship between the average particle size and CV of the particle growth

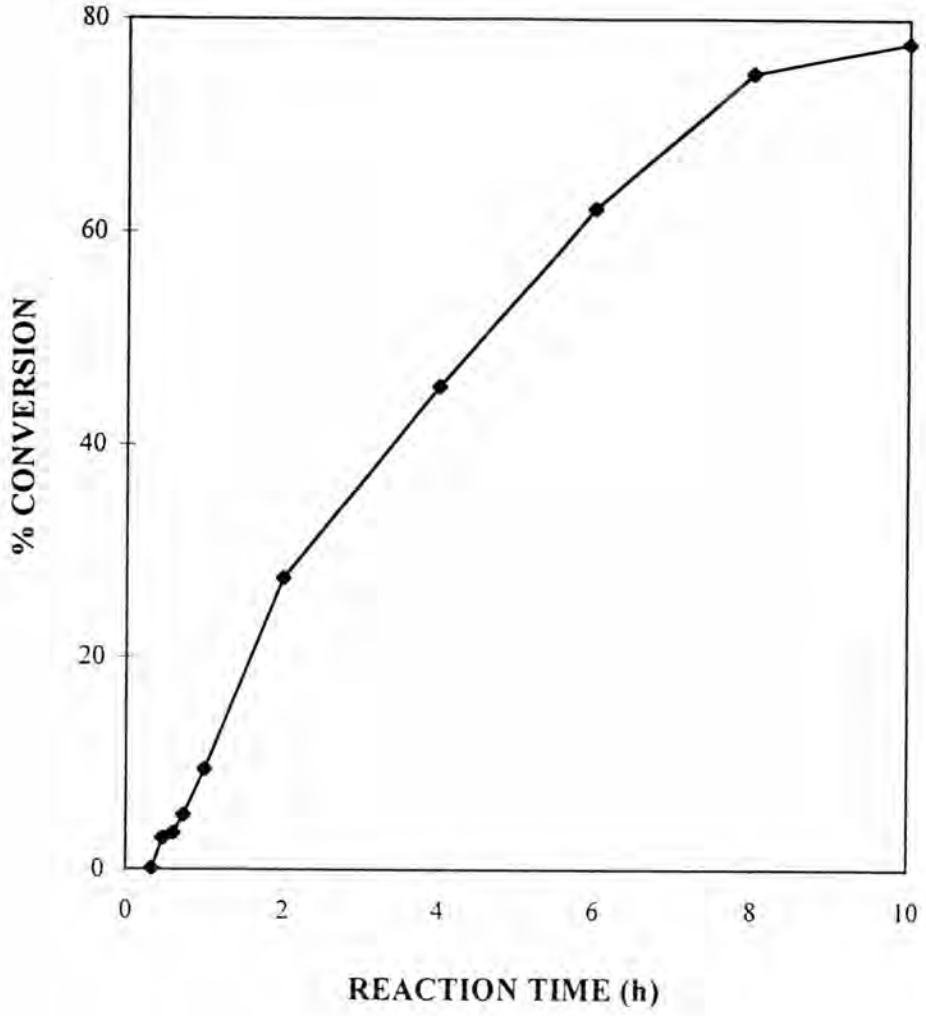

Figure 4.118 Rate of polymerization of styrene and methyl methacrylate in ethanol/water with PVP K-30 as a matrix polymer

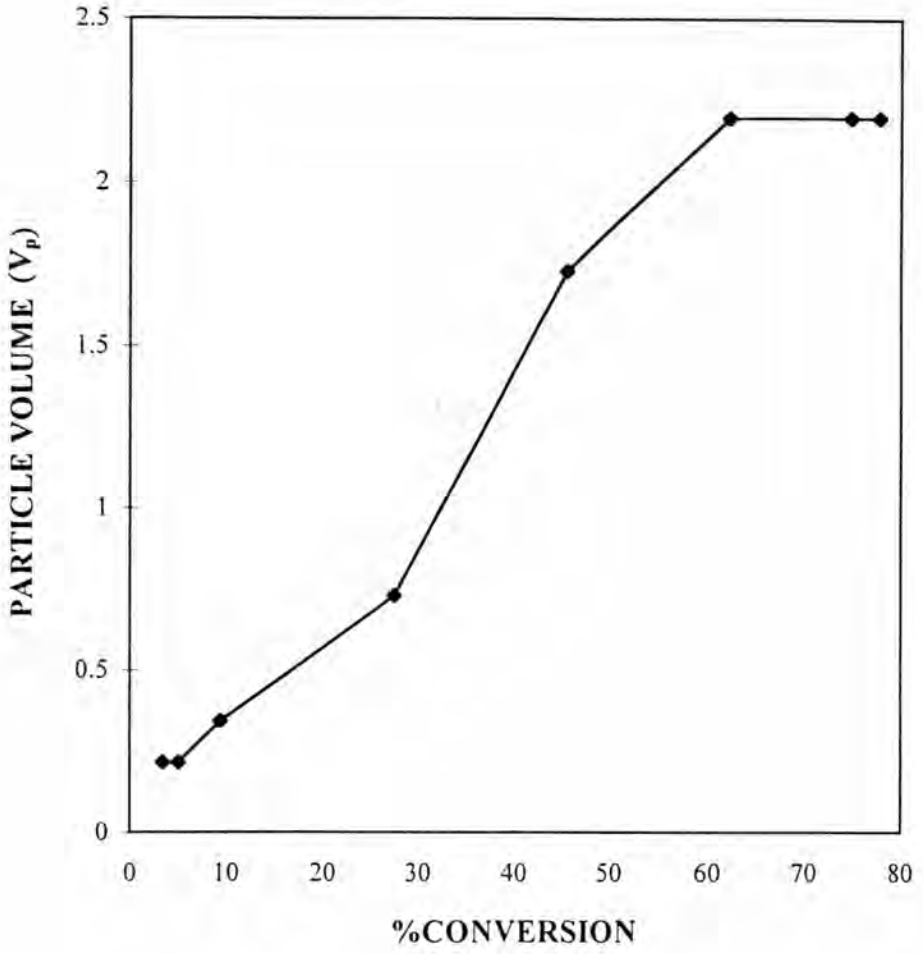

Figure 4.119 Particle volume versus conversion during growth of poly(styrene-*co*-methyl methacrylate) particles

4.8 Differential Scanning Calorimetry

Thermal transition in homopolymers of styrene and methyl methacrylate were examined by DSC. Using the DSC technique, T_g values were recorded according to the midpoint method for a heating rate of 5°C/min.

The PS revealed a T_g of 97.82°C and poly(methyl methacrylate) revealed a T_g of 114.42°C as shown in Figures 4.120 and 4.121, respectively. These homopolymers have one glass transition, whereas the random copolymers of poly(styrene-*co*-methyl methacrylate) display more than a single glass transition.

In Figure 4.122-1.1, it is found that copolymer of styrene and methyl methacrylate having 75% styrene and controlled by 8 wt% PVP K-30 has two glass transition temperatures. T_g values of them are 95.10°C and 111.79°C. Besides, it is seen that poly(styrene-*co*-methyl methacrylate) controlled by 10 wt% PVP K-30 have T_g values at 96.86°C and 113.62°C as shown in Figure 4.124-1.1.

From the DSC curves, it shows that the decomposition temperature of poly (styrene-*co*-methyl methacrylate) is about 400°C. The T_d value of the copolymer is similar to that of polystyrene (Figure 4.120). The decomposition temperature of poly (methyl methacrylate) is at 373°C as shown in Figure 4.121. It is seen that the decomposition temperatures of poly(styrene-*co*-methyl methacrylate) and polystyrene are higher than that of poly(methyl methacrylate).

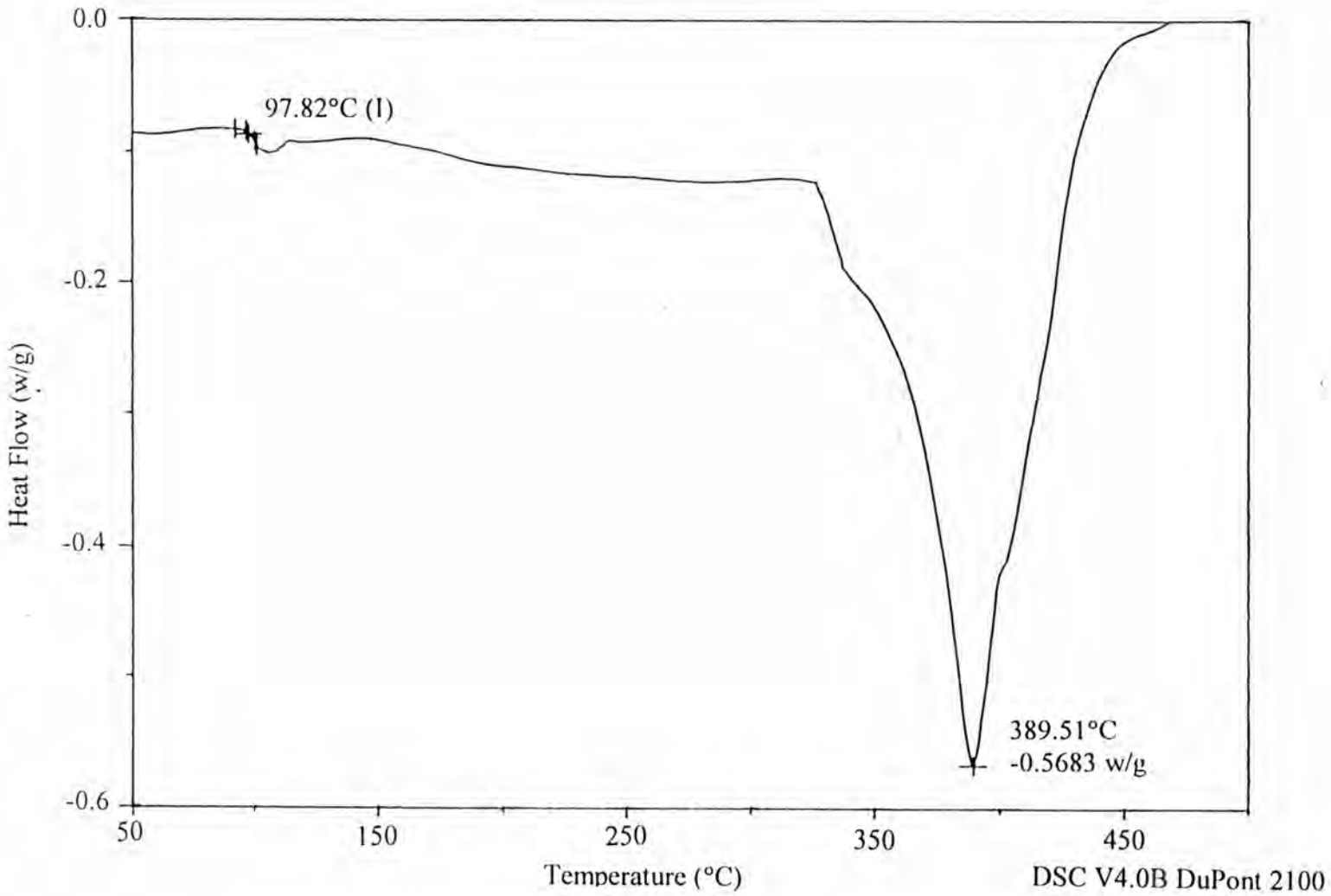

Figure 4.120 DSC curve of polystyrene prepared by dispersion polymerization

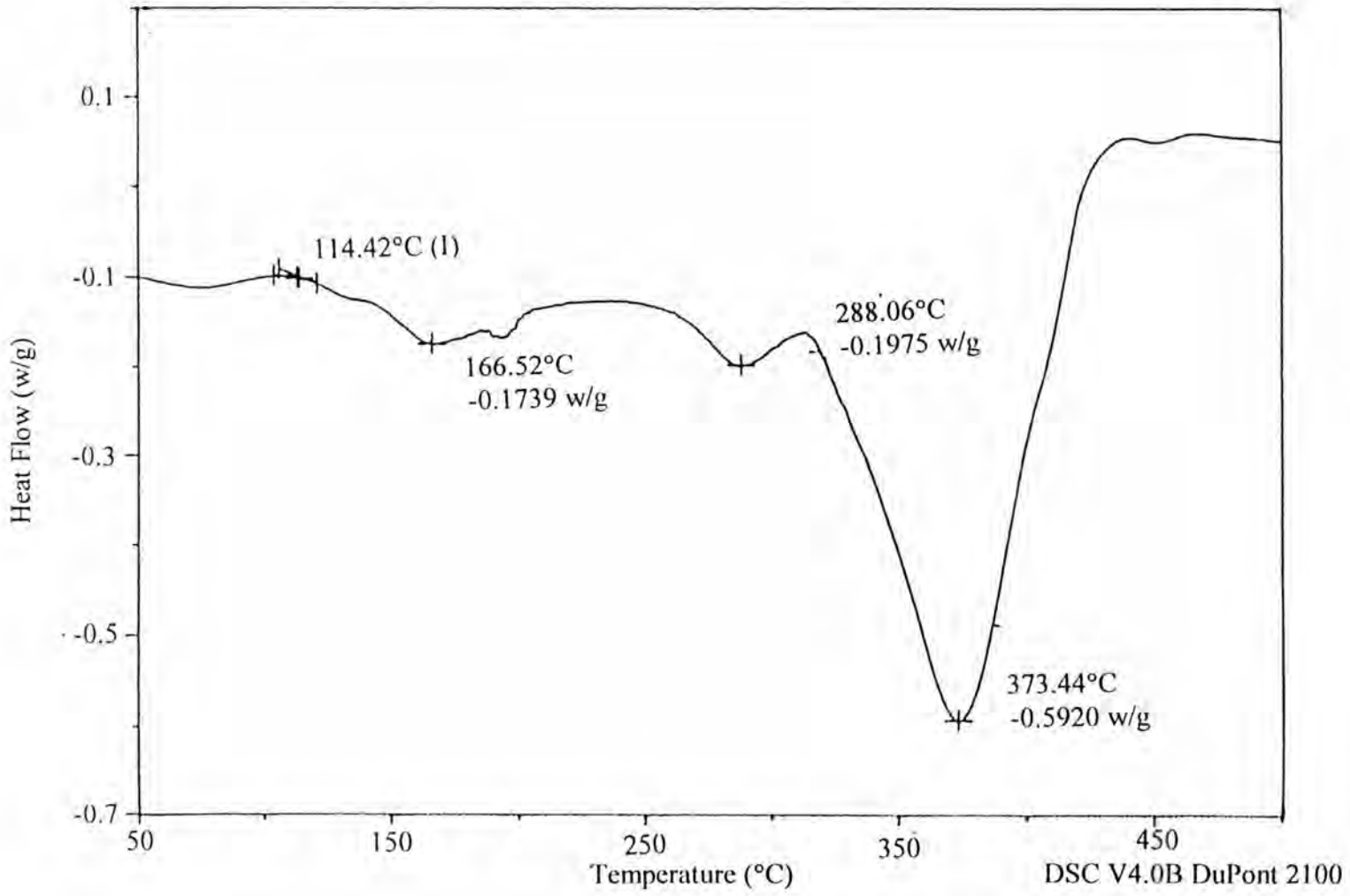

Figure 4.121 DSC curve of poly(methyl methacrylate) prepared by dispersion polymerization

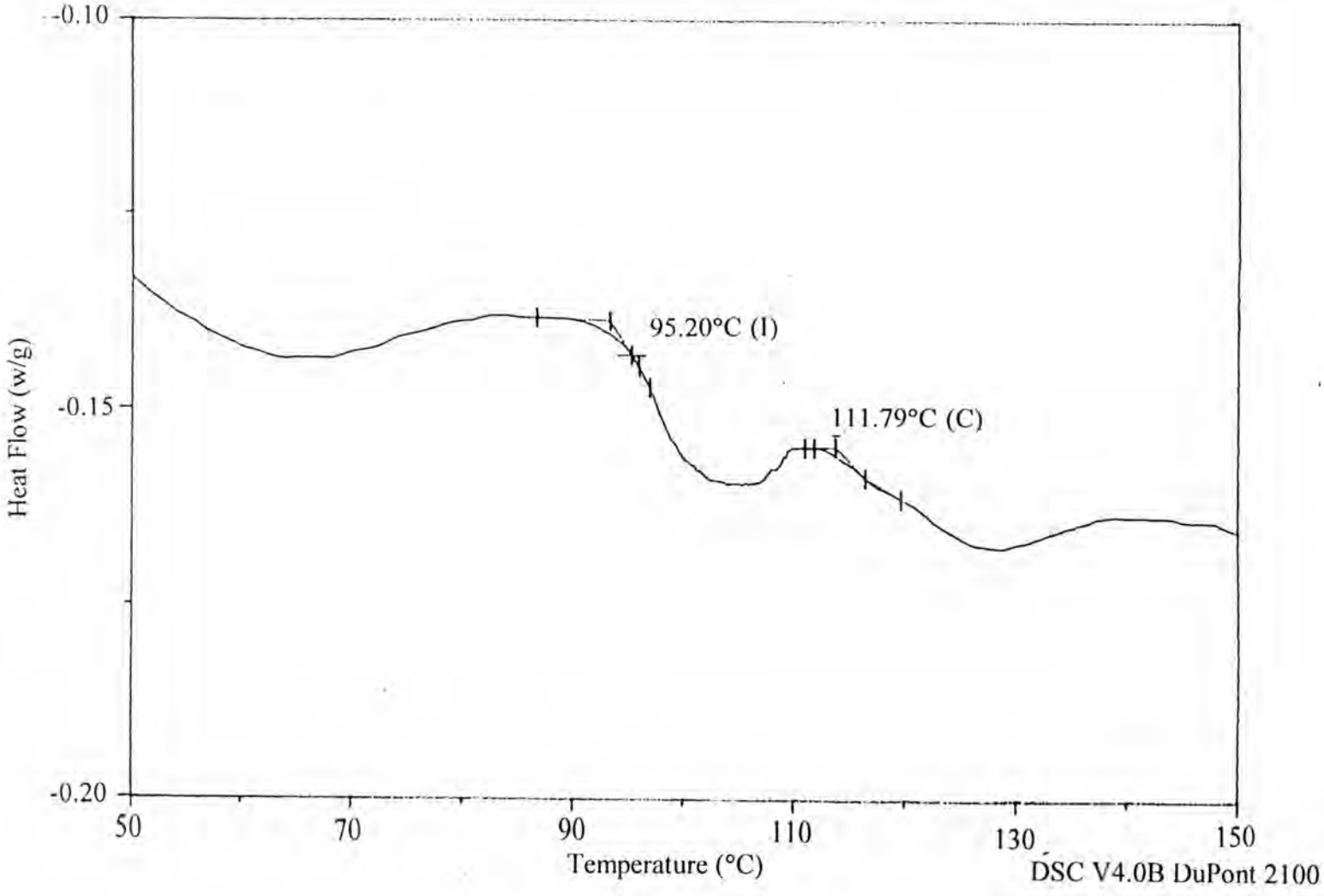

Figure 4.122-1.1 DSC curve of glass transition temperature of poly(styrene-*co*-methyl methacrylate) controlled by 8 wt% PVP K-30

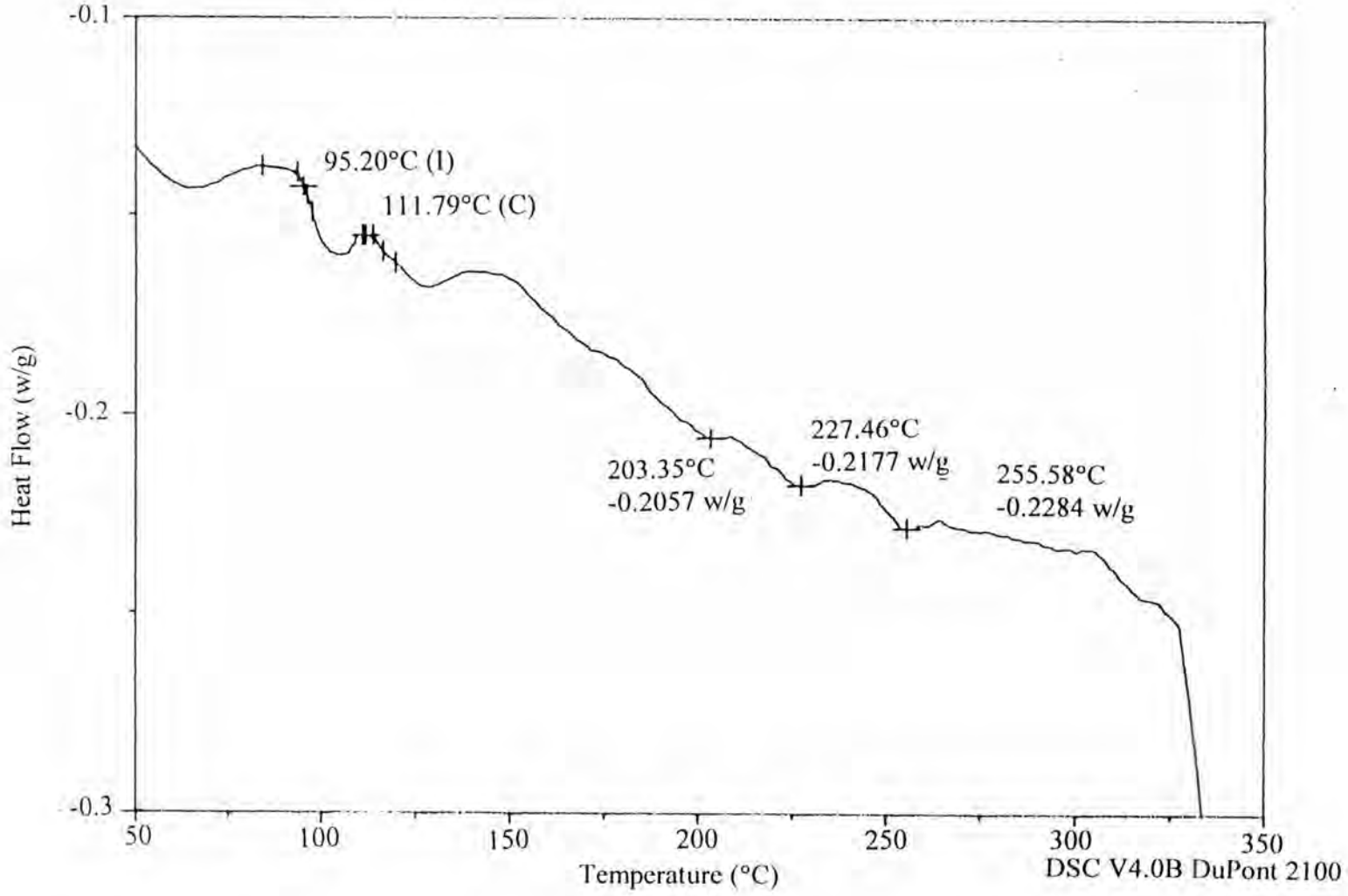

Figure 4.122-1.2 DSC curve of glass transition temperature of poly(styrene-*co*-methyl methacrylate) controlled by 8 wt% PVP K-30

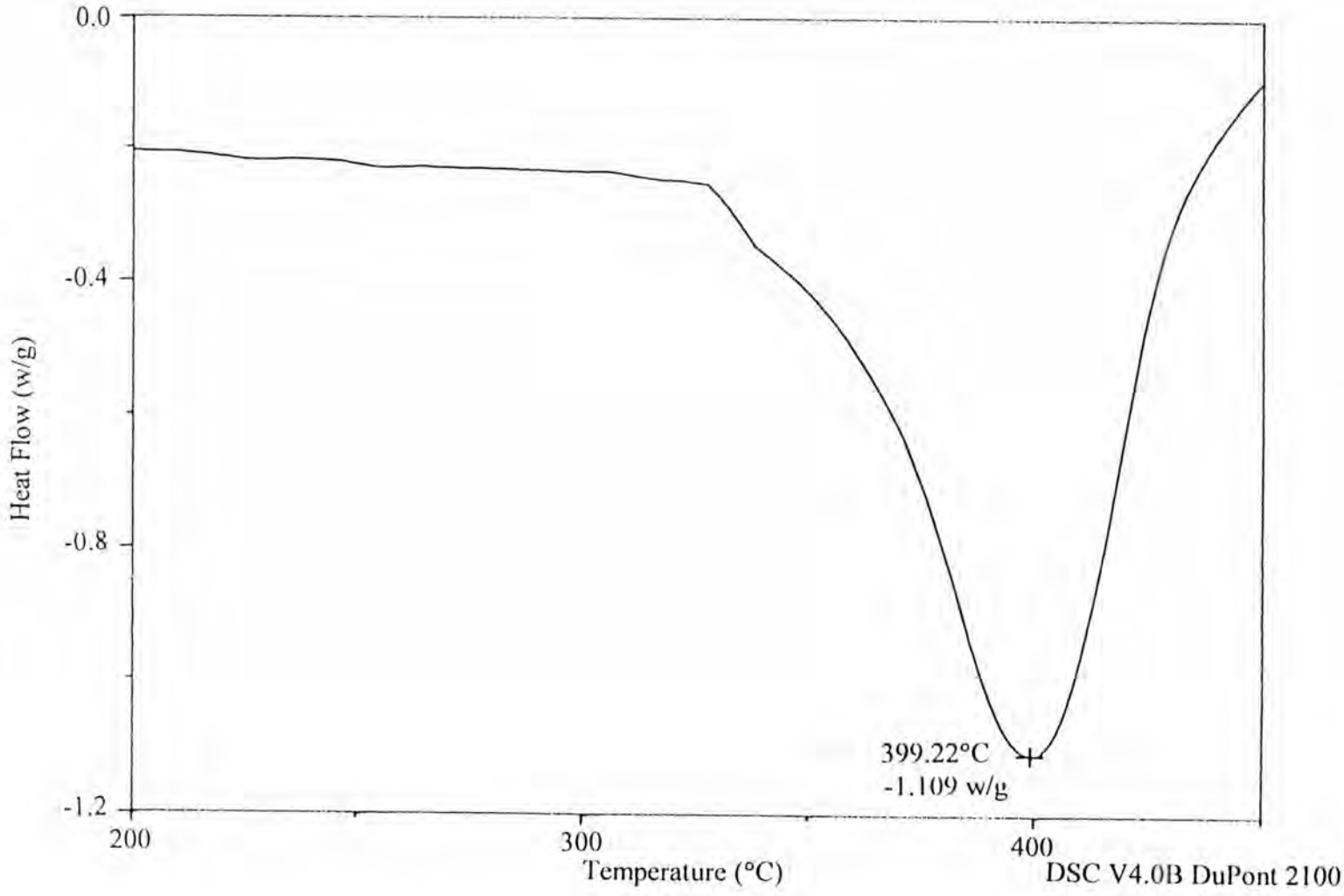

Figure 4.122-2 DSC curve of decomposition temperature of poly(styrene-*co*-methyl methacrylate) controlled by 8 wt% PVP K-30

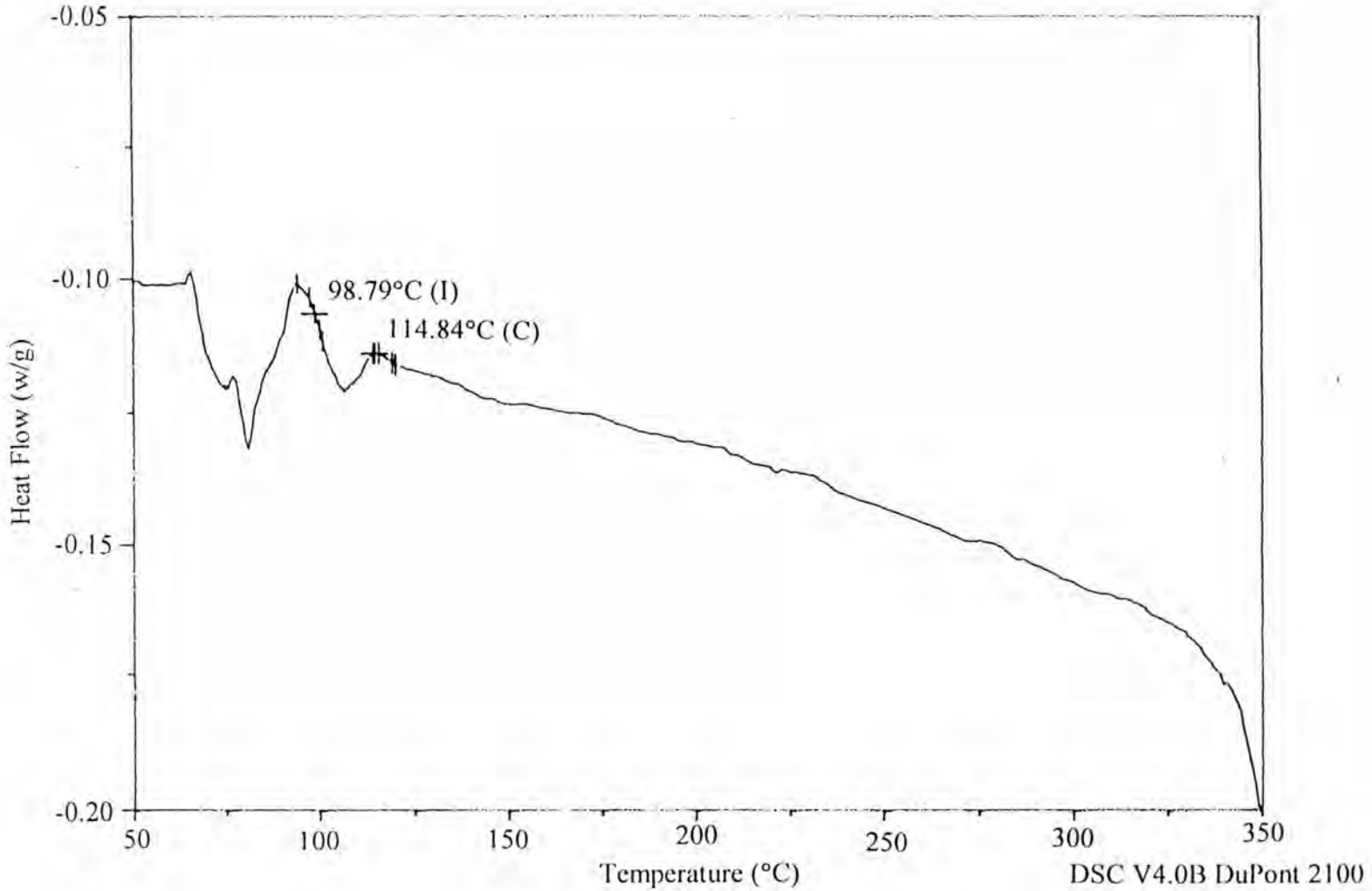

Figure 4.123-1 DSC curve of glass transition temperature of poly(styrene-*co*-methyl methacrylate) controlled by 10 wt% PVP K-30

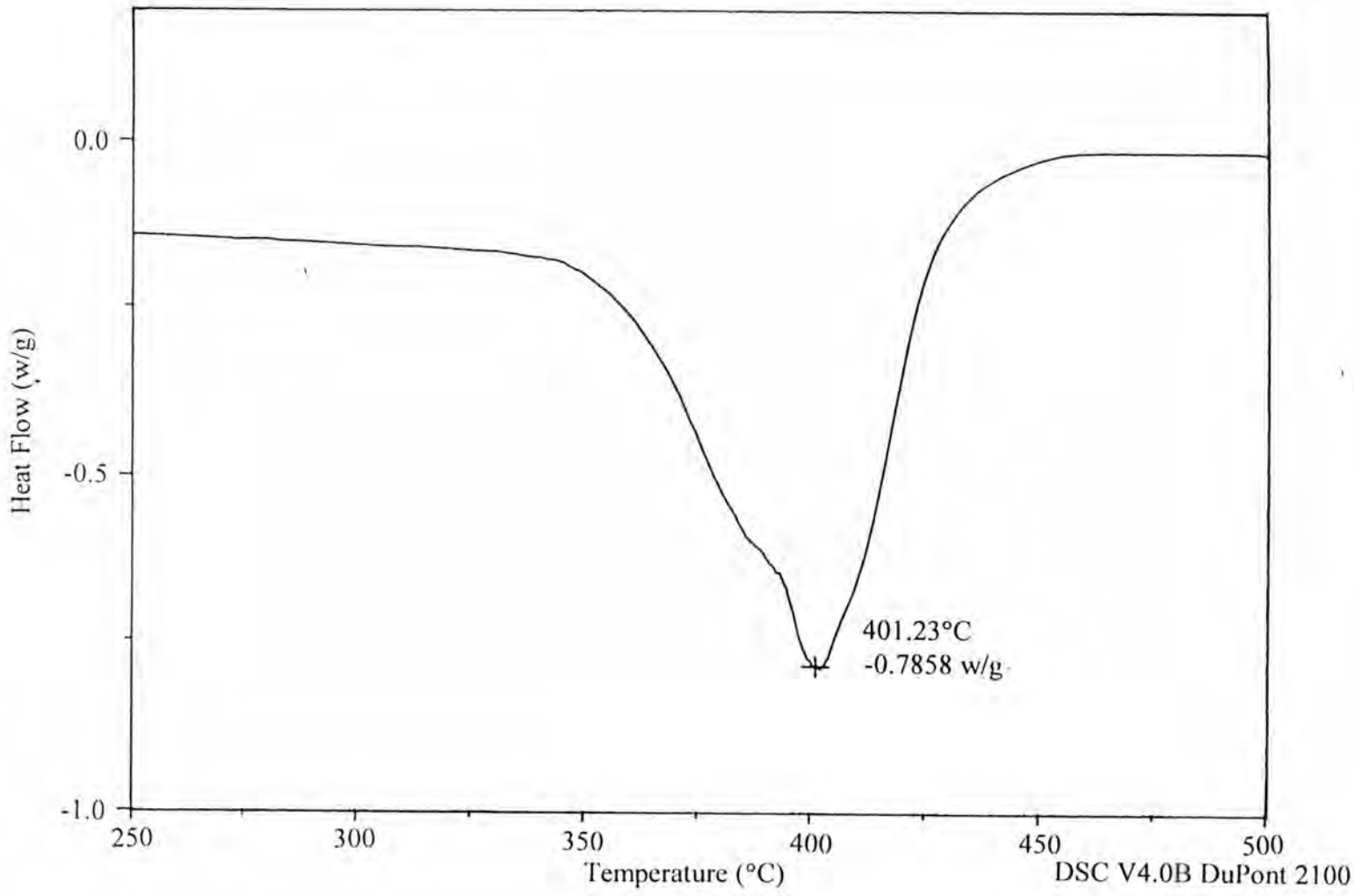

Figure 4.123-2 DSC curve of decomposition temperature of poly(styrene-*co*-methyl methacrylate) controlled by 10 wt% PVP K-30

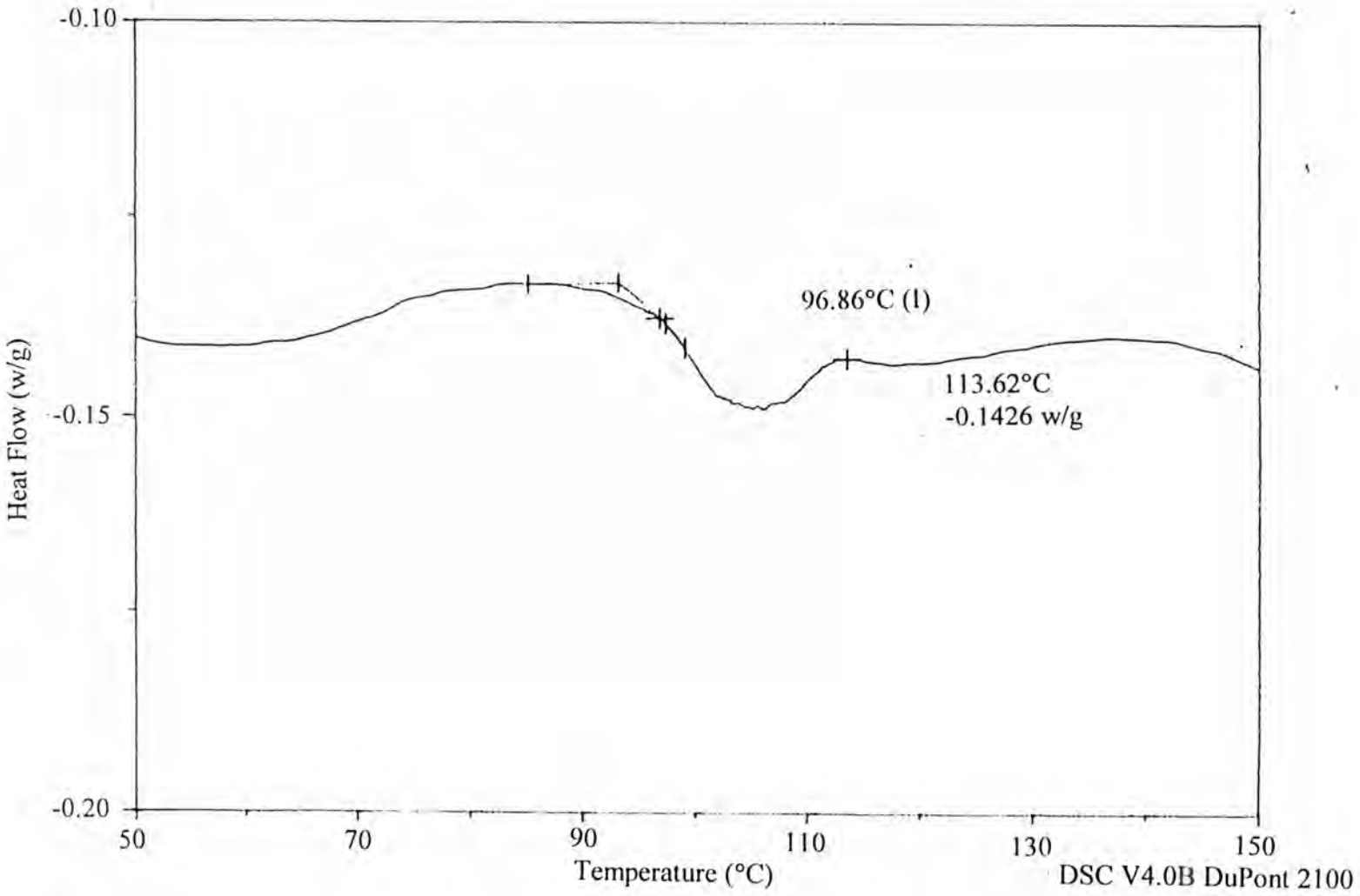

Figure 4.124-1.1 DSC curve of glass transition temperature of poly(styrene-*co*-methyl methacrylate) controlled by 12 wt% PVP K-30

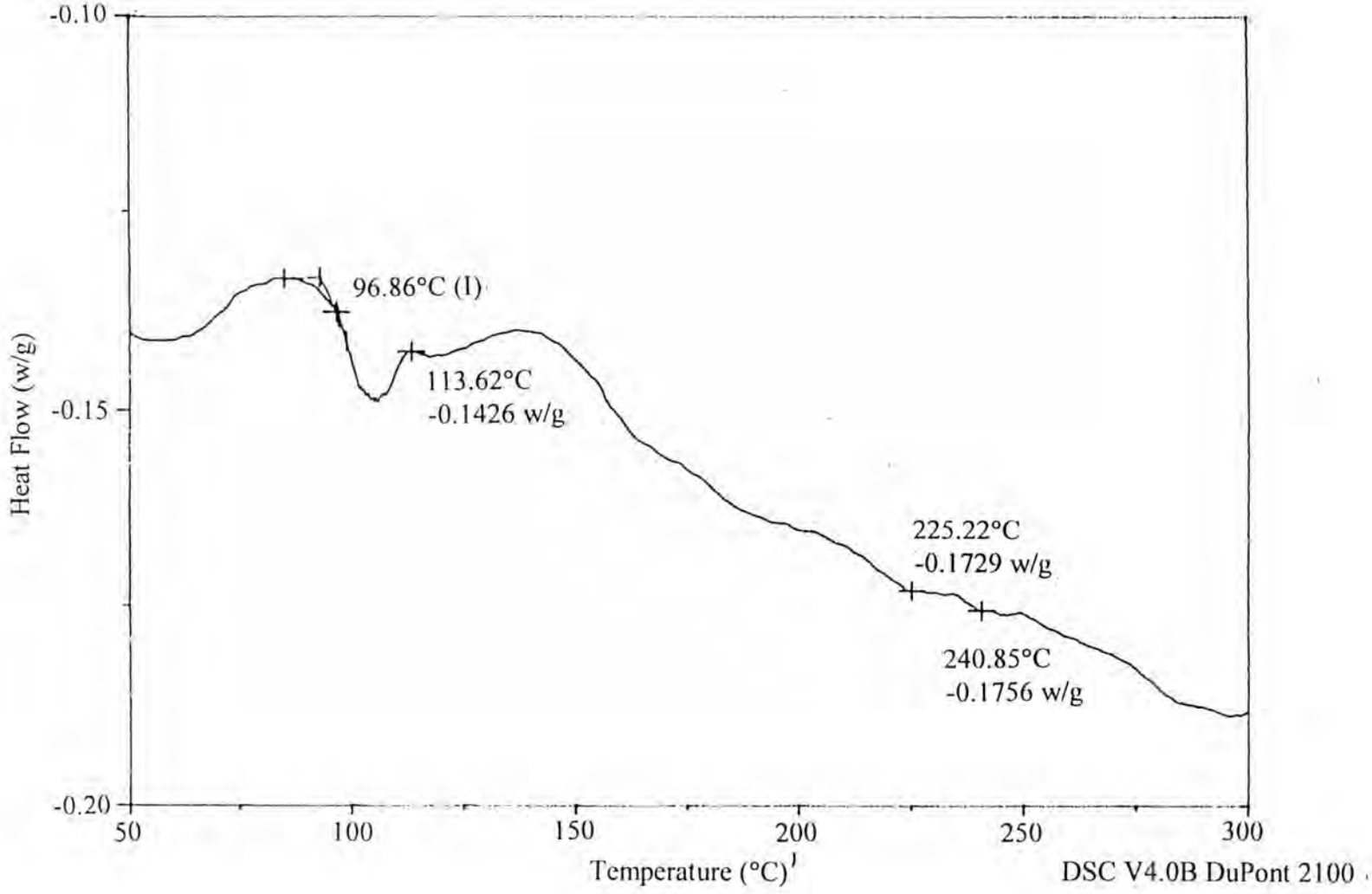

Figure 4.124-1.2 DSC curve of glass transition temperature of poly(styrene-*co*-methyl methacrylate) controlled by 12 wt% PVP K-30

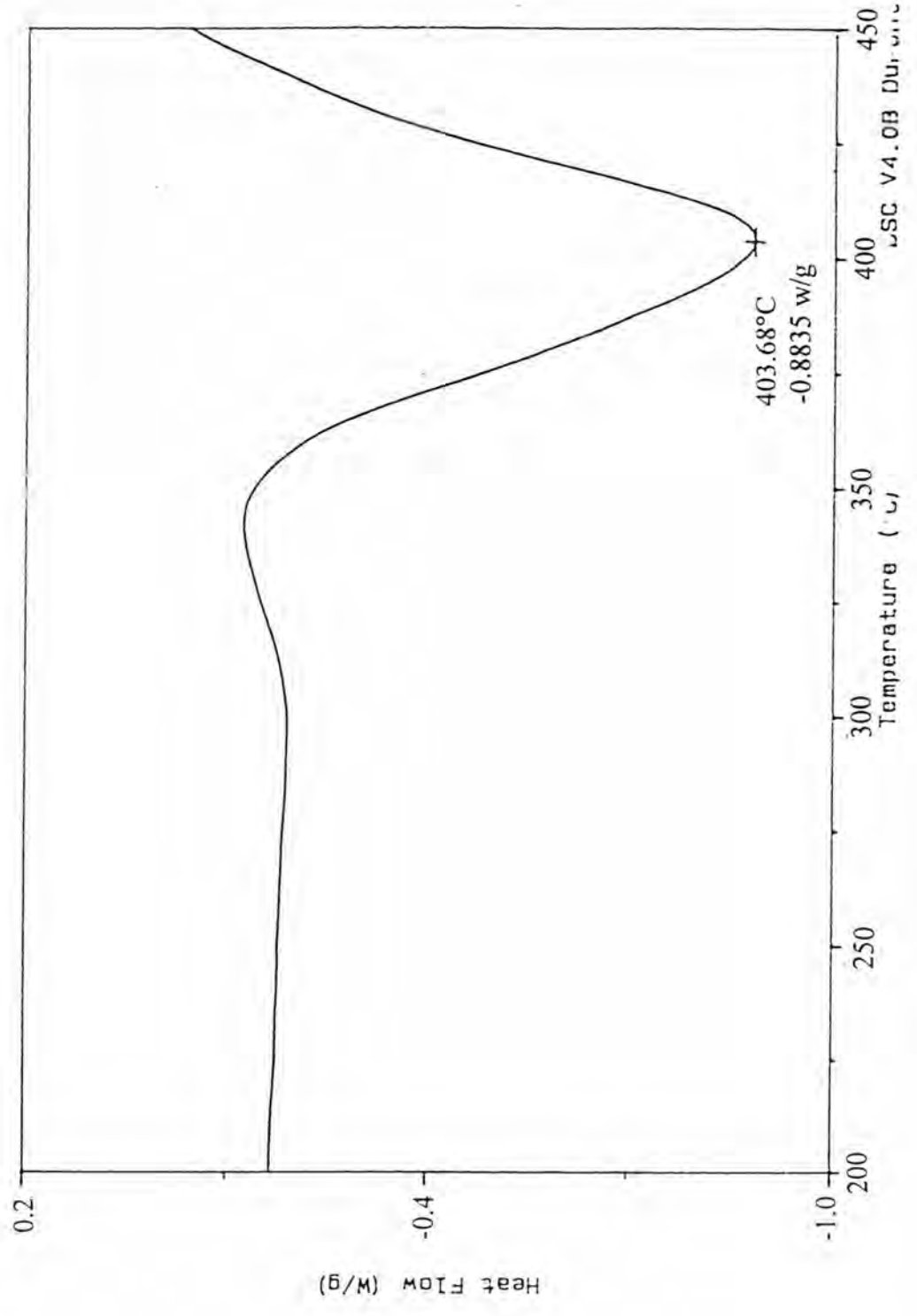

Figure 4.124-2 DSC curve of decomposition temperature of poly(styrene-*co*-methyl methacrylate) controlled by 12 wt% PVP K-30